STUDIES ON
THE HEAVY ATOM EFFECT
ON THE NUCLEAR SHIELDING CONSTANT
AND
THE MOLECULAR INTERACTION
BETWEEN THE CLOSED- AND OPEN-SHELL MOLECULES
BY N M R

KAZUNAKA ENDO
KYOTO UNIVERSITY
1973

STUDIES ON
THE HEAVY ATOM EFFECT
ON THE NUCLEAR SHIELDING CONSTANT
AND
THE MOLECULAR INTERACTION
BETWEEN THE CLOSED-AND OPEN-SHELL MOLECULES
BY N M R

BY

KAZUNAKA ENDO

DEPARTMENT OF HYDROCARBON CHEMISTRY

FACULTY OF ENGINEERING

KYOTO UNIVERSITY

1973

PREFACE

This article summarizes the studies on the heavy atom effect on the chemical shielding constant and the molecular interaction between the proton-donor molecules and a free radical from experimental and theoretical examinations of nmr, performed by the author during 1969-1973.

In the course of the present study the author intended to understand the nmr parameters such as coupling constant, chemical shielding tensor, and relaxation times based on the perturbation theory in quantum mechanics.

Especially throughout the studies on the interaction between the open- and closed-shell molecules, the author discusses this interaction in view of the static (time-average) field from the measurement of the nmr contact shift and deals with the interaction in a viewpoint of the dynamic (time-dependent) field from the relaxation phenomena.

In Part I, the author gives the theory on the nuclear shielding constant using the third-order perturbation method involving into the spin-orbit interaction. In Chapter 2, the author presents the expression for the new type of the shielding constant including the spin-orbit interaction in order to interprete the phenomenon of the heavy atom effect;" The nucleus bonded to the heavy atom such as bromine or iodine resonates at abnormally high field". In Chapter 2-4, the new expression in simplified form with average excitation energy approximation is presented and the physical image for the heavy atom effect on the shielding

constant is made clear. As the application of this theory, the proton chemical shift for the hydrogen halides is calculated in detail.

Part II describes that the nmr contact shifts study provides a potential tool for the investigation of molecular interaction between a nitroxide radical and the closed-shell molecules. In Chapter 2, it is shown that the donor molecules induced by the hydrogen-bond with nitroxide radical yield fruitful information on the nature of the hydrogen bond with the free radical. In section 2 the author mentions a correlation between ^{13}C contact shifts and ^{13}C-H nuclear spin coupling constants. This correlation is interpreted in terms of finite perturbation theory of nuclear spin coupling constants in which the ^{13}C-H coupling constant is related to the electron spin density on the ^{13}C nucleus induced when spin density is placed finitely on the proton. The potential utility of this relation in the prediction of sign and magnitude of long-range ^{13}C-H coupling constants is stated. In section 4 the author studies ^{1}H and ^{13}C contact shifts for various protic substances induced by the addition of di-tert-butyl nitroxide radical (DTBN). The formation constants, enthalpies, limiting ^{1}H and ^{13}C contact shifts and spin densities on the H and C atoms are determined for the proton-donor molecule/DTBN hydrogen-bond interaction from ^{1}H and ^{13}C contact shift measurements at various temperatures. The theoretical studies on this closed- and open-shell bimolecular system are also performed by unrestricted Hartree-Fock SCF MO (INDO method) calculation. In Chapter 3, as a part of

these continuing studies on the interaction between closed- and open-shell molecules, the author performs ^{13}C nmr contact shift studies on DTBN...alkyl halides interaction which are explained in terms of a charge-transfer interaction.

Part III deals with the ^{1}H relaxation study of the hydrogen-bond in proton-donor/DTBN radical system in order to obtain the informations about intermolecular dynamic behaviors. In Chapter 2, ^{1}H relaxation times in proton-donor solutions of DTBN radical are measured in wide temperature ranges and at three different frequencies. The results are discussed in terms of the relaxation theories proposed by Swift-Connick and Solomon-Bloembergen. The activation energies, the lifetimes for the chemical exchange, the closest distance that the proton approaches the odd electron, and the relaxation mechanism are determined from the measurement of the ^{1}H relaxation times.

Finally summary and general conclusion of the present thesis are presented at the end of this work.

ACKNOWLEDGEMENT

The author would like to express his sincere gratitude to Professor Teijiro Yonezawa and Dr. Isao Morishima for their continuing guidances and encouragements during the study of the present work.

He wishes to thank Professor Hiroshi Kato, Dr. Takashi Kawamura and Dr. Hiroshi Nakatsuji for their helpful advices and encouragements. He is indebted to Dr. Kazuyuki Akasaka and Mr. Sadaharu Shirako for their helpful discussions and suggestions. It is also his great pleasure to thank Mrs. Koji Okada, Kenichi Yoshikawa, Toshiro Inubushi, and Koji Ishiwara, with whom the author has collaborated and had many useful discussions throughout his course of study.

In the studies of molecular orbital calculations given in Part I and II, the author indebted to Dr. Hideyuki Konishi and Mr. Kimihiko Hirao for their computor programs used, to whom the author wishes to thank. He also wants to express many thanks to Mrs. Takeshi Matsui, Noboru Nakayama for their assistances in the operation of nmr instrument.

Lastly he expresses his sincere gratitude to his parents and wife.

Kazunaka Endo

Kyoto

April, 1973

CONTENTS

PART I

THE INTRAMOLECULAR HEAVY ATOM EFFECT ON THE NUCLEAR SHIELDING CONSTANT

Chapter 1. Introduction

Since Ramsey proposed the theory of nuclear magnetic shielding in molecules, there have been a large number of studies dealing with various theoretical methods to calculate the shielding constant in molecules. The nuclear shielding constant has been interpreted in terms of the first-order diamagnetic term and of the second-order paramagnetic term by the perturbation theory. For proton chemical shift, first- and second-order terms are considered to be important, with comparable contributions deriving from local electronic enviroment of the proton and the electrons in the remainder of the molecules. In relation to the nucleus other than the proton, the chemical shift is usually discussed to be dominated by the second-order paramagnetic contribution. However, the chemical shielding constant for the nucleus bound to the balogen cannot be explained by the first- and second-order terms. Thus the author studied the effect of the heavy atom on the nuclear shielding tensor.

Experimentally it is well known that the nucleus bonded to the heavy atom such as bromine or iodine resonates at abnormally high field. For example, the proton chemical shift of hydrogen halides, HX, shows abnormal trend when X= Br or I. This is well illustrated in Fig. 1[1] which gives the plot of proton chemical shift vs. the electronegativity of X. The similar abnormal trend is also encountered for ^{13}C chemical shifts for methyl halides, CH_3X[2]. The upfield bias of the chemical shift for the nucleus

Figure 1. The proton chemical shifts of HX compounds plotted against the electronegativity of X'(see Ref. 2).

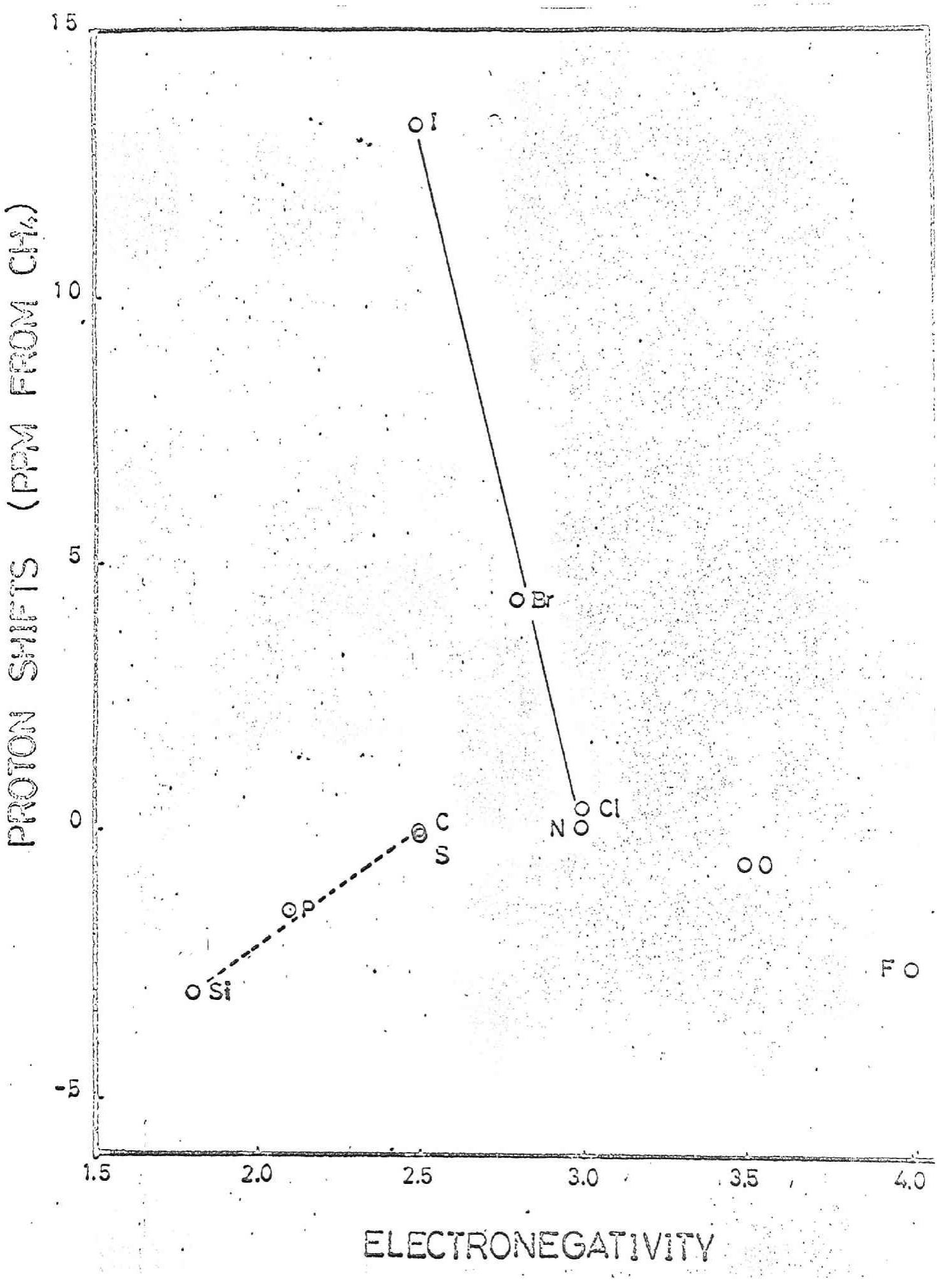

bonbed to the heavy atom has been attracted by many workers[3]. These abnormal observations have been explained that two situations[3] contribute to the paramagnetic term:

(a) the nucleus bonded to the halogen atom are very anisotropic

(b) the halogen atom has the low-lying excited state.

But its origin has yet been in debate.

The present study examine " the effect of electron spin on the shielding constant" through the large spin-orbit interaction (σ_{LS}) characteristic of the heavy atom. As to the effect of electron spin on the nuclear shielding constant, Ramsey[4,5] said in his original paper that, without accidental degeneracies, the magnetic shielding field from the electron spins should be higher orders of smallness than the other contributions. Slichter[6] has also suggested that for the heteronuclear diatomic molecules there may be a different induced orbital moment which, through the spin-orbit coupling, could induce the shift due to spin polarization. Recently Nakagawa et al.[7,8] have proposed the spin-polarization shift due tc such a spin-orbit interaction. They explained qualitatively substituent effects caused by halogens in aromatic proton nmr spectra in terms of the LS shift.

This thesis deals with the more comprehensive study of this spin-polarization shift by the molecular orbital method using third-order perturabation theory. The expression for the new type of shielding constant σ_{LS} is presented in its complete from and in simplified form with the average excitation energy approximation.

Chapter 2. The Effect of the Heavy Atom on the Nuclear Shielding Constant

1. General Theory

A. General Considerations

For the molecule having a heavy atom in an external magnetic field, the Hamiltonian of an N-electron system including the spin-orbit coupling interaction is written as follows;

$$\mathcal{H}=\sum_{K=1}^{N}\left\{\frac{1}{2m}\left\{\mathbb{P}_K-\frac{e}{c}\mathbb{A}_K(\mathfrak{q})\right\}^2+2\beta\mathbb{S}_K\cdot\{\nabla_K\times\mathbb{A}_K(\mathfrak{q})\}+\lambda\mathbb{L}_K\mathbb{S}_K+V(|\mathbb{r}_K|)\right\}, \tag{1}$$

where $V(|\mathbb{r}_K|)$ is the potential energy function, $\lambda\mathbb{L}_K\cdot\mathbb{S}_K$ is the spin-orbit coupling interaction, and $\mathbb{A}_K(\mathfrak{q})$ is the vector potential acting on electron k, which is given by

$$\mathbb{A}_K(\mathfrak{q})=\frac{1}{2}\{\mathbb{H}\times(|\mathbb{r}_K-\mathfrak{q})\}+\frac{(|\mathbb{M}_A\times\mathbb{r}_{AK}\}}{r_{AK}^3}\quad, \tag{2}$$

where $\mathbb{H}$ is a homogeneous magnetic field, $\mathbb{M}_A$ is an infinitesimally small dipole at the position of the atom A, $\mathbb{r}_K$ denotes the position of electron K, $\mathfrak{q}$ is a purely arbitrary constant and arises from the arbitrariness of the gauge of the vector potential, and $\mathbb{r}_{AK}$ denotes the position of electron k with respect to the atom A. With the function $\phi(\mathfrak{q})$ defined by

$$\phi(\mathfrak{q})=\frac{1}{2}((\mathbb{H}\times\mathfrak{q}|)\mathbb{r}_K). \tag{3}$$

we used the following gauge invariant atomic orbitals

$$\tilde{\chi}(K)=\chi(K)\exp(ie\{\phi(\mathfrak{q})-\phi(\mathfrak{a})\}/\hbar c) \tag{4}$$

where $\mathfrak{a}$ is the position of the nucleus and $\chi(K)$ is the atomic

orbital in the absence of a magnetic field. The orbitals $\tilde{\chi}(K)$ are in accord with the choice of origin q for the vector potential. Then the shielding constant of the atom A is obtained from usual third-order perturbation theory

$$\sigma_K = \left(\frac{\partial^2}{\partial\mu_K \partial H_K}\left\{\langle 0|\mathcal{H}|0\rangle - \sum_{n\neq 0}\left\{\frac{\langle 0|\mathcal{H}|n\rangle\langle n|\mathcal{H}|0\rangle}{E_n - E_0}\right\}\right.\right.$$

$$+\sum_{1\neq 0}\sum_{m\neq 0}\left\{\frac{\langle 0|\mathcal{H}|1\rangle\langle 1|\mathcal{H}|m\rangle\langle m|\mathcal{H}|0\rangle}{(E_1 - E_0)(E_m - E_0)}\right\}$$

$$\left.\left. -\langle 0|\mathcal{H}|0\rangle\sum_{n'\neq 0}\left\{\frac{\langle 0|\mathcal{H}|n'\rangle\langle n'|\mathcal{H}|0\rangle}{(E_{n'} - E_0)^2}\right\}\right\}\right)_{\mu=H=0} \qquad (5)$$

It is to be noted that the matrix elements $\langle 1|\mathcal{H}|m\rangle$ are independent of the choice of origin for the vector potential. In order to calculate the matrix elements $\langle 1|\mathcal{H}|m\rangle$ the phase factors $\exp(i\delta)$ should be taken into account, but it is seen that for our choice of the origins in the Hamiltonian most terms which depend on δ may be neglected; for a calculation of the one-center integrals the phase factors become 1, in the evaluation of the two-center integrals they can be expanded in the power series. The first term is 1, the second term is neglected because of the imaginary part, and the other terms do not contribute to the shielding constant because they contain higher powers of H.

We make the assumption that the exact wave functions for the corresponding electronic states in Eq.(5) are approximately built from Hartree-Fock MO's. The wave functions[9] for the ground and the

lowest excited states are written as a single determinant of the form

$$^1\Phi_0 = (\varphi_1\alpha)(\varphi_1\beta)\cdots(\varphi_n\alpha)(\varphi_n\beta)$$

$$^1\Phi_{i\to j} = (\varphi_1\alpha)(\varphi_1\beta)\cdots(\varphi_{i-1}\beta)\frac{1}{\sqrt{2}}\{(\varphi_i\alpha)(\varphi_j\beta)-(\varphi_i\beta)(\varphi_j\alpha)\}(\varphi_{i+1}\alpha)\cdots(\varphi_n\beta)$$

$$^3\Phi_{i\to j} = (\varphi_1\alpha)(\varphi_1\beta)\cdots(\varphi_{i-1}\beta)\left\{\begin{array}{c}(\varphi_i\alpha)(\varphi_j\alpha)\\ \frac{1}{\sqrt{2}}\{(\varphi_i\alpha)(\varphi_j\beta)+(\varphi_i\beta)(\varphi_j\alpha)\}\\ (\varphi_i\beta)(\varphi_j\beta)\end{array}\right\}(\varphi_{i+1}\alpha)\cdots(\varphi_n\beta),$$

where $^1\Phi_0$ is the total wave function for the ground state, $^1\Phi_{i\to j}$ denotes the total wave function for a singlet state, $^3\Phi_{i\to j}$ is for a triplet state; the subscript $i\to j$ labels excitation of a single electron from φ_i to φ_j, and $\varphi(K)$ is an eigenfunction of the Hartree-Fock operator $h(K)$ with orbital energy ϵ_i,

$$h(K)\varphi_i(K) = \epsilon_i\varphi_i(K). \qquad (7)$$

In the case of the molecules XA_n, the coodinate system will be shown in Fig. 2, where we use a coordinate system with the origin on the nucleus X and the z-axis along the line XA and R is the distance between atoms A and X.

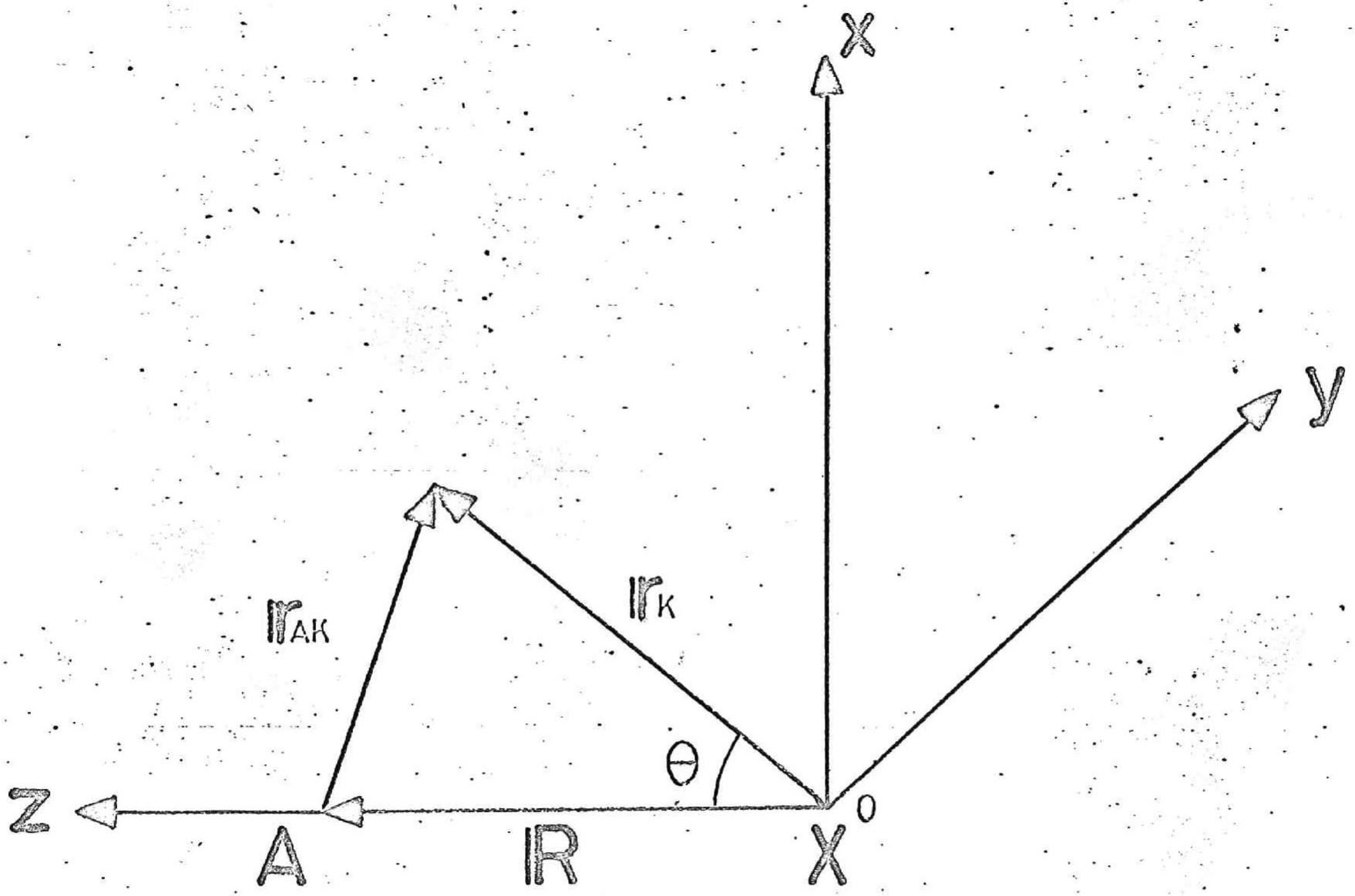
X
y
z
A
R
X
0
θ
r_AK
r_K

B. The First-order perturbation Term

The first term in Eq. (5) is written as

$$\langle {}^1\Phi_0|\mathcal{H}|{}^1\Phi_0\rangle = \sum_{i=1}^{N} \frac{1}{2m}\langle \varphi_i(K)|(P_K - \frac{e}{c}A_K(q))^2|\varphi_i(K)\rangle \qquad (8)$$

This expression is divided into three parts: the first part which contains only atomic orbitals centered on the atom X, the second part which contains only AO's centered on the atom A and the third part which contains both the atomic orbitals of the atom X and the atom A. Because each term is independent of the choice of origin for the vector potential, this origin is chosen in such a way as to facilitate the calculations. Therefore, in the first part the origin is placed on the nucleus X, in the second and the third parts on the nucleus A. Here we consider the diamagnetic contribution to the average shielding constand

$$\sigma' = \frac{1}{3}(\sigma_x + \sigma_y + \sigma_z). \qquad (9)$$

Expand each molecular orbital as a linear combination of the gauge invariant atomic orbitals

$$\varphi_i(K) = \sum_q C_{qi}\tilde{\chi}_q(K). \qquad (10)$$

Then σ_{dia} is expressed as;

$$\sigma_{dia} = \frac{1}{3}\alpha^2 \sum_{i=1}^{occ}\sum_{a,b} C_{ai}C_{bi}\left\{\langle \chi_a(K)|\frac{1}{r_{AK}} - \frac{RZ_{AK}}{r_{AK}^3}|\chi_b(K)\rangle \right.$$

$$\left. + \langle \chi_a(K)|\frac{1}{r_{AK}}|\chi_b(K)\rangle\right\}, \qquad (11)$$

where α is the fine-structure constant.

C. The Second-order Perturbation Term

For the second-order contribution we can obtain two shielding constants $\sigma^{\mu\mu}_{para}$ and σ'_{para}. The former is given as;

$$\sigma^{\mu\mu}_{para} = -\alpha^2 \mathrm{Re}\Big(\sum_{i=1}^{occ}\sum_{j}^{occ}({}^1E_{ji} - E_0)^{-1}\Big\{\langle\varphi_i(K)|[(\mathbf{r}_{AK}\times\nabla)_\mu/r_{AK}^3|\varphi_j(K)\rangle$$
$$\times\langle\varphi_j(K)|[(\mathbf{r}_K - \mathbf{q})\times\nabla]_\mu|\varphi_i(K)\rangle + \langle\varphi_i(K)|[(\mathbf{r}_K-\mathbf{q})\times\nabla]_\mu|\varphi_j(K)\rangle$$
$$\times\langle\varphi_j(K)|[(\mathbf{r}_{AK}\times\nabla)_\mu/r_{AK}^3|\varphi_i(K)\rangle\Big\}\Big), \qquad (12)$$

where ${}^1E_{ji} - E_0 = \epsilon_j - \epsilon_i - J_{ji} + 2K_{ji}$ is the singlet excitation energy from φ_i to φ_j[9].

Substitution of Eq. (10) into Eq. (12) yields

$$\sigma^{\mu\mu}_{para} = -\alpha^2 \mathrm{Re}\Big(\sum_{a,b,c,d}\Big\{\langle\chi_a(K)|[(\mathbf{r}_{AK}\times\nabla)_\mu/r_{AK}^3|\chi_b(K)\rangle$$
$$\times\langle\chi_c(K)|[(\mathbf{r}_K-\mathbf{q})\times\nabla]_\mu|\chi_d(K)\rangle + \langle\chi_a(K)|[(\mathbf{r}_K-\mathbf{q})\times\nabla]_\mu|\chi_b(K)\rangle$$
$$\times\langle\chi_c(K)|[(\mathbf{r}_{AK}\times\nabla)_\mu/r_{AK}^3|\chi_d(K)\rangle\Big\}\sum_{i=1}^{occ}\sum_{j}^{unocc}({}^1E_{ji}-E_0)^{-1}C_{ai}C_{bj}C_{cj}C_{di}\Big). \qquad (13)$$

For the latter, σ'_{para}, the second-order perturbation term, is written as follows;

$$-\frac{2\langle{}^1\Phi_0|\partial\mathcal{H}_1|{}^3\Phi_{i\to j}\rangle\langle{}^3\Phi_{i\to j}|\gamma_e\hbar\mathbf{H}\cdot\hat{\mathbf{S}}|{}^1\Phi_0\rangle}{{}^3E_{ji} - E_0}, \qquad (14)$$

where $\gamma_e \hbar H_l \cdot \hat{\$}$ is the spin zeeman interaction, ${}^3E_{ji} - E_0$ is the triplet excitation energy from φ_i to φ_j, and

$$\mathcal{H}_1 = 2\beta \sum_{K=1}^{n} \left(\frac{1}{r_{AK}^3} \left\{ \frac{3(\hat{\$}_K \cdot \mathbf{r}_{AK})(\mu_A^l \cdot \mathbf{r}_{AK})}{r_{AK}^2} - (\hat{\$}_K \cdot \mu_A^l) \right\} + \frac{8}{3} \pi (\hat{\$}_K \cdot \mu_A^l)\, \delta(r_K) \right). \tag{15}$$

Hereafter, let us consider the role of electron spin for diamagnetic molecules. Since the ground-state wave function ${}^1\Phi_0$ is a spin zero function, all matrix elements of the spin Zeeman interaction in the z-direction to excited states vanish:

$$\langle {}^3\Phi_{i\to j} | \gamma_e \hbar H_0 \hat{S}_z | {}^1\Phi_0 \rangle = 0 \tag{16}$$

The ground state is therefore strictly decoupled from all other states as far as the spin Zeeman coupling is concerned: then σ_{para}^{l} is zero.

D. The Third-order Perturbation Term

For the third-order contribution including the spin-orbit coupling interaction, we can also obtain three shielding constants $\sigma_{LS}^{\mu\mu}(1)$, $\sigma_{LS}^{\mu\mu}(2)$, and $\sigma_{LS}^{\mu\mu}(3)$. For the first term $\sigma_{LS}^{\mu\mu}(1)$, the third-order perturbation expressions are written as;

$$\sigma_{LS}^{\mu\mu}(a) = \left[\frac{\partial^2}{\partial \mu_k \partial H_k} \left(\frac{\langle {}^1\Phi_0 | \mathcal{H}_2 | {}^3\Phi_{i\to j} \rangle \langle {}^3\Phi_{i\to j} | \mathcal{H}_3 | {}^3\Phi_{i'\to j'} \rangle \langle {}^3\Phi_{i'\to j'} | \mathcal{H}_1 | {}^1\Phi_0 \rangle}{({}^3E_{ji} - E_0)({}^3E_{j'i'} - E_0)} \right) \right]_{\mu=H=0}, \tag{17}$$

$$\sigma_{LS}^{\mu\mu}(b) = \left[\frac{\partial^2}{\partial \mu_k \partial H_k} \left(\frac{\langle {}^1\Phi_0 | \mathcal{H}_2 | {}^3\Phi_{i\to j} \rangle \langle {}^3\Phi_{i\to j} | \mathcal{H}_1 | {}^1\Phi_{i'\to j'} \rangle \langle {}^1\Phi_{i'\to j'} | \mathcal{H}_3 | {}^1\Phi_0 \rangle}{({}^3E_{ji} - E_0)({}^1E_{j'i'} - E_0)} \right) \right]_{\mu=H=0}, \tag{18}$$

$$\sigma_{LS}^{\mu\mu}(c)=\left[\frac{\partial^2}{\partial\mu_K\partial H_K}\left(\frac{\langle {}^1\Phi_0|\mathcal{H}_3|{}^1\Phi\rangle\langle {}^1\Phi_{i\to j}|\mathcal{H}_1|{}^3\Phi_{i'\to j'}\rangle\langle {}^3\Phi_{i\to j'}|\mathcal{H}_2|{}^1\Phi_0\rangle}{({}^1E_{ji}-E_0)({}^3E_{j'i'}-E_0)}\right)\right]_{\mu=H=0}, \tag{19}$$

$$\sigma_{LS}^{\mu\mu}(d)=\left[\frac{\partial^2}{\partial\mu_K\partial H_K}\left(\frac{\langle {}^1\Phi_0|\mathcal{H}_3|{}^1\Phi_{i\to j}\rangle\langle {}^1\Phi_{i\to j}|\mathcal{H}_2|{}^3\Phi_{i\to j'}\rangle\langle {}^3\Phi_{i\to j'}|\mathcal{H}_1|{}^1\Phi_0\rangle}{({}^1E_{ji}-E_0)({}^3E_{j'i'}-E_0)}\right)\right]_{\mu=H=0} \tag{20}$$

$$\sigma_{LS}^{\mu\mu}(e)=\left[\frac{\partial^2}{\partial\mu_K\partial H_K}\left(\frac{\langle {}^1\Phi_0|\mathcal{H}_1|{}^3\Phi_{i\to j}\rangle\langle {}^3\Phi_{i\to j}|\mathcal{H}_2|{}^1\Phi_{i'\to j'}\rangle\langle {}^1\Phi_{i'\to j'}|\mathcal{H}_3|{}^1\Phi_0\rangle}{({}^3E_{ji}-E_0)({}^1E_{j'i'}-E_0)}\right)\right]_{\mu=H=0}, \tag{21}$$

$$\sigma_{LS}^{\mu\mu}(f)=\left[\frac{\partial^2}{\partial\mu_K\partial H_K}\left(\frac{\langle {}^1\Phi_0|\mathcal{H}_1|{}^3\Phi_{i\to j}\rangle\langle {}^3\Phi_{i\to j}|\mathcal{H}_3|{}^3\Phi_{i'\to j'}\rangle\langle {}^3\Phi_{i'\to j'}|\mathcal{H}_2|{}^1\Phi_0\rangle}{({}^3E_{ji}-E_0)({}^3E_{j'i'}-E_0)}\right)\right]_{\mu=H=0}, \tag{22}$$

where

$$\mathcal{H}_2=\sum_{K=1}^{n}\lambda\mathbb{L}_K\cdot\mathbb{S}_K, \tag{23}$$

and

$$\mathcal{H}_3=(e/2mc)\sum_{K=1}^{n}\mathbb{H}\cdot(\mathbb{L}_K-\mathbb{q}\times\mathbb{P}_K)=(e/2mc)\sum_{K=1}^{n}\mathbb{H}\cdot[(\mathbb{r}_K-\mathbb{q})\times\mathbb{P}_K] \tag{24}$$

In the evaluation of the matrix elements of the perturbation Hamiltonian $\mathcal{H}_1$ we neglect the dipolar interaction, because it is much smaller than Fermi contact interaction.

Expanding the wave functions in terms of the molecular orbitals,

Eq. (17) become

$$\sigma_{L\cdot S}^{\mu}(a)=\frac{2\pi}{3}\alpha^2\lambda\Bigg\{\sum_{i=1}^{occ}\sum_{jj'}^{unocc}\frac{\langle\varphi_i(K)|(\mathbb{L}_K)_\mu|\varphi_j(K)\rangle\langle\varphi_{j'}(K)|(\mathbb{L}_K-q\times\mathbb{P}_K)_\mu|\varphi_{j'}(K)\rangle\langle\varphi_{j'}(K)|\delta(r_{AK})|\varphi_{i'}(K)\rangle}{({}^3E_{ji'}-E_o)({}^3E_{j'i'}-E_o)}$$

$$-\sum_{ii'}^{occ}\sum_{j}^{unocc}\frac{\langle\varphi_i(K)|(\mathbb{L}_K)_\mu|\varphi_j(K)\rangle\langle\varphi_i(K)|(\mathbb{L}_K-q\times\mathbb{P}_K)_\mu|\varphi_{i'}(K)\rangle\langle\varphi_j(K)|\delta(r_{AK})|\varphi_{i'}(K)\rangle}{({}^3E_{ji'}-E_o)({}^3E_{ji'}-E_o)}$$

$$+2\sum_{im}^{occ}\sum_{j}^{unocc}\frac{\langle\varphi_i(K)|(\mathbb{L}_K)_\mu|\varphi_j(K)\rangle\langle\varphi_m(K)|(\mathbb{L}_K-q\times\mathbb{P}_K)_\mu|\varphi_m(K)\rangle\langle\varphi_j(K)|\delta(r_{AK})|\varphi_{i'}(K)\rangle}{({}^3E_{ji'}-E_o)({}^3E_{ji'}-E_o)}\Bigg\}. \tag{25}$$

In order to calculate the third-order perturbation term, we neglect overlap between different atoms, and consider only the interactions of the valence electrons in the molecules XA_n. Thus the matrix elements appearing in Eq. (25) are approximated as follows;

$$\langle\varphi_i(K)|(\mathbb{L}_K)_\mu|\varphi_j(K)\rangle=[\mathbb{C}_i^X\times\mathbb{C}_j^X]_\mu,$$

$$\langle\varphi_j(K)|\delta(r_{AK})|\varphi_i(K)\rangle=C_{sj'}^A C_{si'}^A|S(0)|^2, \text{ etc,} \tag{26}$$

Where the components of the vectors $\mathbb{C}_\nu^X$ are the coefficients of the corresponding p_X, p_Y and p_Z orbital in the atom X, C_{sj}^A is the coefficient of the s orbital in the atom A, and $|S(0)|^2$ is the electron orbital probability density of the atom A at $r_{AK}=0$. Subsitution Eq. (26) into Eq. (25), we obtain

$$\sigma_{LS}^{\mu\mu}(a) = -\frac{2\pi}{3}\alpha^2\lambda\Bigg\{\sum_{i}^{occ}\sum_{jj'}^{unocc}\frac{[\mathbb{C}_i^X\times\mathbb{C}_j^X]_\mu[\mathbb{C}_j^X\times\mathbb{C}_{j'}^X]_\mu\, C_{sj}^A C_{si}^A}{({}^3E_{ji}-E_0)({}^3E_{j'i}-E_0)}$$

$$-\sum_{ii'}^{occ}\sum_{j}^{unocc}\frac{[\mathbb{C}_i^X\times\mathbb{C}_j^X]_\mu[\mathbb{C}_{i'}^X\times\mathbb{C}_{i'}^X]_\mu C_{sj}^A C_{si'}^A}{({}^3E_{ji}-E_0)({}^3E_{ji'}-E_0)}$$

$$+2\sum_{im}^{occ}\sum_{j}^{unocc}\frac{[\mathbb{C}_i^X\times\mathbb{C}_j^X]_\mu[\mathbb{C}_m^X\times\mathbb{C}_m^X]_\mu C_{sj}^A C_{si}^A}{({}^3E_{ji}-E_0)^2}\Bigg\}|S(0)|^2 \qquad (27)$$

The shielding constants $\sigma_{LS}^{\mu\mu}(b)$, ... , $\sigma_{LS}^{\mu\mu}(f)$ are derived as $\sigma_{LS}^{\mu\mu}(a)$ is done. Therefore we obtain the expression for the shielding constant $\sigma_{LS}^{\mu\mu}(1)$;

$$\sigma_{LS}^{\mu\mu}(1) = -\frac{4}{3}\pi\lambda\alpha^2|S(0)|^2\Bigg\{\sum_{i}^{occ}\sum_{jj'}^{unocc}[\mathbb{C}_i^X\times\mathbb{C}_j^X]_\mu[\mathbb{C}_j^X\times\mathbb{C}_{j'}^X]_\mu C_{sj}^A C_{si}^A$$

$$\times\left(\frac{1}{({}^3E_{ji}-E_0)({}^3E_{j'i}-E_0)}+\frac{1}{({}^1E_{ji}-E_0)({}^3E_{j'i}-E_0)}\right)+\sum_{i}^{occ}\sum_{jj'}^{unocc}[\mathbb{C}_i^X\times\mathbb{C}_j^X]_\mu$$

$$\times C_{sj}^A C_{sj'}^A[\mathbb{C}_{j'}^X\times\mathbb{C}_i^X]_\mu\{({}^3E_{ji}-E_0)({}^1E_{ji}-E_0)\}^{-1}-\sum_{ii'}^{occ}\sum_{j}^{unocc}[\mathbb{C}_i^X\times\mathbb{C}_j^X]_\mu$$

$$\times[\mathbb{C}_{i'}^X\times\mathbb{C}_{i'}^X]_\mu C_{sj}^A C_{si'}^A\{({}^3E_{ji}-E_0)({}^3E_{ji'}-E_0)\}^{-1}+\{({}^1E_{ji}-E_0)({}^3E_{ji'}-E_0)\}^{-1}\Bigg]$$

$$-\sum_{i,\nu}^{occ}\sum_{j}^{unocc}\{(\mathbb{C}_i^X\times\mathbb{C}_j^X)_\mu C_{S\nu}^A C_{S\nu}^A\{(\mathbb{C}_j^X\times\mathbb{C}_\nu^X)_\mu\{({}^3E_{j\nu}-E_0)({}^1E_{j\nu}-E_0)\}^{-1}$$

$$+2\sum_{i,m}^{occ}\sum_{j}^{unocc}\{(\mathbb{C}_i^X\times\mathbb{C}_j^X)_\mu\{(\mathbb{C}_m^X\times\mathbb{C}_m^X)_\mu C_{Sj}^A C_{Si}^A\{{}^3E_{j\nu}-E_0\}^{-2}. \tag{28}$$

In the derivation of the second term $\sigma_{LS}^{\mu\mu}(2)$, we considered Eq. (16) and used the third-order perturbation term. The shielding constant $\sigma_{LS}^{\mu\mu}(2)$ is expressed as;

$$\sigma_{LS}^{\mu\mu}(2)=\left\{\frac{\partial^2}{\partial\mu_K\partial H_K}\left(\frac{\langle{}^1\Phi_0|\partial\mathcal{H}_2|{}^3\Phi_{i\to j}\rangle\langle{}^3\Phi_{i\to j}|\gamma_e\hbar H|\cdot\hat{S}_K|{}^1\Phi_{i\to j}\rangle\langle{}^1\Phi_{i\to j}|\partial\mathcal{H}_4|{}^1\Phi_0\rangle}{({}^3E_{j\nu}-E_0)({}^1E_{j'\nu}-E_0)}\right.\right.$$

$$\left.\left.+\frac{\langle{}^1\Phi_0|\partial\mathcal{H}_4|{}^1\Phi_{i\to j}\rangle\langle{}^1\Phi_{i\to j}|\gamma_e\hbar H|\cdot\hat{S}_K|{}^3\Phi_{i\to j'}\rangle\langle{}^3\Phi_{i\to j'}|\partial\mathcal{H}_2|{}^1\Phi_0\rangle}{({}^1E_{j\nu}-E_0)({}^3E_{j'\nu}-E_0)}\right)\right\} \tag{29}$$

where

$$\partial\mathcal{H}_4=(e/mc)\sum_{K=1}^{n}\frac{\mu_A'\cdot(\mathbb{L}_K-(\mathbb{R}\times\mathbb{P}_K))}{r_{AK}^3}=(e/mc)\sum_{K=1}^{n}\frac{\mu_A'\cdot((\mathbb{r}_K-\mathbb{R})\times\mathbb{P}_K)}{r_{AK}^3}. \tag{30}$$

Expansion of the wave functions in terms of the molecular orbitals yields

$$\sigma_{LS}^{\mu\mu}(2)=\frac{\lambda}{2}\alpha^2\left\{\sum_{i=1}^{occ}\sum_{j,j'}^{unocc}\frac{\langle\varphi_i(K)|(\mathbb{L}_K)_\mu|\varphi_j(K)\rangle\langle\varphi_j(K)|\varphi_{j'}(K)\rangle\langle\varphi_{j'}(K)|\frac{(\mathbb{L}_K-(\mathbb{R}\times\mathbb{P}_K))_H}{r_{AK}^3}|\varphi_i(K)\rangle}{({}^3E_{j\nu}-E_0)({}^1E_{j'\nu}-E_0)}\right.$$

$$-\sum_{i=1}^{occ}\sum_{j,j'}^{unocc}\frac{\langle\varphi_i(K)|(\mathbb{L}_K)_\mu|\varphi_j(K)\rangle\langle\varphi_i(K)|\varphi_{j'}(K)\rangle\langle\varphi_{j'}(K)|(\mathbb{L}_K-(\mathbb{R}\times\mathbb{P}_K))_\mu/r_{AK}^3|\varphi_i(K)\rangle}{({}^3E_{ji}-E_0)({}^1E_{ji'}-E_0)}$$

$$+\sum_{i=1}^{occ}\sum_{j,j'}^{unocc}\frac{\langle\varphi_i(K)|(\mathbb{L}_K-(\mathbb{R}\times\mathbb{P}_K))_\mu/r_{AK}^3|\varphi_j(K)\rangle\langle\varphi_j(K)|\varphi_{j'}(K)\rangle\langle\varphi_{j'}(K)|(\mathbb{L}_K)_\mu|\varphi_i(K)\rangle}{({}^1E_{ji}-E_0)({}^3E_{ji'}-E_0)}$$

$$-\sum_{i,i'=1}^{occ}\sum_{j}^{unocc}\frac{\langle\varphi_i(K)|(\mathbb{L}_K-(\mathbb{R}\times\mathbb{P}_K))_\mu/r_{AK}^3|\varphi_j(K)\rangle\langle\varphi_{i'}(K)|\varphi_i(K)\rangle\langle\varphi_j(K)|(\mathbb{L}_K)_\mu|\varphi_{i'}(K)\rangle}{({}^1E_{ji}-E_0)({}^3E_{ji'}-E_0)}\Bigg\} \tag{31}$$

Substitution of Eq. (10) into Eq. (31) gives

$$\sigma_{LS}^{\mu\mu}(2)=\lambda\alpha^2\Bigg\{\sum_{i=1}^{occ}\sum_{j,j'}^{unocc}\sum_{a,b,c,d,e,f}\Big\{\big\{({}^3E_{ji}-E_0)(E_{j'i}-E_0)\big\}^{-1}C_{ia}C_{jb}C_{jc}C_{jd}C_{j'e}C_{if}$$

$$\times\langle\chi_a(K)|(\mathbb{L}_K)_\mu|\chi_b(K)\rangle\langle\chi_c(K)|\chi_d(K)\rangle\langle\chi_e(K)|(\mathbb{L}_K+(\mathbb{R}\times\mathbb{P}_K))_\mu/r_{AK}^3|\chi_f(K)\rangle\Big\}$$

$$-\sum_{i,i'=1}^{occ}\sum_{j}^{unocc}\sum_{a,b,c,d,e,f}\Big\{\big\{({}^3E_{ji}-E_0)({}^1E_{ji'}-E_0)\big\}^{-1}C_{ia}C_{jb}C_{i'c}C_{id}C_{je}C_{i'f}$$

$$\times\langle\chi_a(K)|(\mathbb{L}_K)_\mu|\chi_b(K)\rangle\langle\chi_c(K)|\chi_d(K)\rangle\langle\chi_e(K)|(\mathbb{L}_K-(\mathbb{R}\times\mathbb{P}_K))_\mu/r_{AK}^3|\chi_f(K)\rangle\Big\}\Bigg\}. \tag{32}$$

Where the Hermitian property was used. In the case os the molecules XA_n, a calculation of $\sigma_{LS}^{\mu\mu}(2)$ revealed that it is very small. The numerical calculation shows that the second term $\sigma_{LS}^{\mu\mu}(2)$ is in the order of 10^{-9} for hydrogen iodide. There-

fore this term was neglected in the present treatment.

For the third term $\sigma_{LS}^{\mu\mu}(3)$, we also used the third-order perturbation theory. The shielding constant $\sigma_{LS}^{\mu\mu}(3)$ is given as;

$$\sigma_{LS}^{\mu\mu}(3) = \left[\frac{\partial^2}{\partial\mu_K \partial H_K}\left\{ \frac{\langle {}^1\Phi_0|\mathcal{H}_2|{}^3\Phi_{i\to j}\rangle\langle {}^3\Phi_{i\to j}|\frac{1}{2m}(P_K - \frac{e}{c}A_K(q_l))^2|{}^3\Phi_{i\to j}\rangle\langle {}^3\Phi_{i\to j}|\mathcal{H}_2|{}^1\Phi_0\rangle}{({}^3E_{ji} - E_0)({}^3E_{j'i'} - E_0)} \right.\right.$$

$$\left.\left. - \langle {}^1\Phi_0|\frac{1}{2m}(P_K - \frac{e}{c}A_K(q_l))^2|{}^1\Phi_0\rangle \frac{\langle {}^1\Phi_0|\mathcal{H}_2|{}^3\Phi_{i\to j}\rangle\langle {}^3\Phi_{i\to j}|\mathcal{H}_2|{}^1\Phi_0\rangle}{({}^3E_{ji} - E_0)^2} \right\}\right]_{\mu=H=0}. \tag{33}$$

Each term of $\sigma_{LS}^{\mu\mu}(3)$ contains the matrix elements of the first-order perturbation term and of the spin-orbit interaction which appears twice in this third-order perturbation expression. Thus the third term $\sigma_{LS}^{\mu\mu}(3)$ is relatively small so that it can be neglected. In fact, even in the case of the hydrogen iodide, each term of $\sigma_{LS}^{\mu\mu}(3)$ is smaller than 10^{-8}.

E. The Nuclear Shielding Constant

Combining Egs. (11), (13), and (28), the nuclear shielding constant σ is obtained as follows;

$$\sigma = \sigma_{dia} + \frac{2}{3}(\sigma_{para}^{xx} + \sigma_{LS}^{xx}(1)). \tag{34}$$

In this form, the evaluation of σ requires a knowledge of the coefficients C_{ia} of the atomic orbitals $\chi_a(K)$, matrix elements over the atomic orbitals $\chi_a(K)$, and the excitation

energies. In Appendix, we employ the general equation to obtain a simplified expression for $\sigma_{LS}^{\mu\mu}(1)$ in terms of parameters related to bond properties, using appropriate approximations.

2. Calculation of the Proton Shift

In this section we will present the results of the numerical calculation of the shielding constant for HX molecules with an aid of the expression derived in II. In order to calculate the proton shift of the hydrogen halides we used the semi-empirical SCF-LCAO MO[10] for all valence electron systems. The wave functions of the hydrogen halides are shown in Table I.

σ_{dia} is given from Eq. (II) as follows;

$$\sigma_{dia} = \frac{1}{3}\alpha^2 \sum_{i=1}^{occ} \sum_{a,b} C_{ia} C_{ib} \left\{ \langle \chi_a(K) | \frac{1}{r_{HK}} - \frac{R Z_{HK}}{r_{HK}^3} | \chi_b(K) \rangle + \langle \chi_a(K) | \frac{1}{r_{HK}} | \chi_b(K) \rangle \right\}. \quad \text{(II-1)}$$

The first term in Eq. (II-1) contains only wave functions which are centered on the halogen nucleus, and the second term contains only wave functions which are centered on the hydrogen and both halogen and hydrogen atomic orbitals which are centered on the hydrogen. The various integrals which appear in Eq (II-1) are listed in Table II. For a calculation of the first-order pertur-

Table I. SCF orbital coefficients and energies of HX.

Molecule	MO	1h	s	P_z	P_x P_y	E (eV)
	1	0.341960	0.934964	-0.094336	0.0	-40.465443
HF	2	-0.380137	0.229469	0.896013	0.0	-16.465443
R(0.917A)[a]	3	0.0	0.0	0.0	1.000000	-15.081669
	4					
	5	0.859395	-0.270529	0.433884	0.0	2.771950
	1	0.472576	0.853630	-0.222922	0.0	-27.842008
HCl	2	-0.349398	0.413486	0.840803	0.0	-15.695439
R(1.274A)[a]	3	0.0	0.0	0.0	1.000000	-13.930910
	4					
	5	0.809069	-0.319455	0.493311	0.0	2.429752
	1	0.490182	0.836575	-0.244669	0.0	-26.359921
HBr	2	-0.377122	0.456631	0.805771	0.0	-14.683530
R(1.414A)[a]	3	0.0	0.0	0.0	1.000000	-12.396140
	4					
	5	0.785812	-0.302705	0.539323	0.0	2.531140
	1	0.538804	0.776785	-0.326856	0.0	-21.901690
HI	2	-0.349578	0.558716	0.752085	0.0	-13.500885
R(1.609A)[a]	3	0.0	0.0	0.0	1.000000	-11.773998
	4					
	5	0.766827	-0.290589	0.572306	0.0	1.859848

a. R is the H-X bond length.

bation term two-center integrals are considered.

The second-order contribution $\sigma_{para}^{\mu\mu}$ is obtained from Eq. (13);

$$\sigma_{para}^{\mu\mu} = -2\alpha^2 Re\Big[\sum_{a,b,c,d}\Big\{\langle\chi_a(K)|[(\mathbf{r}_K-\mathbf{R})\times\nabla]_\mu/r_{HK}^3|\chi_b(K)\rangle$$

$$\times\langle\chi_c(K)|[\mathbf{r}_K\times\nabla]_\mu|\chi_d(K)\rangle\Big\}\sum_{i=1}^{occ}\sum_{j}^{unocc}(E_{ji}-E_0)^{-1}C_{ai}C_{bj}C_{cj}C_{di}\Big].$$

(II -2)

Here only one-center integrals are retained for the sake of simplicity. Although the two-center integrals may contribute substantially to the second-order perturbation term. However, the present calculations agree approximately with Hameka's more labourious results[11] (see Table III). All quantities which are required for a calculation of $\sigma_{para}^{\mu\mu}$ are listed in Table IV.

For a calculation of $\sigma_{LS}^{\mu\mu}$ we used Eq. (28) directly. All quantities which are required for the evaluation of $\sigma_{LS}^{\mu\mu}(1)$ are listed in Table V. Here also the one-center integrals are retained. Because the calculations of two-center integrals are more complicated than those of the second-order perturbation term, and one-center integrals strongly influences the results.

We calculated integrals which appear in the formular of all the perturbation terms after the Hameka's[11] and Musher's[12] methods.

Especially in the case of the hydrogen fluoride the values calculated by semi-empirical SCF MO were compared with the results

Table II. Intergrals which appear in the formulae of the first-order perturbation term of the proton shielding constant.

	$\langle nSx \mid nSx \rangle$	$\langle nSx \mid nZx \rangle$	$\langle nZx \mid nZx \rangle$	$\langle nXx \mid nXx \rangle$	$\langle 1h \mid nSx \rangle$	$\langle 1h \mid nZx \rangle$
F	0.027393	-0.135914	-0.079398	0.076688	0.366153	0.371684
Cl	0.055015	-0.074792	-0.020010	0.092528	0.345577	0.434180
Br	0.082226	-0.031432	0.037315	0.104682	0.323847	0.396549
I	0.105617	0.012862	0.095961	0.100445	0.309230	0.442876

Table III. The calculated values of σ_{para} (ppm unit)

	HF	HCL	HBr	HI
Present result	-10.45	-3.27	-3.03	-2.29
Hameka's result	-6.82	-4.20	-3.17	-1.66

Table IV. Quantites which are required for the evaluation of σ_{para}.

	$^1E_{ji}-E_o$ (eV)	$\langle nYx \mid 1/r^3_{Hk} \mid nYx \rangle$
F	6.95455	0.182657
Cl	8.19057	0.061470
Br	7.74982	0.039822
I	6.73167	0.023412

Table V. Quantities which are required for a calculation of $\sigma_{LS}^{\mu\mu}(1)$.

	λ(eV)	$^1E_5-E_1$(eV)	$^1E_5-E_2$(eV)	$^1E_5-E_{3,4}$(eV)	$^3E_5-E_1$(eV)	$^3E_5-E_2$(eV)	$^3E_5-E_{3,4}$(ev)
F	0.034	34.37744	9.16056	6.95455	31.36235	7.02593	5.84618
Cl	0.073	23.86486	10.59241	8.19057	20.71661	9.26911	7.43476
Br	0.307	23.38723	10.70583	7.74982	20.31057	9.33111	7.10374
I	0.632	19.33507	9.73385	6.73385	16.09366	8.32262	6.25097

by non-empirical SCF MO[13]. All the results are listed in Table VI.

The ^{1}H and ^{13}C LS shift for the halides are calculated by Eq(v-6) using "ΔE approximation". In Table VII the results of ^{1}H LS shift for the hydrogen halides are given. The values of ^{1}H LS shift which was calculated using ΔE=8eV are in satisfactory agreement with ones obtained from Eq. (28).

In Table VIII the values of ^{13}C LS shift for the methyl halides are calculated using Eq.(IV-6), but it should be noted that we can not use this equation strictly. Because in the methyl halides there are two atoms associated with the spin-orbit interactions. Thus the spin-orbit interaction of the carbon is neglected because of smallness of magnitude, and C^{13} LS shift is evaluated by semi-empirical SCF LCAO MO[10] for all valence electron systems. The calculated values are too small relatively to reproduce the trend of the experimental results of C^{13} chemical shift for the methyl halides. However, ΔE values of 8eV and 10eV appear to be somewhat large in view of the lowest excitation energy for CH_3I(4.0eV)[14]. Therefore one should take less magnitude of ΔE value (5eV, for example) which leads to more refined value of $\sigma_{LS}(1)$ (11.6×10^{-6}).

Table VI. Calculated proton shielding constants for hydrogen halides (ppm unit)

	non-empirical	semi-empirical			
	HF	HF	HCl	HBr	HI
σ_{dia}	10.38	5.06	6.35	8.88	9.98
σ_{para}	-16.09	-10.45	-3.72	-3.03	-2.29
$\sigma_{LS}(1)$	0.07	0.37	0.59	2.98	8.21
total	-5.64	-5.02	3.22	8.83	15.90

Table VII. The ^{1}H LS shielding constants ($\sigma_{LS}(1)$).

	Exact[a]	ΔE Approximation	
		8(ev)	10(eV)
HF	0.37	0.28	0.18
HCl	0.59	0.70	0.45
HBr	2.98	3.32	2.18
HI	8.21	7.34	4.69

a: Calculated without ΔE approximation.

Table VIII. The ^{13}C LS shielding constants (ppm unit).

CH_3X	ΔE Approximation	
	(8 eV)	(10 eV)
CH_3F	0.15	0.10
CH_3Cl	0.48	0.30
CH_3Br	2.36	1.51
CH_3I	4.56	2.92

Table IX. The proton chemical shifts of hydrogen halides

		Relative to HF (ppm unit)			Relative to HCl (ppm unit)	
		HCl	HBr	HI	HBr	HI
Hameka's results	σ_{dia}	3.58	5.66	8.57	2.08	5.17
	σ_{para}	2.62	3.65	5.16	1.03	2.54
	σ_{total}	6.20	9.31	13.91	3.11	7.71
Our results	σ_{dia}	1.29	3.82	4.92	2.53	3.63
	σ_{para}	6.73	7.42	8.16	0.69	1.43
	σ_{LS}	0.22	2.61	7.84	2.39	7.62
	σ_{total}	8.24	13.85	20.92	5.61	12.68
Obs.[a]	EX	2.95	7.28	15.90	4.33	12.80

a. Ref. 1.

3. Discussion

In Table IX, our calculated values including Hameka's calculated results are compared with experimental results for the proton chemical shift of hydrogen halides. Our calculated results, relative to HF, differ from the experimental values by about 5×10^{-6}. However, it is apparent that our results coincide fairly well with the experimental values, when the values are respect to HCl. For hydrogen halides there is no satisfactory wavefunction available except the HF and HCl molecules, so we used the semi-empirical SCF-LCAO MO[10] for all valence electron systems. However, it appears that the increase of the LS shift (σ_{LS}) in going from HF to HI may be attributed to the greater spin polarization in the molecules containing the heavy atoms.

A. The Significance of the LS Shift

Inspection of Table VI shows that the values of σ_{LS} (1) are as large as σ_{para} for HBr and HI; the LS shift makes a contribution substantially to the proton shifts for the HBr and HI. Table IX also shows that Hameka's results, relative to HCl, are smaller than the experimental ones. When we add the present value of $\sigma_{LS}(1)$ to the Hameka's theoretical value of σ which neglects the LS shift, the agreement with experiment is satisfactory (Table IX).

It is clear from the above discussion that the new shift, $\sigma_{LS}(1)$, cannot be ignored in comparison with σ_{para}. The LS shift appears to have an important contribution to the abnormal upfield

to hydrogen chloride, are plotted vs. the electronegativity of

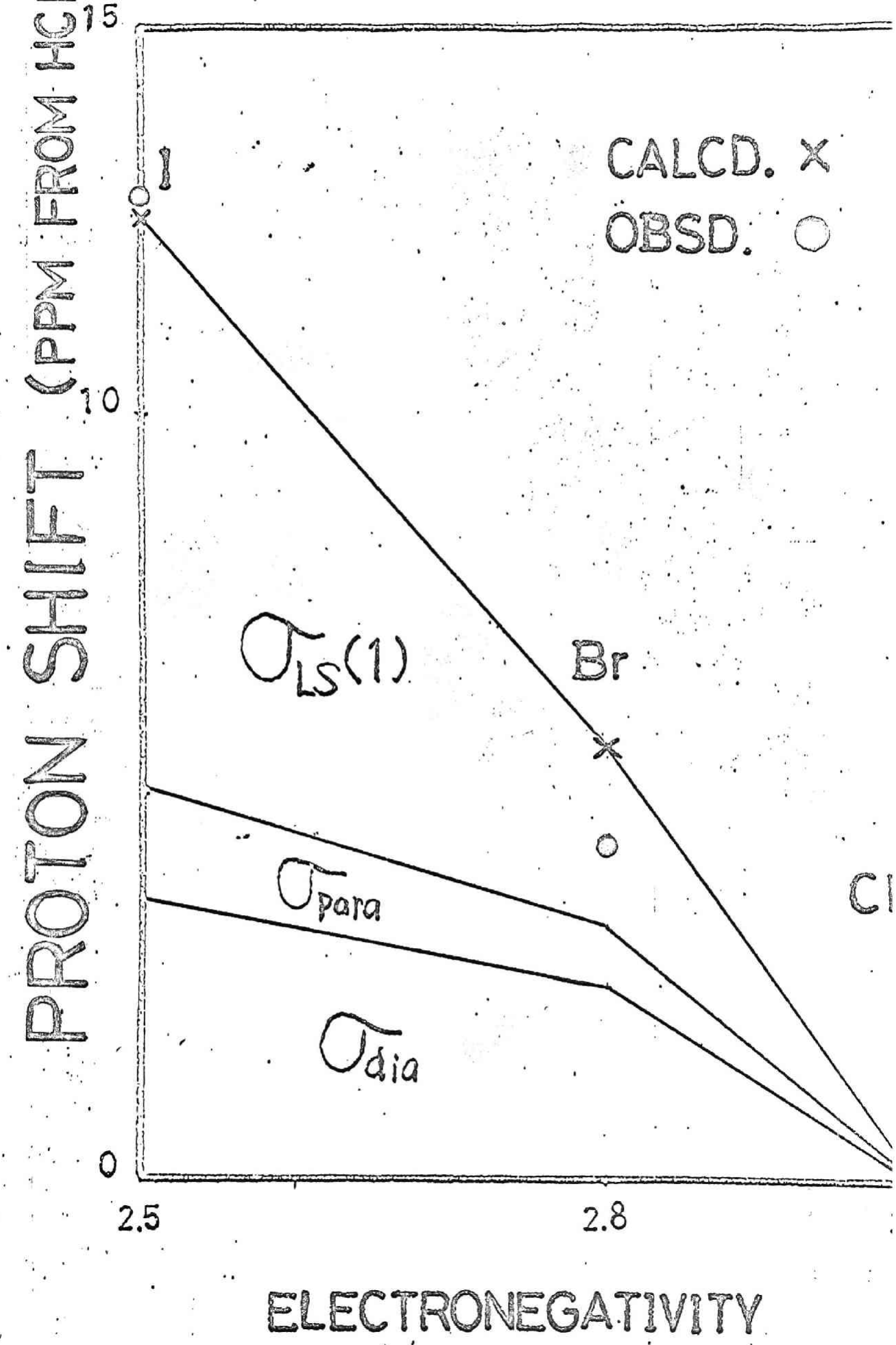

trend of the proton chemical shift in hydrogen halides (Fig. 3)

B. The Implication of the LS Shift

In the diamagnetic substances the contributions of the electron spins to the chemical shielding appear in the higher-order perturbation calculations.[4,5] When one considers the effects of the heavy atoms of iodine and bromine which are characterized by the large spin-orbit interactions, the higher-order perturbation theory should be used.

Though the LS shift $\sigma_{LS}(1)$ has already been explained by Nakagawa et al.[6,7], our derivation (Eq.(IV-6)) will be amenable to see the physical meaning of $\sigma_{LS}(1)$; in molecules such as HBr and HI, the heavy atom has many electrons, so the orbital angular momentum of the heavy atom is induced by an external magnetic field. In succession, the orbital moment induces a spin polarization into the bond through the spin-orbit interaction of the heavy atoms, and the spin polarization contributes to the chemical shifts on the hydrogen through Fermi contact interaction of a nucleus with electrons. Alternatively, this shift is interpreted in the sence that a localized triplet exciton is induced on the heavy atom by the spin-orbit interaction, transmitting to the neighboring atom through the bond. Thus the LS shift arises on the neighnoring atom through Fermi contact interaction of a nucleus with electrons.

Finally, we can consider that Eq.(IV-6) includes the terms which are similar to the atom-atom polarizability, so when the

LS shift is large, it won't give only a contribution to the chemical shift on the nearest-neighboring atom, but also on the near atoms.

4. Appendix

For the third-order contributions $\sigma_{LS}^{xx}(1)$ to the shielding od the nucleus A, a general formula is given from Eq.(28) as;

$$\sigma_{LS}^{xx}(1)=-\frac{4\pi}{3}\lambda\alpha^2\Big\{\sum_{i}^{occ}\sum_{j,j'}^{unocc}[\mathbb{C}_i^B\times\mathbb{C}_j^B]_x[\mathbb{C}_j^B\times\mathbb{C}_{j'}^B]_x C_{sj'}^A C_{si}^A$$

$$\times\left[({}^3E_{ji}-E_0)^{-1}({}^3E_{j'i}-E_0)^{-1}+({}^1E_{ji}-E_0)^{-1}({}^3E_{j'i}-E_0)^{-1}\right]$$

$$+\sum_{i}^{occ}\sum_{jj'}^{unocc}[\mathbb{C}_i^B\times\mathbb{C}_j^B]_x C_{sj}^A C_{sj'}^A[\mathbb{C}_{j'}^B\times\mathbb{C}_i^B]_x\left[({}^3E_{ji}-E_0)({}^1E_{j'i}-E_0)\right]^{-1}$$

$$-\sum_{i,i'}^{occ}\sum_{j}^{unocc}[\mathbb{C}_i^B\times\mathbb{C}_j^B]_x[\mathbb{C}_{i'}^B\times\mathbb{C}_i^B]_x C_{sj}^A C_{si'}^A\left[({}^3E_{ji}-E_0)^{-1}({}^3E_{ji'}-E_0)^{-1}\right.$$

$$\left.+({}^1E_{ji}-E_0)^{-1}({}^3E_{ji'}-E_0)^{-1}\right]-\sum_{i,i'}^{occ}\sum_{j}^{unocc}[\mathbb{C}_i^B\times\mathbb{C}_j^B]_x C_{si'}^A C_{si}^A[\mathbb{C}_j^B\times\mathbb{C}_{i'}^B]_x$$

$$\times\left[({}^3E_{ji}-E_0)({}^1E_{j'i'}-E_0)\right]^{-1}+2\sum_{i,m}^{occ}\sum_{j}^{unocc}[\mathbb{C}_i^B\times\mathbb{C}_j^B]_x[\mathbb{C}_m^B\times\mathbb{C}_m^B]_x$$

$$\times C_{sj}^A C_{si}^A({}^3E_{ji}-E_0)^{-2}\Big\}|S(0)|^2. \qquad \text{(IV-1)}$$

We now use the " ΔE approximation" by replacing all differences ${}^3E_{ji}-E_0$ by an average ΔE. Then each term in Eq. (IV-1) becomes a product of two factors,one containing over occupied MO's and the other a sum over unoccupied MO's. The x component is expressed

as follows;

$$O_{LS}^{xx}(1) = -\frac{\pi\lambda\alpha^2|S(0)|^2}{6(\Delta E)^2}\{2(P_{YBSA}Q_{YBZB}Q'_{ZBSA}+P_{ZBSA}Q_{YBZB}Q'_{YBSA}$$

$$-P_{YBSA}Q_{ZBZB}Q'_{YBSA}-P_{ZBSA}Q_{YBYB}Q'_{ZBSA})+P_{YBZB}Q_{ZBSA}Q'_{YBSA}$$

$$+P_{YBZB}Q_{YBSA}Q'_{ZBSA}-P_{ZBZB}Q_{YBSA}Q'_{YBSA}-P_{YBYB}Q_{ZBSA}Q'_{ZBSA}$$

$$-2(P_{YBZB}Q_{ZBSA}P'_{YBSA}+P_{ZBYB}Q_{YBSA}P'_{ZBSA}-P_{ZBZB}Q_{YBSA}P'_{YBSA}$$

$$-P_{YBYB}Q_{ZBSA}P'_{ZBSA})-(P_{YBSA}Q_{ZBYB}P'_{ZBSA}+P_{ZBSA}Q_{YBZB}P'_{YBSA}$$

$$-P_{ZBSA}Q_{YBYB}P_{ZBSA}-P_{YBSA}Q_{ZBZB}P'_{YBSA})+2(P_{YBSA}Q_{ZBSA}P'_{YBZB}$$

$$+P_{ZBSA}Q_{YBSA}P'_{YBZB}-P_{ZBSA}Q_{YBSA}P'_{YBZB}-P_{YBSA}Q_{ZBSA}P'_{YBZB})\},$$

(IV-2)

where P_{ab} is an element of the charge-bond-order matrix and Q_{ab} is defined similarly for unoccupied orbitals as;

$$P_{ab} = 2\sum_{i=1}^{occ} C_{ai}C_{bi}, \qquad \text{(IV-3)}$$

$$Q_{ab} = 2\sum_{j}^{unocc} C_{aj}C_{bj}. \qquad \text{(IV-4)}$$

When overlap is neglected, we can use the relation

$$P_{ab} + Q_{ab} = 2\delta_{ab} \qquad \text{(IV-5)}$$

to express the sums over unoccupied MO's as sums over occupied MO's. Thus the third-order contributions $\sigma_{LS}^{xx}(1)$ is simplified as;

$$\sigma_{LS}^{xx}(1) = -\frac{\pi\lambda\alpha^2|S(0)|^2}{(\Delta E)^2}\{2P_{YBSA}P_{YBZB}P_{ZBSA}$$

$$-P_{YBSA}^2P_{ZBZB} - P_{ZBSA}^2P_{YBYB} + P_{YBSA}^2 + P_{ZBSA}^2\}.$$

(IV-6)

References

1) W. G. Schneider, H.J. Bernstein, and J. A. Pople, J. Chem. phys., 28, 601 (1958).

2) H. Spiesecke and W. G. Schneider, J. Chem. phys., 35, 722 (1961).

3) Emsley, Feeny, and Sutcliffe, High-resolution NMR Spectroscopy II, Pergamon, New York, (1966).

4) N. F. Ramsey, phys. Rev., 78, 699 (1950).

5) N. F. Ramsey, phys. Rev., 86, 243 (1952).

6) C. P. Slichter, Principle of Magnetic Resonance, p.114, Harper and Row, New York, (1963).

7) N. Nakagawa, S. Shinada and S. Obinata, The 6th NMR Symposium, p.8, Kyoto, (1967).

8) Y. Nomura, Y. Takeuchi, and N. Nakagawa, Tetrahedron Letters, 8, 639 (1969).

9) C. C. J. Roothaan, Revs. Modern phys., 23, 69 (1951).

10) T. Yonezawa, H. Konishi and H. Kato, Bull. Chem. Soc.,Japan, 42, 933 (1969).

11) H. F. Hameka, Mol. phys. 2, 64 (1959).

12) J. I. Musher, J. Chem. phys., 40, 2399 (1964).

13) A. M. Karo and L. C. Allen, J. Amer. Chem. Soc., 80, 4496 (1958).

14) K. Kimura, and S. Nagakura, Spectrochimica Acta, 17, 166 (1961).

15) The effect of interaction on the anisotropy of ^{13}C chemical shift for CH_3I has been studied experimentally and theoretically (I.Morishima, A.Mizuno and T.Yonezawa, Chem.Phys.Letters, in press).

Chapter 3. Conclusion

In Part I of this thesis the theory on the nuclear shielding constant is studied by using the third-order perturbation method involving into the spin-orbit interaction.

In Chapter 2, the new typed expression of the shielding constant including the LS interaction is presented to explain the abnormal upfield trend of the chemical shift for the nucleus bonded to the heavy atom. In Chapter 2-3, as the application of this theory, the proton chemical shift for the hydrogen halides was calculated in detail. The numerical calculations using semi-empirical SCF wavefunctions gave substantial contribution(51 %) of this shielding effect(σ_{LS}) to the total shielding of the hydrogen iodide. Therefore, it is emphasized that the σ_{LS} term cannot be ignored in comparison with σ_{para}, and has an important contribution to the abnormal upfield trend of the proton chemical shift in hydrogen halides. In Chapter 2-4 the author described the expression for the new type with the average excitation energy approximation. This simplified expression enables us to clear the physical image for the heavy atom effect on the shielding constant. Thus, from this expression, it is shown that the LS shift arises on the neighboring atom through Fermi contact interaction of a nucleus with electrons.

PART II

THE INTERACTION BETWEEN THE CLOSED- AND OPEN-SHELL MOLECULES BY NMR CONTACT SHIFT

Chapter I Introduction

Fifty years ago Latimar and Rodebeesh showed that the great usefulness of the concept of the hydrogen-bond in explaining many physical properties of substances containing hydrogen atoms attached to electronegative atoms. Since that time more and more application of the hydrogen-bond have been made, and more and more has been learned about the nature of hydrogen-bond. A great majority of phenomena connected with the hydrogen-bond can be interpreted if this bond is considered as describing an interaction in which the electro-static charge-migration as well as the short-range repulsion effects are simultaneously important. The fundamental similarity between the hydrogen-bond and charge-transfer(or covalent bond) interaction has been emphasized. Recently MO theoretical studies have been performed for various hydrogen-bond systems. Nonempirical and semi-empirical SCF MO calculations have been proved to be successful in producing hydrogen-bond energies, charge distributions and most stable conformations. All these studies are associated with closed-shell molecules.

In this thesis the author is concerned with the hydrogen-bond between closed and open-shell molecules which has been studied experimentally and theoretically. Here he describes the results of n m r contact shifts and MO theoretical studies for the hydrogen bonding in the proton-donor molecules/nitroxide radical system in view of static(time average) field.

In Chapter 2 (published in Journal of the American Chemical Society, 93, 2048(1971), Chemical Physics letters, 9, 143(1971), ibid, 9, 203(1971) and Journal of the Chemical physics, in press (1973)),

the molecular interaction between a nitroxide radical and the proton-donor molecules is studied by the n m r contact shift measurements and molecular orbital calculations. In section 1, it is shown that the donor molecules induced by the hydrogen-bond with nitroxide radical yield fruitful information on the nature of the hydrogen-bond with the free radical. In section-2 the author mentions a correlation between ^{13}C contact shifts and ^{13}C-H nuclear spin coupling constants. This correlation is explained in terms of finite perturbation theory of nuclear spin coupling constants in which the ^{13}C-H coupling constant is related to the electron spin density on the ^{13}C nucleus induced when spin density is placed finitely on the proton. The potential utility of the relation in the prediction of sign and magnitude of long-range ^{13}C-H coupling constants is also stated.

In section 3 SCF molecular orbital calculations using INDO method are performed for dimethyl nitroxide(DMNO) methanol and DMNO-acetylene hydrogen-bond systems. Negative spin density of the hydroxyl proton of methanol which has been confirmed by our provious n m r studies is reproduced only for the model where the hydroxyl proton is placed directly over the oxygen p-πorbital.

In section 4 ^{1}H and ^{13}C Fermi contact shifts induced by the hydrogen-bond with DTBN radical are observed for various proton downfield ^{13}C contact shifts of the donor molecules are interpreted in terms of the spin polarization mechanism of electron spin transfer from DTBN to the protic substances. The formation constants, enthalpies, limiting ^{1}H and ^{13}C contact shifts and spin densities on the H and C atoms are also determined for the proton-donor/DTBN hydrogen-bond interaction from ^{1}H and ^{13}C contact shift measurements at various temperatures. The theoretical studies of this closed -

and open-shell bimolecular system are performed by unrestricted Hartree-Fock SCF MO(INDO method) calculations.

In chaper 3, as a part of these continuing studies on the interaction between closed and open-shell molecules, (Chemical Physics Letters, 14, 372(1972), Journal of the American Chemical Society, 94, 4812(1972) the author performs ^{13}C n m r. contact shift study of the electron donor-accepton interaction between halogenated molecules and the nitroxide radical. ^{13}C n m r contact shifts induced by the addition of DTBN radical are observed for holomethanes, haloethanes, and halobenzenes. These results are interpreted in terms of the charge-transfer interaction between the DTBN radical and halogenated molecules in the manner of C-X DTBN interaction. Approximate values of the formation constants, enthalpies, limiting ^{13}C contact shifts, and spin densities on the carbon are determined for this C T Complex formation.

Theoretical studies on this interaction system are also performed by the unrestricted Hartree-Fock SCF-MO(INDO method) calculations. The stabilization energies and spin densities on the acceptor carbon are well reproduced by the MO calculation. In the basis of the present experimental and theoretical studies the mechanism of halogen abstraction reaction is discussed briefly.

Chapter 2. The Interaction between the Proton Donor Molecules and a Nitroxide Radical.

Section 1. ^{1}H and ^{13}C Contact Shift of Protic Molecules in Presence of the Nitroxide Radical.

Studies on Nuclear Magnetic Resonance Contact Shifts Induced by Hydrogen Bonding with Organic Radicals. I. ^1H and ^{13}C Contact Shifts of Protic Molecules in the Presence of the Nitroxide Radical

Sir:

During the last 20 years considerable interest has been manifested in the study of the hydrogen bond (H bond).[1] A great majority of phenomena connected with the H bond can be explained if this bond is considered as describing an interaction in which the electrostatic charge-migration (covalent bond) as well as the short-range repulsion effects are simultaneously important. The fundamental similarity between the H-bond and charge-migration (or charge-transfer or co-covalent bond) interaction has been emphasized.[1c] Recently MO theoretical studies have been performed for various H-bond systems and proved to be successful in producing H-bond energies, charge distributions, and most stable conformations.[2] All these studies are associated with closed-shell molecules. In the present work we are concerned with the H bond between closed-shell and open-shell molecules which has been studied less experimentally and theoretically. We wish to report here preliminary results of nmr contact-shift and MO theoretical studies for the H bonding in the protic molecule–nitroxide radical system.[3]

In order to assess the importance of covalent bonding in the XH···Y H-bonding system, we have studied proton and ^{13}C contact shifts for various proton donor molecules, XH, induced by the presence of di-*tert*-butyl nitroxide (DTBN), the proton acceptor. We have also carried out unrestricted Hartree–Fock (UHF) calculations using Pople's INDO method[4] for the above H-bond system to substantiate the observed contact shifts. The observation of the XH proton contact shift is expected to reflect directly the electron spin density transferred through the H bond from DTBN. This H-bond contact shift will serve as a measure of covalent character or strength of the XH···Y H-bond interaction. In addition, the contact shifts for other protons and carbons in the XH molecule will allow us to see the mode of electron spin distribution in the XH molecule.

We have observed the effect on ^1H and ^{13}C resonance positions of several XH molecules upon addition of increasing amounts of DTBN.[5] The hydroxyl proton of methanol, for example, in CCl_4 experienced an upfield shift and broadening when a small amount of DTBN was added, while methyl protons were almost unaffected. This upfield shift is proportional to the concentration of added DTBN and is more pronounced for a more acidic XH proton such as in phenol. The observed upfield shifts of the XH proton in the various proton donor molecules are plotted against the DTBN concentration (Figure 1).[6]

The upfield shift is most likely caused by the Fermi contact interaction for the XH proton of that fraction of the XH molecule which is specifically H bonded to DTBN. We have also examined the temperature dependence of this upfield shift. The resulting linear dependence of the shift on $1/T$ (Curie law behavior) may be characteristic of the contact shift.[7,8]

(1) (a) G. Pimentel and A. L. McClellan, "The Hydrogen Bond," W. H. Freeman, San Francisco, Calif., 1960; (b) D. Hadzi, Ed., "Hydrogen Bonding," Pergamon Press, Oxford, 1959; (c) S. Bratoz, *Advan. Quantum Chem.*, 3, 209 (1966).

(2) K. Morokuma, H. Kato, T. Yonezawa, and K. Fukui, *Bull. Chem. Soc. Jap.*, 38, 1263 (1965); K. Morokuma and L. Pederson, *J. Chem. Phys.*, 48, 3275 (1968); P. Kollman and L. C. Allen, *ibid.*, 51, 3286 (1969); A. S. N. Murthy and C. N. R. Rao, *Chem. Phys., Lett.*, 2, 123 (1968); W. Adam, A. Grimison, R. Hoffmann, and G. Zuazaga de Ortiz, *J. Amer. Chem. Soc.*, 90, 1509 (1968), and other recent papers.

(3) To our knowledge, study of the nmr contact shifts of solvent molecules in the presence of organic radicals has been quite limited [see N. A. Sysoeva, A. U. Stepanyants, and A. L. Buchachenko, *Zh. Strukt. Khim.*, 9, 311 (1968)]. Very recently, de Boer, *et al.*, have reported contact shift data for the solvent molecule (tetrahydrofuran) dissolving radical anions: E. de Boer, A. M. Grotens, and J. Smid, *J. Amer. Chem. Soc.*, 92, 4742 (1970); *Chem. Commun.*, 1035 (1970).

(4) J. A. Pople, D. L. Beveridge, and P. A. Dobosh, *ibid.*, 90, 4201 (1968).

(5) Pmr spectra were obtained at various temperatures on a Jeolco high-resolution nmr spectrometer (60 MHz) using TMS as an internal standard. The concentration of all XH molecules was 2.5×10^{-3} *M* in CCl_4 solution. To this solution, DTBN was added drop by drop (from 3.3×10^{-5} to 16.5×10^{-5} *M*) until the XH proton signal was too broad to be observed. Natural-abundance ^{13}C nmr spectra were recorded with a Jeolco C-60HL spectrometer (15.1 MHz) using a complete proton-decoupling technique.

(6) Since the exchange of the proton donor molecules between H-bonded and nonbonded sites is rapid on the nmr time scale, the spectra are time averaged, the various proton resonances being shifted from their normal diamagnetic values by an amount which is proportional to the concentration of the H-bonded species. Thus as DTBN is added, the proton resonances of the XH molecule shift toward the resonance position of the H-bonded species. The relative values of this shift for various XH molecules are of significance in the present study. The relative values of the slope in the linear relation for various XH molecules may approximately correspond to the relative H-bonding contact shifts in this labile molecular interaction.

(7) This temperature dependence of the shift is, of course, partly caused by the temperature dependence of the equilibrium of the H-bond interaction.

(8) In the diamagnetic solution, the XH proton signal is displaced to lower field by H bonding;[1a,b] this usual downfield shift and upfield contact shift occur simultaneously for the present H-bond systems. However, the contact shift appears to be predominant in the observed DTBN-induced shift; addition of a diamagnetic proton acceptor, in place of DTBN, to the solution of the XH molecule had no substantial effect on the XH proton shift. Therefore, DTBN-induced upfield shifts strongly suggest negative electron spin density on the XH proton induced by H bonding with DTBN, although the apparent values of the relative shifts obtained from Figure 1 are not quantitatively related to the relative values of the induced spin densities.

Inspection of Figure 1 shows that H-bonding contact shifts fall generally in the order of proton-donating ability of the X–H group, which is well established[1a,b] by various spectroscopic methods. However, it is interesting to note that the C–H proton in chloroform experiences a substantial contact shift, comparable with that for other more acidic O–H groups. The acid strength determined by ir spectroscopy (the shift of the X–H stretching frequency) is in the order acetic acid > phenol > methanol > amine > chloroform.[1a,9a] Therefore, the large contact shift for chloroform appears to imply that the covalent character in the H bond is quite large for the C–H group, as compared with the N–H and O–H groups.[9b,10] This is also seen in the sizable contact shift for the acetylenic proton in phenylacetylene in comparison with diethylamine.[9b,12] Another feature apparent from the data in Figure 1 is the unexpectedly small contact shift for acetic acid. This may be due to the self-association (dimer formation) of acetic acid, which is less sensitive to the H bond.

In order to look at the manner of electron spin distribution on the various parts of XH molecule, we have observed ^{13}C contact shifts for $CHCl_3$, CH_2Cl_2, CH_3OH, and $C_6H_5C{\equiv}CH$ as well as proton shifts induced by the presence of DTBN (Table I).[13] Addition of DTBN

Table I. Proton and Carbon Contact Shifts and Spin Densities Induced by Hydrogen Bonding with DTBN

Molecule	Nucleus	Obsd contact shift[a] Obsd, ppm	Rel value	Rel spin density
	OH	+1.12	+1.00	−1.00
CH_3OH	CH_3	−0.23	−0.205	+0.205
	^{13}C	−1.0	−0.893	+0.148
$CHCl_3$	H	+0.69	+1.00	−1.00
	^{13}C	−9.4	−13.6	−2.31
CH_2Cl_2	H	+0.20	+1.00	−1.00
	^{13}C	−2.4	−12.0	+1.99
$C_6H_5C_2{\equiv}C_1H$	H	+0.15	+1.00	−1.00
	$^{13}C_1$	−2.21	−14.7	−2.44
	$^{13}C_2$	−0.40	−2.65	−0.44

[a] Measured as neat liquid in the presence or absence of DTBN (1×10^{-4} *M*).

shifts the ^{13}C resonances of these molecules to lower field, indicating positive spin density on the carbon. This ^{13}C downfield shift for $CHCl_3$, CH_2Cl_2, and $C_6H_5C{\equiv}CH$ is more pronounced in its magnitude than are

(9) (a) This order of acid strength determined by the ir frequency shift corresponds to that of the H-bond energy (see C. A. Coulson, "Valence," Oxford University Press, London, 1961); (b) the apparent contact shifts are affected by the shift of the H-bonded species and by the equilibrium constant. Therefore, one should not take the observed shift as the shift directly proportional to the H-bond contact shift. However, one may be allowed to take the relative value of the shifts as proportional to the H-bond shift.

(10) The contribution of the covalent bond structure in the XH···Y H-bond system has been theoretically shown to be 6% at most for the OH···O system.[1c,11] The above finding would be acceptable if the covalent bond contribution in the CH···O system is more important than in the OH···O and the NH···O systems.

(11) C. A. Coulson and V. Danielson, *Ark. Fys.*, 8, 239, 245 (1954).

(12) Although the concomitant downfield shift of the XH proton due to H-bond formation is considered to reduce the apparent upfield contact shift, particularly for protons more acidic than C–H protons, the contribution of this downfield shift is minor, as evidenced by the diamagnetic solution with corresponding concentration of the diamagnetic proton acceptor such as trimethylamine oxide or dimethyl sulfoxide.

(13) In order to obtain the relative magnitudes of the ^1H and ^{13}C contact shifts (Table I), we have measured ^1H and ^{13}C spectra for neat liquids of these molecules in the absence or presence of DTBN.

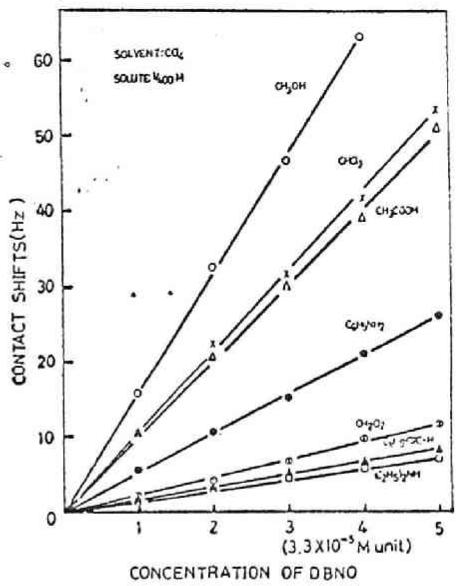

Figure 1. Plots of the proton shift induced by di-*tert*-butyl nitroxide (DBNO) *vs.* concentration of DBNO for various protic substances. The solute concentration is 2.5×10^{-2} *M* in CCl_4.

the proton contact shifts in these molecules. This ^{13}C shift is evidently due to the Fermi contact interaction, not to the effect of bulk susceptibility. This is apparent from the fact that the phenyl ring carbons in phenylacetylene are hardly affected by the addition of DTBN. It should also be noted that the addition of the diamagnetic proton acceptor does not change the ^{13}C shift.

The relative contact shifts ($\Delta\delta_C/\Delta\delta_H$) of the proton and ^{13}C are related to the relative value of the spin densities (ρ_{SC}/ρ_{SH}) on the proton 1s and the carbon 2s atomic orbitals by the relation

$$\frac{\rho_{SC}}{\rho_{SH}} = \frac{|\phi_{SH}(\gamma_H)|^2}{|\phi_{SC}(\gamma_C)|^2}\frac{\Delta\delta_C}{\Delta\delta_H}$$

where $|\phi_{SN}(\gamma_N)|^2$ is the square of the 1s or 2s atomic orbital at the nucleus N.[4] The relative spin densities obtained by this relation are also given in Table I. Nonlocal distribution of the spin densities on the proton and carbon atoms is clearly seen.

In order to substantiate the observed ^1H and ^{13}C contact shifts, INDO calculations were performed for dimethyl nitroxide (DMN)–methanol and DMN–acetylene systems. We assumed that the nitrogen, oxygen, and carbon atoms in DMN were coplanar. The bond distances used are NO, 1.215 and NC, 1.550 Å and the CNC bond angle is assumed to be 120°. The corresponding values for donor molecules methanol and acetylene were obtained from Sutton's compilation.[14] The geometrical structures for the H-bond system adopted here are the π and σ type, where the XH proton is directly over the p_π orbital of the oxygen atom with the X–H bond axis perpendicular to the N–O bond and in the σ plane, respectively. The spin densities calculated for each H-bond model were obtained for the structure with energy optimization. The results are summarized in Table II. The experimental trend of the induced spin densities on the ^1H and ^{13}C nuclei is well reproduced only for the π model both for DMN–methanol and DMN–acetylene systems. The σ model fails to explain the observed ^1H and ^{13}C contact shifts in these

(14) L. E. Sutton, Ed., *Chem. Soc., Spec. Publ.*, No. 11 (1958).

Table II. Results of INDO Calculations for Proton Donor...Nitroxide Systems

Proton donor	$R_{O\cdots H_1}$[a] (Å)		Calcd spin densities[b] and stabilization energies[c] π model	σ model[d]
Methanol	1.50	ρ_{OH}	−0.016	0.002
		ρ_C	0.000	0.000
		ΔE, kcal/mol[e]	8.87	10.10
Acetylene	1.75	ρ_{H_1}	−0.010	0.002
		ρ_{C_2}	0.008	−0.002
		ρ_{C_1}	0.000	0.000
		ρ_{H_4}	0.001	0.000
		ΔE, kcal/mol[e]	1.29	1.20

[a] Obtained by energy optimization. [b] Spin densities on the hydrogen 1s and carbon 2s atomic orbitals. [c] Energy differences between two conformations for finite and infinite separations of proton donor and dimethyl nitroxide. [d] Calculated for the model where ∠NOH = 120°. [e] Numbering of the atoms: $(CH_3)_2N-O\cdots H_1-C_2\equiv C_1-H_4$.

two systems; the downfield ^{13}C contact shifts in two acetylenic carbons (C_1 and C_2) require the π model.

The appearance of negative and positive spin densities in the C–H group can be explained by a spin polarization mechanism. Because positive spin density is residing on the oxygen p_π orbital, the transfer process will preferentially involve an electron in the O···H bond with a spin antiparallel to that of the oxygen electron. This results in a slight excess of positive electron spin density on another site (carbon) of the C–H bond, leading to a slight amount of unpairing of the electrons in the C–H bond. This may also be the case for other XH···DTBN systems. As is inferred from the above discussion, polarization of electron spins may propagate through the bonds and induce positive or negative spin density on the various parts of the XH molecule. Therefore, the way in which electron spin distributes itself in XH molecules is expected to follow the trend of nuclear spin coupling constants. The relative ^{13}C contact shift, *i.e.*, the relative spin densities, for acetylenic carbons (C_1 and C_2) in phenylacetylene (ρ_{C_2}/ρ_{C_1} = 0.18) is well correlated with the relative values of the $^{13}C_1-H$ and $^{13}C_2\equiv C_1-H$ nuclear spin coupling constants ($J_{C_1\equiv C-H}/J_{C_1-H}$ = +251/+49 = 0.20). This correlation appears to hold for the trend in the directly bonded $^{13}C-H$ coupling constants in $CHCl_3$, CH_2Cl_2, and $C_6H_5C\equiv CH$.[15]

This nonlocal distribution of electron spin density is also seen in the stereospecific proton contact shifts for various protons in the XH molecules. We have examined the proton nmr spectrum of 4-methylpiperidine, for example, in the presence of DTBN. Quite different values of the downfield contact shifts for α-axial and α-equatorial protons were observed, while the NH proton exhibited a pronounced upfield shift. The observation of a greater downfield contact shift for an α-axial proton than for an equatorial one ($\Delta\delta_{ax}/\Delta\delta_{eq}$ = 5) is in accord with the conformation of the N–H group located preferentially at the axial position,[16] in which these protons are separated by the "zig-zag" route, the favorable arrangement for electron spin distribution and nuclear spin coupling.[17]

From the present work we can conclude that the contact shifts induced by H bonding between protic substances and the nitroxide radical serve as a sensitive probe for elucidation of the covalent character of the H bond and of the mode of electron spin distribution on the proton donor molecules. Further theoretical studies on this H-bonding system will appear elsewhere.[18]

(15) I. Morishima, K. Endo, and T. Yonezawa, *Chem. Phys. Lett.*, in press.
(16) T. Yonezawa, I. Morishima, and Y. Ohmori, *J. Amer. Chem. Soc.*, 92, 1267 (1970); I. Morishima, K. Okada, M. Ohashi, and T. Yonezawa, *Chem. Commun.*, 33 (1971).
(17) I. Morishima and T. Yonezawa, *J. Chem. Phys.*, in press.
(18) I. Morishima, K. Endo, and T. Yonezawa, *Chem. Phys. Lett.*, in press.

Chapter 2

Section 2 A Correlation between ^{13}C Contact Shifts Induced by ^{13}C-H...Nitroxide Hydrogen Bond and ^{13}C-H Nuclear Spin Coupling Constants

STUDIES ON THE NMR CONTACT SHIFTS INDUCED BY HYDROGEN BONDING WITH NITROXIDE RADICAL. A CORRELATION BETWEEN ^{13}C CONTACT SHIFTS INDUCED BY ^{13}C-H... NITROXIDE HYDROGEN BOND AND ^{13}C-H NUCLEAR SPIN COUPLING CONSTANTS

^{1}H and ^{13}C NMR contact shifts have been observed for chloroform, methylene chloride and phenylacetylene in the presence of di-tertbutyl nitroxide radical (DBNO). Upfield and downfield contact shifts were observed for ^{1}H and ^{13}C NMR resonances, respectively. The relative values of ^{13}C contact shifts with respect to ^{1}H contact shifts are linearly correlated with directly bonded ^{13}C-H spin coupling constants. This correlation is interpreted in terms of finite perturbation theory of nuclear spin coupling constants in which the ^{13}C-H coupling constant is related to the electron spin density on the ^{13}C nucleus induced when spin density is placed finitely on the proton. The potential utility of this relation in the prediction of sign and magnitude of long-range ^{13}C-H coupling constants is also stated.

In previous papers [1,2] we have reported the results of proton contact shifts for a variety of the proton donor molecules, XH, induced by the presence of stable radical, di-tert-butyl nitroxide (DBNO), which serves as the proton acceptor, Y, and stressed the importance of the covalent effect in the XH... Y hydrogen bonding. The observation of the XH proton contact shift presents direct evidence of the covalent character of the XH... Y hydrogen bond which induces electron spin density on the XH proton interacting with DBNO [1]*. The observed negative spin density (i.e., upfield contact shifts) on the XH proton is most likely due to the spin polarization mechanism. The induced negative spin density on the XH proton propagates through the bonds on the various nuclei in the XH molecule [2]. The modes of spin distribution through various types of σ-bonds can thus be detected from the NMR contact shift measurements. Such contact shifts have been shown to have a potential utility in the studies of electronic and geometrical structures of the XH molecule [2].

In the present work, we have examined ^{13}C contact shifts induced by the ^{13}C-H... DBNO hydrogen bond and we wish to report a correlation between ^{13}C contact shifts and ^{13}C-H nuclear spin coupling constants. It has been well established that the C-H group serves as a proton donor in the hydrogen bond interaction. The observed upfield (^{1}H) and downfield (^{13}C) contact shifts show that the hydrogen bond between C-H bond and DBNO induces negative and positive spin densities on the proton and ^{13}C of the C-H bond, respectively. Since the mode of electron spin distribution appears to be associated with that of nuclear spin coupling, the relative value of ^{13}C contact shifts with respect to the C-H proton is expected to be correlated to ^{13}C-H nuclear spin coupling constants. Here we have examined this idea for chloroform ($CHCl_3$),

* In the diamagnetic solution, the XH proton in the proton donor molecule experiences a downfield shift by hydrogen bonding. In this paramagnetic solution, this usual downfield shift and the upfield contact shift occur simultaneously. However, the contact shift appears to be predominant in the observed DBNO-induced shift. This has been also confirmed from the temperature dependence of the XH upfield shift. The resulting linear dependence of the shift on $1/T$ (Curie law behavior) may be characteristic of the contact shift which is related to the electron spin density.

methylene chloride (CH_2Cl_2) and phenylacetylene ($C_6H_5C \equiv CH$).

Proton and ^{13}C NMR spectra were obtained on a Jeol-3H-60HL spectrometer at 60MHz and 15.1 MHz respectively. ^{13}C NMR spectra were recorded with complete-proton decoupling technique using the external locking mode. Samples of the neat liquids in the absence and presence of DBNO were made in 5 mm tubes for ^1H NMR and in 8mm tubes for ^{13}C NMR in the same concentration of DBNO**. Since the exchange of the proton donor molecules between complexed (hydrogen bonded) and uncomplexed sites is rapid on the NMR time scale, the spectra are time-averaged, the various ^1H and ^{13}C resonances being shifted from their normal diamagnetic values by an amount which is proportional to the concentration of the hydrogen bonded species. Thus as DBNO is added to the proton donor molecule, the ^1H and ^{13}C resonances of the XH molecule shift toward the resonance positions of the hydrogen bonded species. Thus the ^1H and ^{13}C chemical shifts from the neat liquid to the paramagnetic solution containing a varying amount of DBNO were measured. The ^{13}C contact shifts relative to the ^1H contact shifts which are of significant use in this case were obtained from the slopes of linear plots of the ^1H and ^{13}C shifts versus concentration of added DBNO. The results were summarized in table 1. The relative contact shifts of the proton and $^{13}C(\Delta\delta_C/\Delta\delta_H)$ are related to the relative value of the spin densities (ρ_{SC}/ρ_{SH}) on the proton 1s and the carbon 2s atomic orbitals by the relation:

$$\frac{\rho_{SC}}{\rho_{SH}} = \frac{|\phi_{SH}(r_H)|^2}{|\phi_{SC}(r_C)|^2} \frac{\Delta\delta_C}{\Delta\delta_H},$$

where $|\phi_{SN}(r_N)|^2$ is the square of the 1s or 2s atomic orbital at the nucleus N [3]. The value of $|\phi_{SH}(r_H)|^2/|\phi_{SC}(r_C)|^2$ (=0.166) was taken from ref. [3]. The relative spin densities obtained by this relation are also given in table 1. The results are compared with ^{13}C-H spin coupling constants in table 1. The induced spin densities on ^{13}C nuclei in some molecules relative to $CHCl_3$ are in agreement with $J_{^{13}C-H}$ relative to $CHCl_3$.

The agreement between relative ^{13}C contact shifts induced by ^{13}C-H... DBNO hydrogen bonding and ^{13}C-H nuclear spin coupling constant may be interpreted in terms of Pople's finite perturbation theory (FPT) of the nuclear spin coupling constant [4, 5]. The FPT approach of ^{13}C-H spin coupling is based on the scheme that $J_{^{13}C-H}$ is proportional to the electron spin density induced on the ^{13}C nucleus when electron spin density is finitely placed on the H atom. This finite perturbation at the H atom possibly corresponds to the hydrogen bond interaction between the C-H proton and DBNO in which a small amount of electron spin is induced on the proton by the presence of DBNO. In order to substantiate the observed ^1H and ^{13}C contact shifts and the above treatment of correlation between contact shifts and nuclear spin coupling constant, we have carried out molecular orbital calculations of electron spin densities for the C-H... DBNO hydrogen bonded system

** The concentration of DBNO ranges from 1×10^{-4}M to 1×10^{-3}M. The absolute shifts were -0.2 to -0.5ppm for the proton resonances and 1 to 10ppm for ^{13}C resonances.

Table 1
Proton and ^{13}C contact shifts induced by C-H... DBNO hydrogen bond and ^{13}C-H nuclear spin coupling constants

Molecule	Nucleus	Contact shifts relative to H shifts	Spin density		$J_{^{13}C-H}$	
			relative to H	relative to ^{13}C in $CHCl_3$	Obs (Hz)	Relative value
$CHCl_3$	H	+ 1.00	-1.00			
	^{13}C	-13.6	+2.26	1.00	209 [a]	1.00
CH_2Cl_2	H	+ 1.00	-1.00			
	^{13}C	-12.0	1.99	0.88	178	0.85
C_6H_5-$C_2\equiv C_1$-H	H	+ 1.00	-1.00			
	$^{13}C_1$	-14.7	+2.44	1.08	+251 [b]	1.20
	$^{13}C_2$	- 2.65	+0.44	0.19	+ 49 [b]	0.24

a) Ref. [7].
b) For the values for acetylene, see ref. [8].

Table 2
Induced spin densities for acetylene-DBNO hydrogen bonding system

Structure of hydrogen bond	$R_{O\ldots H}$ (Å)	Calculated spin densities [a]				Total energy (eV)
		ρ_{H_1}	ρ_{C_2}	ρ_{C_3}	ρ_{H_4}	
π-model	1.50	-0.0102	0.0082	0.0013	0.0013	-1682.322
	1.75	-0.0030	0.0021	0	0.0003	-1682.487
σ-model [b]	1.50	0.0023	-0.0021	-0.0001	-0.0003	-1682.357

a) The numbering for acetylene: $\geq$N-O... H-C $\equiv$ C-H.
1 2 3 4

b) Calculated for the model of N-O...H bond angle = 120°.

using Pople's INDO-UHF (unrestricted Hartree-Fock) method [3]. The INDO calculation for DBNO shows that most of the spin density is placed on the oxygen p_π orbital. The negative spin density on the C-H proton was reproduced only for the π-model of the C-H...DBNO system in which the C-H group is directly over the oxygen atom of the N-O bond with the C-H axis perpendicular to the N-O bond (see table 2). In the π-model (fig. 1) the observed trend of ^{13}C contact shifts for phenylacetylene is also reproduced although the calculated spin densities on the carbon 2s atomic orbital is too small (table 2).

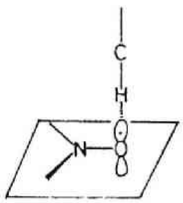

Fig. 1. π-model of the C-H...DBNO hydrogen bond system.

The other possible geometries of the C-H... DBNO system, such as the σ model in which the C-H proton approach the oxygen lone-pair in the σ plane, were ruled out because positive spin densities are always induced on the C-H proton in this model. The positive spin density on the p_π orbital of the oxygen atom polarize the paired electron of the C-H bond and induces negative spin density on the H atom, resulting in the appearance of the positive spin density on the carbon of the C-H bond. Therefore, the spin polarization mechanism plays an important role in the distribution of electron spin densities in the donor molecule. This is a reason for linear correlation between ^{13}C contact shifts and ^{13}C-H nuclear spin coupling through one or two bonds. Since the negative spin density is placed on the C-H proton, the site where the finite perturbation is taking place, the positive (negative) spin density induced on the other nucleus, X, corresponds to the positive (negative) value of the X-H nuclear spin coupling constant. This relation also possibly holds for H-H and ^{13}C-H coupling in other protic molecules...DBNO hydrogen bond systems. From the observation of proton and ^{13}C contact shifts for the protic substances in the presence of DBNO, we are able to predict relative values of the H-H and ^{13}C-H nuclear spin coupling constants. This is particularly useful in the prediction of the long-range coupling constants (including the sign and magnitude). It is usually difficult to observe the nuclear spin coupling constant associated with the carboxyl, hydroxyl or amine proton, because these are highly protic and nuclear spin coupling is usually decoupled due to proton exchange. However, DBNO-induced contact shifts for these molecules are useful in the prediction of these coupling constants. An example is given here for methanol. The relative ^{13}C and proton contact shifts for the methyl group with respect to the hydroxyl proton are -0.21 and -0.89 which correspond to the relative spin densities of 0.205 and 0.148. Since the ratio of $J_{^{13}C\text{-}H}$ and J_{HH} values is related to the spin density on the carbon and proton s atomic orbitals,

$$\frac{J_{^{13}C\text{-}H}}{J_{H\text{-}H}} = \frac{\gamma_C}{\gamma_H} \frac{|\phi_{SC}(r_C)|^2 \rho_{SC}}{|\phi_{SH}(r_H)|^2 \rho_{SH}},$$

the H-H coupling constant can be estimated from the relative value of ρ_{SC} and ρ_{SH}. Comparison of this result with those in table 1 allows us to expect +16.4 Hz and +7.8 Hz for ^{13}C-O-H and H-C-O-H coupling constants. The latter is com-

parable with the observed value of 5.1 Hz [6]. The details on the MO theoretical studies for protic substances... DBNO hydrogen bond system and application of the present method to other coupling cases, such as H-H, ^{14}N-H, and long range ^{13}C-H couplings will be presented elsewhere.

REFERENCES

[1] I. Morishima, K. Endo and T. Yonezawa, Chem. Phys. Letters 9 (1971) 143.

[2] I. Morishima, K. Okada and T. Yonezawa, submitted for publication.

[3] J. A. Pople, D. L. Beveridge and P. A. Dobosh, J. Am. Chem. Soc. 90 (1968) 4201.

[4] J. A. Pople, J. W. McIver and N. S. Ostlund, Chem. Phys. Letters 1 (1967) 365.

[5] J. A. Pople, J. W. McIver and N. S. Ostlund, J. Chem. Phys. 49 (1968) 2965.

[6] E. Grunwald, C. F. Jumper and S. Meiboom, J. Am. Chem. Soc. 84 (1962) 4664.

[7] N. Muller and D. Pritchard, J. Chem. Phys. 31 (1959) 768.

[8] R. M. Lynden-Bell and N. Sheppard, Proc. Roy. Soc. A269 (1962) 385.

Chapter 2

Section 3. Molecular Orbital Studies of Hydrogen Bond and N M R Contact Shifts in Nitroxide Radical/Methanol System

MOLECULAR ORBITAL STUDIES OF HYDROGEN BOND AND NMR CONTACT SHIFTS IN NITROXIDE RADICAL/METHANOL SYSTEM

SCF molecular orbital calculations using INDO method have been performed for dimethyl nitroxide (DMNO)-methanol and DMNO-acetylene hydrogen bond systems. Negative spin density on the hydroxyl proton of methanol which has been confirmed by our previous NMR studies was reproduced only for the model where the hydroxyl proton is placed directly over the oxygen p-π orbital (π-hydrogen bonding). The stabilization energies for these open-shell electron systems were not so greatly different from those for usual closed-shell systems.

1. INTRODUCTION

Recently MO theoretical studies have been performed for various hydrogen bond systems [1]. Nonempirical and semi-empirical SCF calculations have been proved to be successful in producing hydrogen bond energies, charge distributions and most stable conformations. All these studies, however, have dealt with hydrogen bond for closed-shell molecules which have been well established experimentally. In the present work we are concerned with hydrogen bonding between closed- and open-shell molecules. Previously we have studued NMR contact shifts induced by hydrogen bonding with nitroxide radical [2]. This is an example of NMR study on hydrogen bond between closed- and open-shell molecules which affords direct informations on the electron spin densities transferred through hydrogen bonding from radical to a proton donor molecule. This contact shift study promises to offer fruitful informations on the nature and mode of hydrogen bond, particularly the covalency of hydrogen bond. This experimental work stimulated us to undertake a detailed theoretical study of nitroxide/methanol hydrogen bond system to understand the observed NMR contact shifts of methanol and to see hydrogen bond energies, charge distributions and conformations in this hydrogen bond system. There have been no MO theoretical studies on the hydrogen bond between closed- and open-shell molecules.

In the present communication we report preliminary results of unrestricted Hartree-Fock (UHF) calculations for dimethyl nitroxide (DMNO) radical/methanol hydrogen bond system. To search for the geometrical mode of this hydrogen bond system, calculated spin densities on the proton donor molecule for various molecular geometries were compared with the experimental results. The stabilization energy was also compared with that for usual closed molecular system.

2. RESULTS

All the calculations were carried out using Pople's INDO SCF MO method [3]. Bond lengths and angles for DMNO used in the calculations are NO, 1.215 Å, NC, 1.550 Å and $\angle$CNC, 120°. We assumed that the nitrogen, oxygen and carbon atoms were coplanar. The geometrical structures for hydrogen bond system adopted here are σ- and π-hydrogen bond. In the former the hydroxyl proton of methanol is directly over the p_π orbital of the oxygen atom in DMNO with the O-H bond axis perpendicular to the N-O bond. In the π-bridge model, the OH group is over the center of the N-O bond. In the σ-model the OH group is in the σ-plane with the angle (θ) between the N-O bond and the O. . . H-O axis being varied from 0°, 60° and 90° (see fig. 1). We then systematically varied the O-H. . . O length to obtain the geometry corresponding to the lowest energy of the system. Calculated spin densities on the s atomic orbitals and hyperfine

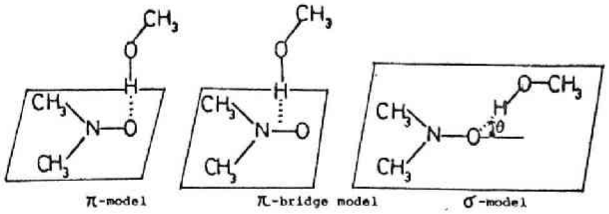

Fig. 1. Hydrogen bond models for DMNO/methanol system.

coupling constants for DMNO and DMNO/methanol hydrogen bond system are summarized in table 1. The table contains the results for π-model which is most probable in terms of induced spin density on the hydroxyl proton of methanol (vide infra). Spin densities induced on the methanol and stabilization energies for different hydrogen bond models are also given in table 1. The energy curves for approach of the methanol molecule to DMNO are given in figs. 2 - 4.

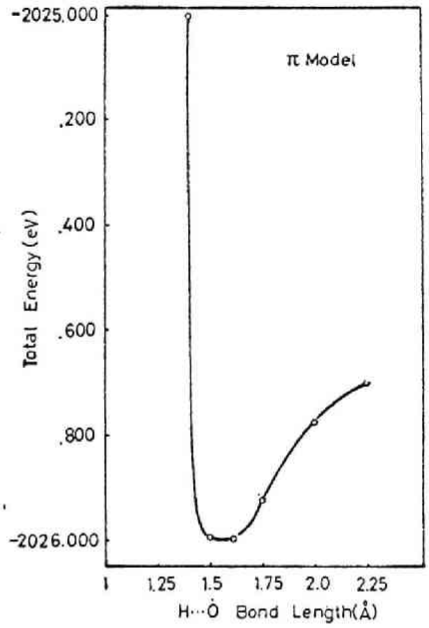

Fig. 2. Energy curve for the motion of the whole molecules in the π model.

3. DISCUSSION

INDO calculation for DMNO shows that most of the spin densities is in the p_π orbital on the oxygen (0.676) and on the nitrogen (0.302). As will be shown in what follows, this π spin density on the oxygen atom is the source of the spin density induced on the hydroxyl proton in the proton donor molecule. The calculated hyperfine coupling constants a_N for various nuclei in DMNO are summarized in table 2 and are compared with the observed results. Although the calculated results are uniformly smaller than the experimental ones, the experimental trend is well reproduced. Recent MO calculations for

Table 1
Stabilization energies and spin densities

Proton donor	Structure	$R_{O\cdots H}$ (Å) a)	Stabilization energy (kcal/mol)	Calculated spin densities on the proton and carbon			
				OH			
CH_3OH	π-model	1.50	8.87	-0.0155			
	π-bridge model	1.75	7.08	0.0030			
	σ-model (θ=60°)	1.50	10.10	0.0023			
	σ-model (θ=90°)	1.75 c)	(-8.58) c)	0.0008 c)			
	σ-model (θ=0°)	1.50	9.89	0.0036			
				H_1	C_2	C_3	H_4
C_2H_2 b)	π-model	1.75	1.29	-0.0030	0.0021	0.0000	0.0003
	σ-model (θ=60°)	1.50	0.81	0.0023	-0.0021	-0.0001	-0.0003

a) The value at energy minimum.
b) The numbering of the atom: $(CH_3)_2N\text{-}O\ldots H_1\text{-}C_2 \equiv C_3\text{-}H_4$.
c) The system is not stabilized for this model.

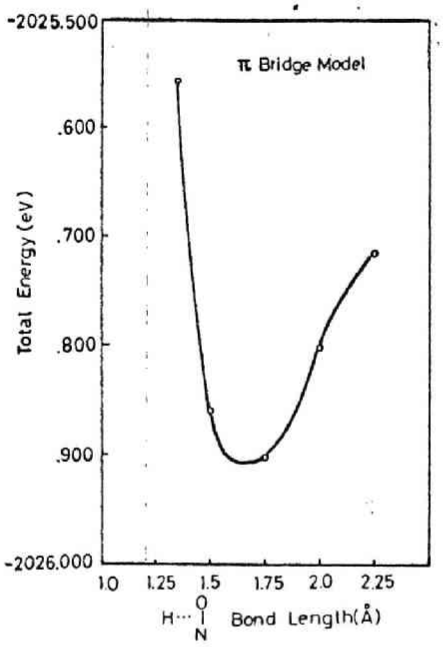

Fig. 3. Energy curve for the motion of the whole molecules in the π bridge model.

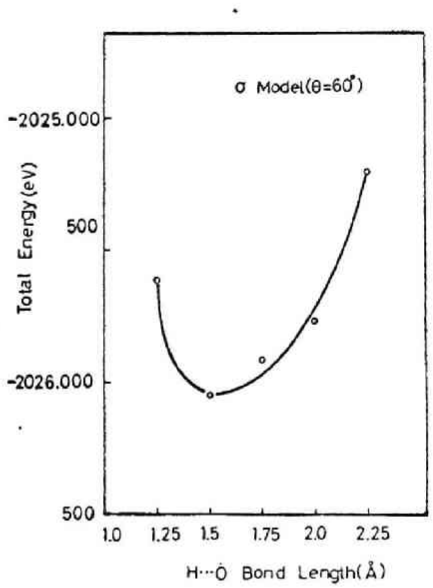

Fig. 4. Energy curve for the motion of the whole molecules in the σ model.

bis(trifluoromethyl) radical [7] and H_2NO [8] have shown that N-O and N-C (or N-H) bonds are not coplanar and deformation from coplanarity is accompanied by the increase of ^{14}N hyperfine coupling constant. This would be the case for DMNO. Our previous contact shift study [2] on on the di-tert-butylnitroxide/methanol hydrogen bond system has shown that the negative spin density (upfield contact shift) is induced on the methanol hydroxyl proton. Therefore, only the π model is justified on the basis of the spin density on the hydroxyl proton. The other models always yield positive spin density irrespective of the O. . . H-O bond length and are therefore ruled out (see table 1). In the σ-model (θ = 90°), the DMNO/methanol system was not stabilized for $R_{O...H}$ ranging 1.50 - 2.00 Å where the induced spin density on the hydroxyl proton was always positive. The π hydrogen bonding was further verified from comparison of the observed ^{13}C contact shifts [2] with the calculated spin densities on the carbon 2s AO's for nitroxide/phenylacetylene system, in which acetylenic proton serves as the proton donor site. The observed downfield ^{13}C contact shifts for both acetylenic carbons are substantiated by the

Table 2
Hyperfine coupling constants for DMNO and DMNO/methanol

Atom	DMNO			DMNO . . . methanol (π-model) [b]			
	Calc.		Obsd.	Calc.			Obsd.
	ρ_s	a_N [a] (G)	$\lvert a_N \rvert$ (G)	ρ_s	a_N [a] (G)	Δa_N [c] (G)	Δa_N [c] (G)
H	0.00838	4.52	12.3 [4]	0.00889	4.80	+0.28	-
^{13}C	-0.00620	- 5.08	6.1 [5]	-0.00646	- 5.29	-0.21	-
^{17}O	0.01232	10.95	19.7 [d]	0.01225	10.88	-0.07	-
^{14}N	0.01667	6.32	15.2 [4]	0.01827	6.93	+0.61	+1.00 [9]

a) Calculated by using proportional constants for each nucleus which relate spin density and hyperfine coupling constant (see ref. [3]).
b) The results for energy optimization.
c) Change of a_N by hydrogen bond.
d) The value for di-sec-butyl nitroxide, ref. [6].

INDO calculations for the π model of DMNO/acetylene hydrogen bond system (see table 1).

The appearance of negative spin density on the hydroxyl and acetylenic protons may be explained qualitatively by the spin polarization mechanism. Because the positive spin density is residing on the oxygen p_π orbital of DMNO, the spin transfer will preferentially involve an electron in the O... H-O bond with a spin antiparallel to that of the oxygen electron. This results in a slight amount of unpairing of the electrons in the X-H bond, leading to a slight excess of positive spin density on another site (X) of the X-H bond.

In table 2 are also given the calculated a_N values for DMNO in DMNO/methanol hydrogen bond system (π model). The variation of a_N values by hydrogen bonding also follows the experimental results for ^{14}N coupling constant [9].

The H... O bond length R for the most stable structure of π type interaction is 1.5 - 1.6 Å (see table 1), which is very close to the result for usual hydrogen bond system of the closed molecule [1]. The calculated value (8.9 kcal/mole) of the stabilization energy for the π-model is slightly less than that (10.1) for the σ model. These values appear to be not far from the hydrogen bond energy calculated for the closed-shell system [1], although the INDO method produces larger value of the hydrogen bond energy than the CNDO method, the currently well accepted method for the hydrogen bond system [1]. The change in charge distributions by hydrogen bond was also not so different from the closed shell system.

It could be concluded from this preliminary study that UHF calculations (INDO method) well explain the observed features of the NMR contact shifts induced by hydrogen bond with nitroxide radical. Extensions of the present theoretical study for other interaction systems including the organic radical are now in progress.

REFERENCES

[1] K. Morokuma, H. Kato, T. Yonezawa and K. Fukui, Bull. Chem. Soc. Japan 38 (1965) 1263;
K. Morokuma and L. Pederson, J. Chem. Phys. 48 (1968) 3275;
A. S. N. Murthy, R. E. Davis and C. N. R. Rao, Theoret. Chim. Acta 13 (1969) 81;
P. Koliman and L. C. Allen, J. Chem. Phys. 51 (1969) 3286.

[2] I. Morishima, K. Endo and T. Yonezawa, J. Am. Chem. Soc., submitted for publication.

[3] J. A. Pople, D. L. Beveridge and P. A. Dobosh, J. Chem. Phys. 47 (1967) 2026; J. Am. Chem. Soc. 90 (1968) 4201.

[4] J. Q. Adams, S. W. Nicksic and J. R. Thomas, J. Chem. Phys. 45 (1966) 654.

[5] G. Chapelet-Letourneux, cited in J. Douady et al., Mol. Phys. 17 (1969) 217.

[6] J. C. Baird, J. Chem. Phys. 37 (1962) 1879.

[7] G. R. Underwood and V. L. Vogel, Mol. Phys. 19 (1970) 621.

[8] A. W. Balloto and L. Burnell, J. Chem. Phys. 53 (1970) 333.

[9] T. Kawamura, S. Matsunami and T. Yonezawa, Bull. Chem. Soc. Japan 40 (1967) 1111.

Chapter 2

Section 4 ^{1}H and ^{13}C Contact Shifts and Molecular Orbital Studies on the Hydrogen Bond of Nitroxide Radical.

Interaction between Closed and Open-shell Molecules. VI. ^{1}H and ^{13}C Contact Shift and Molecular Orbital Studies on the Hydrogen Bond of Nitroxide Radical

Abstract: ^{1}H and ^{13}C Fermi Contact shifts induced by the hydrogen bond with di-tert-butyl nitroxide(DTBN) radical have been observed for various proton donor molecules(X-H). The upfield contact shifts of the X-H proton and downfield ^{13}C contact shifts of the donor molecules were interpreted in terms of the spin polarization mechanism of electron spin transfer from DTBN to X-H molecule. The formation constants, enthalpies, limiting ^{1}H and ^{13}C contact shifts and spin densities on the H and C atoms were also determined for the X-H....DTBN hydrogen bond interaction from ^{1}H and ^{13}C contact shift measurements at various temperatures. The theoretical studies on this closed and open-shell bimolecular system were also performed by unrestricted Hartree-Fock SCF MO(INDO method) calculations. The hydrogen bond energies and spin densities on the X-H molecules were well reproduced by the MO calculations.

The study of the interaction between closed and open-shell molecules would be of particular interest from experimental and theoretical points of view. As a part of our continuous investigation of this problem, we here report a full detail of the nuclear magnetic resonance(nmr) and molecular orbital(MO) theoretical studies of the H-bond(hydrogen bond) between a stable free radical(nitroxide radical) and various proton donor molecules.[1] Although the H-bond has been studied

$$X\text{-}H\ldots\ldots O\text{-}N(t\text{-}Bu)_2$$

spectroscopically and theoretically, there has been only a limited work on the H-bond of the free radical.[2] The study on the intermolecular interaction of the nitroxide radical has been made by the electron spin resonance(esr) method.[3] The esr method, however, can inform us of the change in the hyperfine coupling constant(i.e. electron spin density) or the g value of a free radical itself and gives no information on the electronic structure of the solvent molecule perturbed by the interaction with a free radical. The use of nmr contact shifts could be relevant to the investigation of electron spin distribution on the diamagnetic solvent molecule induced by the interaction with the radical The study of the mode of electron spin transfer from nitroxide radical to the proton donor molecule(X-H) might serve as an sensitive probe for elucidation of the nature of the H-bond. In this sense,

nitroxide radical-induced nmr contact shifts would be useful as a spin label in the study of the molecular interaction between closed and open-shell molecules. Here we have studied proton and ^{13}C contact shifts for various proton donor molecules induced by the addition of di-tert-butyl nitroxide(DTBN) radical, the proton acceptor. We have also carried out unrestricted Hartree-Fock(UHF) MO calculations for this H-bonded bimolecular system to substantiate theoretically observed contact shifts and H-bond energies.

Experimental Section

Materials. DTBN was prepared by referring Briere and Rassat.[4] All of the proton donor molecules used here were commertially available.

Nmr measurements. Proton nmr spectra were obtained at 60 MHz on a Jeolco 3H-60 spectrometer equipped with variable temperature assembly. TMS was used as an internal standard. Completely proton decoupled ^{13}C nmr spectra were obtained at 15.1 MHz on a Jeolco C-60HL spectrometer equipped with the SD-HC heterospin decoupler and IS-60 field/frequency synchronous sweep system of the proton irradiation frequency. Spectra were measured with the external locking mode at various temperatures. ^{13}C chemical shifts were determined on a expanded scale(18ppm per full scan) with the precision of $\pm$ 0.15 ppm. Samples were made in the neat or CCl_4 or C_6H_{12} solution in the absence or presence of varying amount of DTBN in 5 mm(for ^1H nmr) or in

Figure 1. Observed proton contact shifts (at 60 MHz) plotted against the concentration of added DTBN radical.

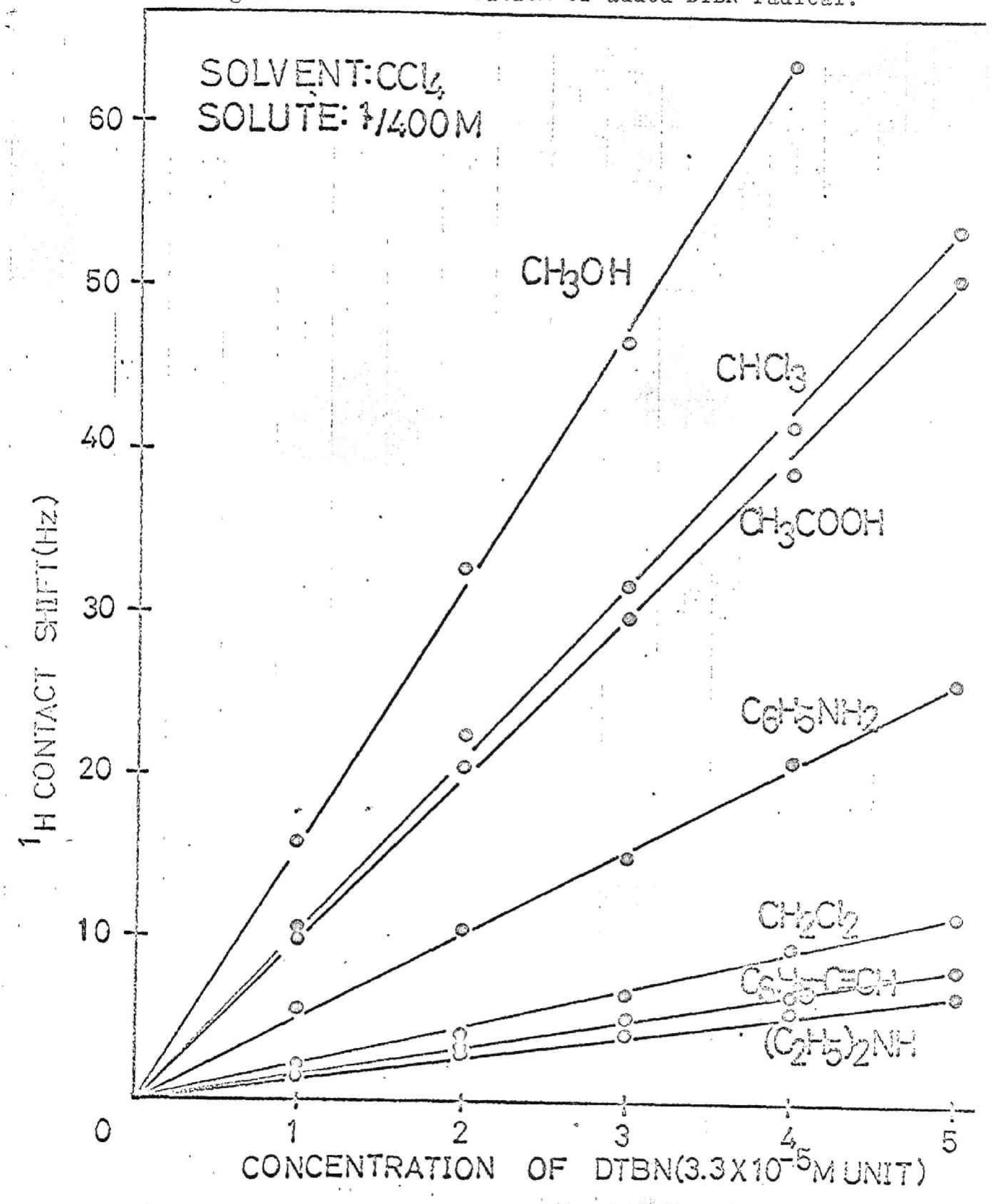

Figure 2. Curie law test of the proton contact shift for chloroform.

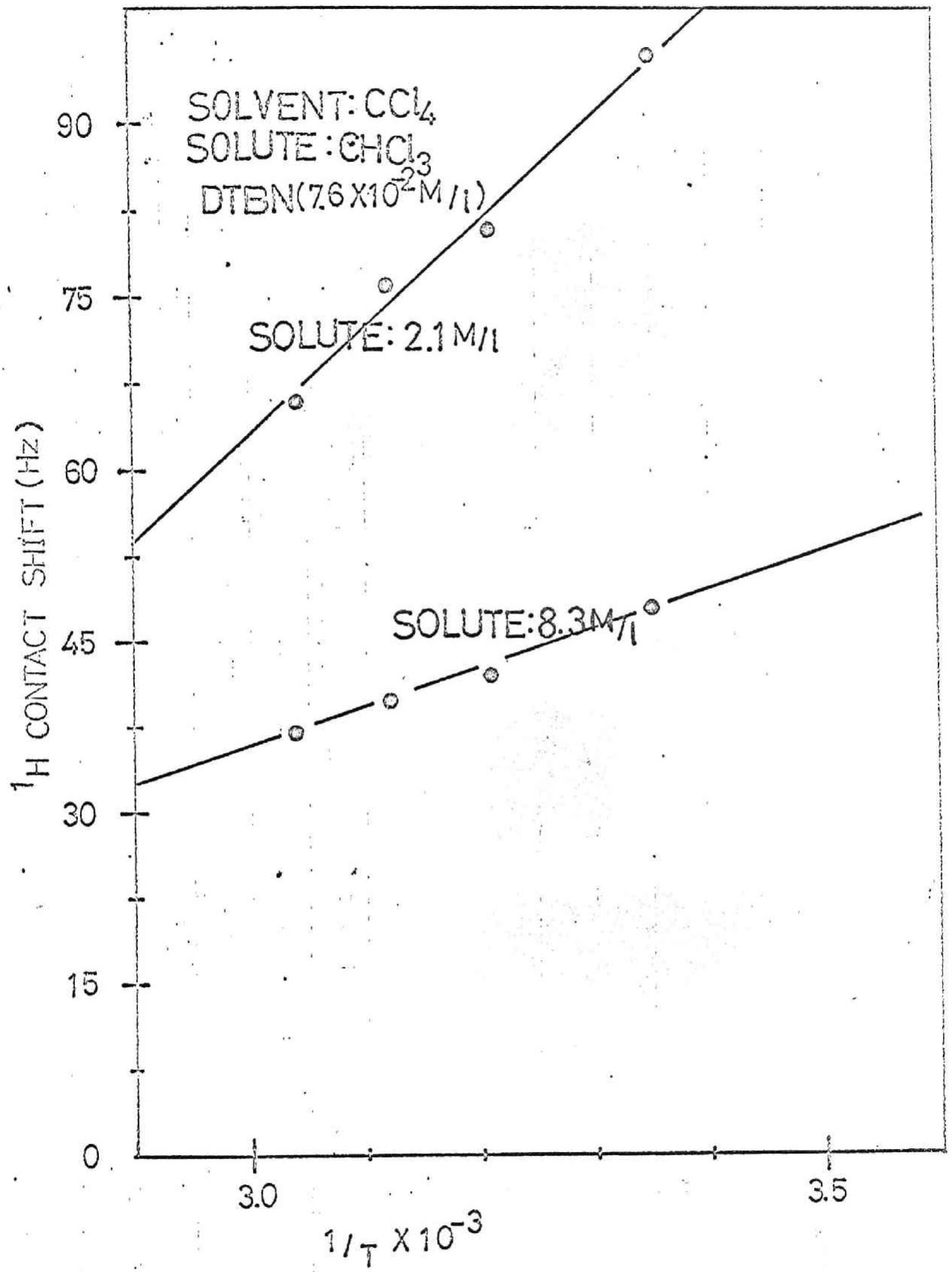

the 8 mm sample tube. The DTBN-induced ^{1}H and ^{13}C contact shifts are the shift change from the diamagnetic solution to the paramagnetic one in the presence of a given amount of DTBN radical.

Results

Proton Contact Shifts. Addition of DTBN radical to the protic molecules shifted quite sensitively the X-H proton to the higher field, to the extent which is proportional to the concentration of DTBN. This is shown in Figure 1 for various proton donor molecules. This DTBN-induced upfield shift followed the Curie law behavior as shown in Figure 2 for chloroform as an example. The upfield proton shift, contrary to the usual downfield shift encountered for the H-bond interaction between closed-shell molecules, is therefore attributable to the Fermi contact shift which is related to the hyperfine coupling constant, a_H, for the X-H proton by the relation [5]

$$\frac{\Delta H}{H} = -a_H \frac{\gamma_e g\beta S(S+1)}{\gamma_H 3kT} \qquad (1)$$

Here a_H is related to the electron spin density ρ_H on the proton by the equation

$$a_H = \frac{8\pi}{3} g\beta\gamma_H |\psi_H(0)|^2 \rho_H \qquad (2)$$

The notations have their usual meaning. [5]

The observed upfield shifts, characteristic of negative spin density on the proton, follows in general the trend of the proton donor ability of the X-H molecules.[1a] The hydroxyl proton of phenol experienced signal broadening and upfield contact shift quite rapidly with the addition of DTBN. Therefore, ^{1}H nmr was not adequate for the study of phenol-DTBN interaction. Thiol(RSH), the proton donor molecule, reacted rapidly with DTBN and was not suitable for the present investigation.

In order to analyse quantitatively the X-H....DTBN H-bond, we have determined the formation constants(K), enthalpies(Δ H) and limiting shifts(Δ,) for the H-bond complex formation

$$\text{X-H} + \text{DTBN} \underset{K}{\rightleftharpoons} \text{X-H...DTBN} \qquad (3)$$

For the case of rapid exchange(which is verified by the linear plot of Figure 1), the observed proton shift, δ , is given by

$$\delta = P_f \delta_f + P_c \delta_c \qquad (4)$$

where p_f and p_c designate the fractions of the free proton donor and of H-bonded complex respectively and δ_f and δ_c are the corresponding proton chemical shifts. Then

$$P_c = \frac{\delta_f - \delta}{\delta_f - \delta_c} = \frac{(XH\cdots DTBN)}{(XH)_\circ} = \frac{\Delta}{\Delta_\circ} \qquad (5)$$

and for the condition of (XH)>> (DTBN),

$$K = \frac{(XH\cdots DTBN)}{(XH)_\circ((DTBN)_\circ - (XH\cdots DTBN))} \qquad (6)$$

where Δ and $\Delta_\circ$, are observed and limiting contact shifts, espectively and ( )$_\circ$ denotes the initial concentration.

Figure 3. Plots of the inverse of the observed proton contact shift against the initial concentration of proton donor (chloroform) (see Eq.(7)) at various temperature.

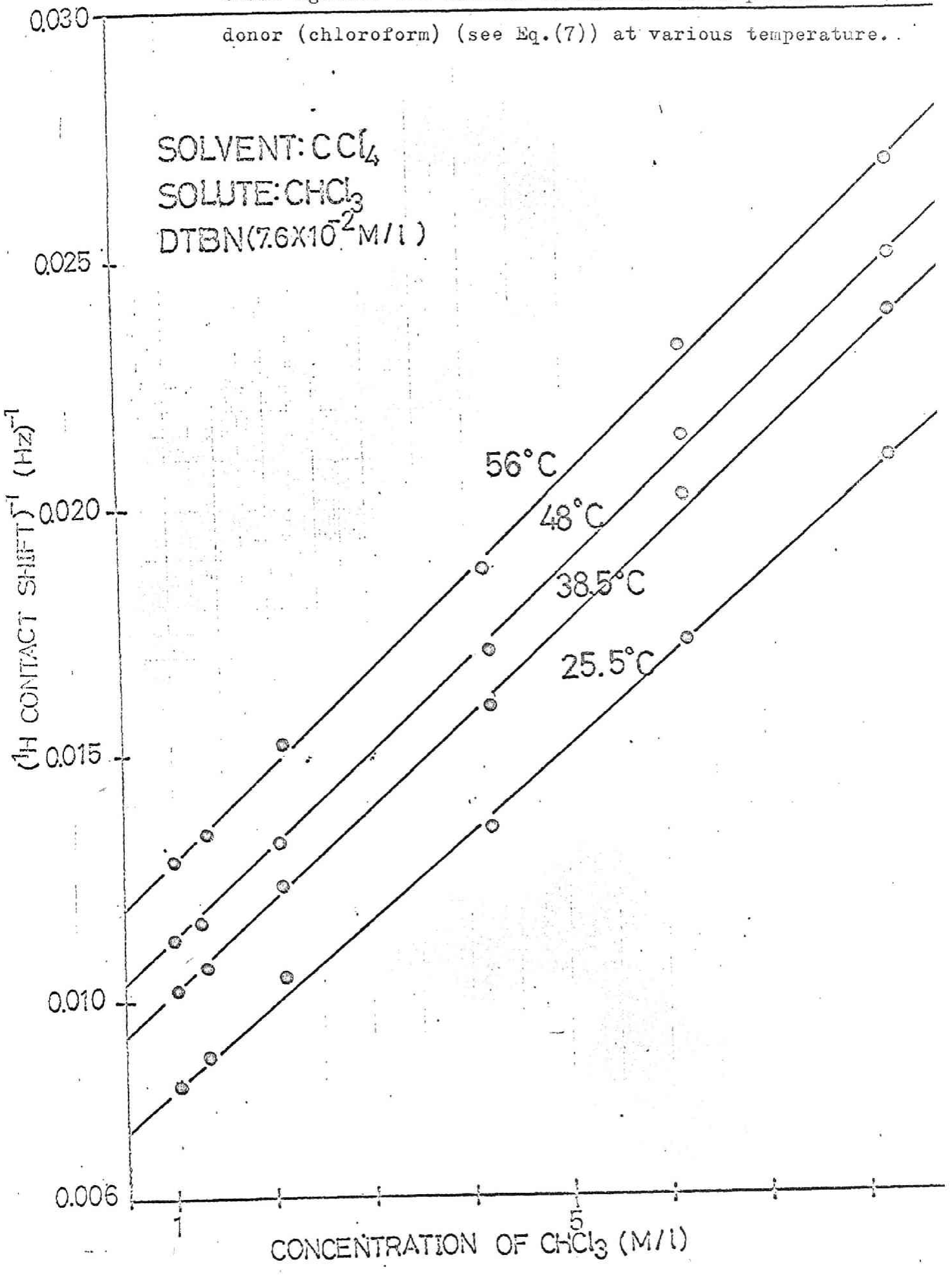

Figure 4. Plots of K v.s. 1/T in the ^{1}H and ^{13}C contact shifts measuments for chloroform.

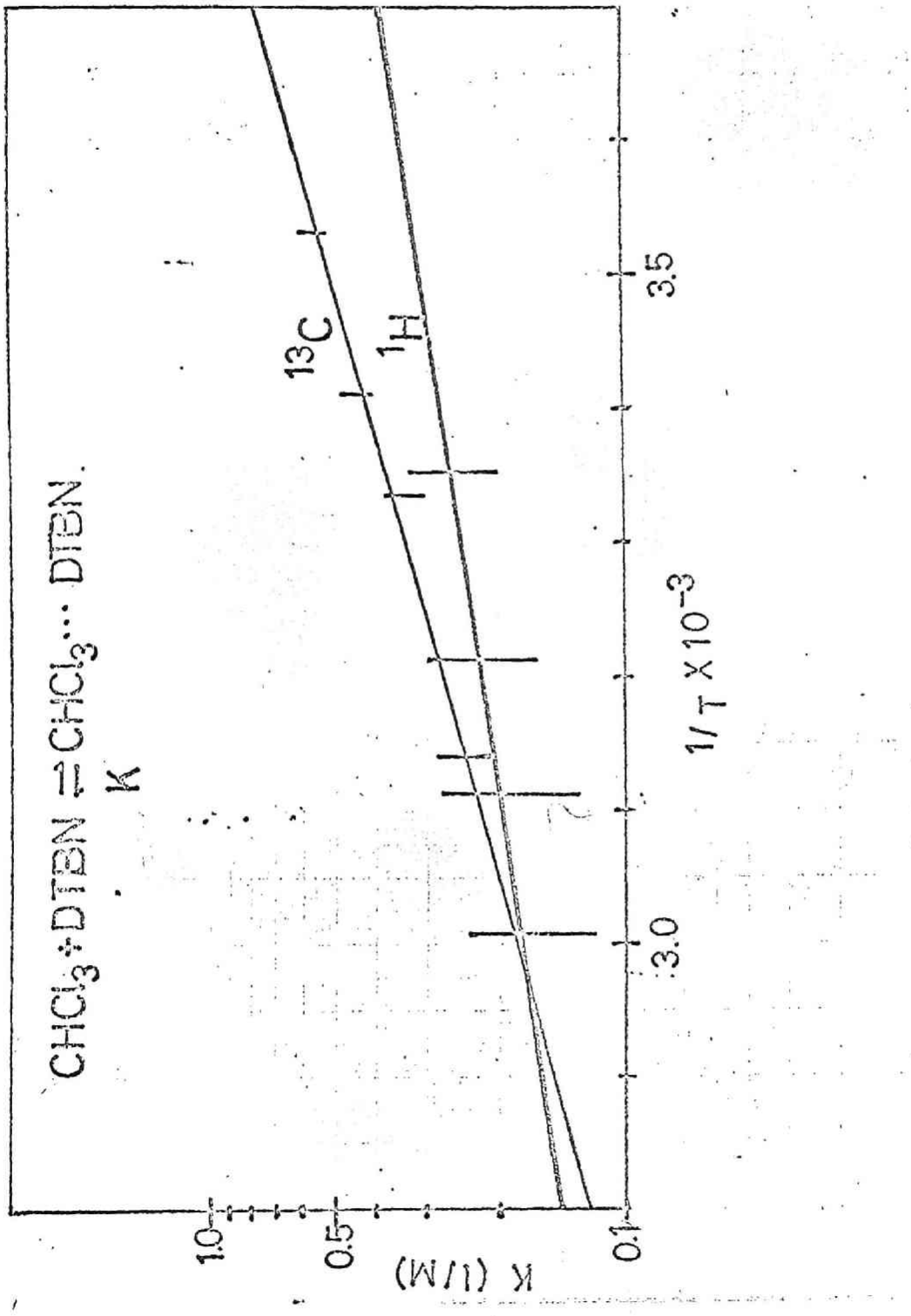

Figure 5. Observed ^{13}C contact shifts protted against the concentration of added DTBN.

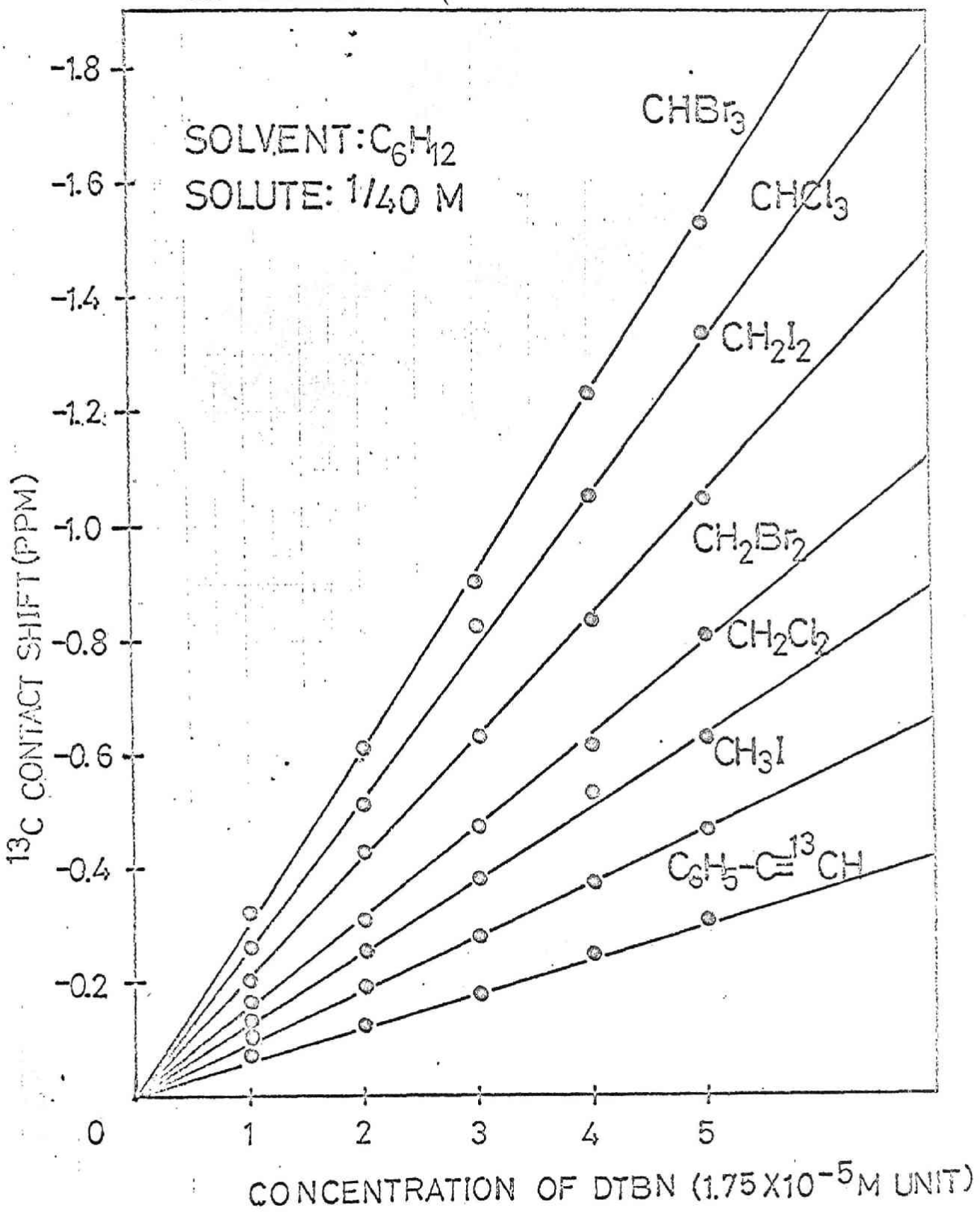

Table 1. Formation Constants, Enthalpies, ^1H Limiting Contact Shifts and Spin Densities on the Proton for Hydrogen Bond Complex Formation with DTBN

Proton Donor	K(l/mol)	ΔH(Kcal/mol)	Proton Limitimg Shift, (ppm)	Spin Density on the proton
$CH_3O\underline{H}$	1.26 ± 0.07 (-4°C)	-4.5 ± 1.0	32 ± 2	-0.00077
	0.53 ± 0.07 (+22°C)		30 ± 2	-0.00080
	0.42 ± 0.08 (+42°C)		29 ± 2	-0.00086
	0.27 ± 0.06 (+57°C)		29 ± 2	-0.00086
			Av.	-0.00082
$C\underline{H}Cl_3$	0.26 ± 0.06(+25°C)	-2.6 ± 1.3	35 ± 2	-0.00093
	0.23 ± 0.06(+38°C)		32 ± 2	-0.00089
	0.20 ± 0.07(+48°C)		32 ± 2	-0.00093
	0.18 ± 0.06(+56°C)		31 ± 2	-0.00091
			Av.	-0.00091
$C_6H_5N\underline{H}_2$	0.51 ± 0.06(+24°C)	-1.1 ± 0.9	4.7 ± 0.7	-0.00013
	0.47 ± 0.07(+42°C)		4.6 ± 0.7	-0.00013
	0.42 ± 0.07(+55°C)		4.3 ± 0.7	-0.00013
	0.40 ± 0.07(±70°C)		3.9 ± 0.7	-0.00012
			Av.	-0.00013

Figure 6. Curie law test of the ^{13}C contact shift for chloroform.

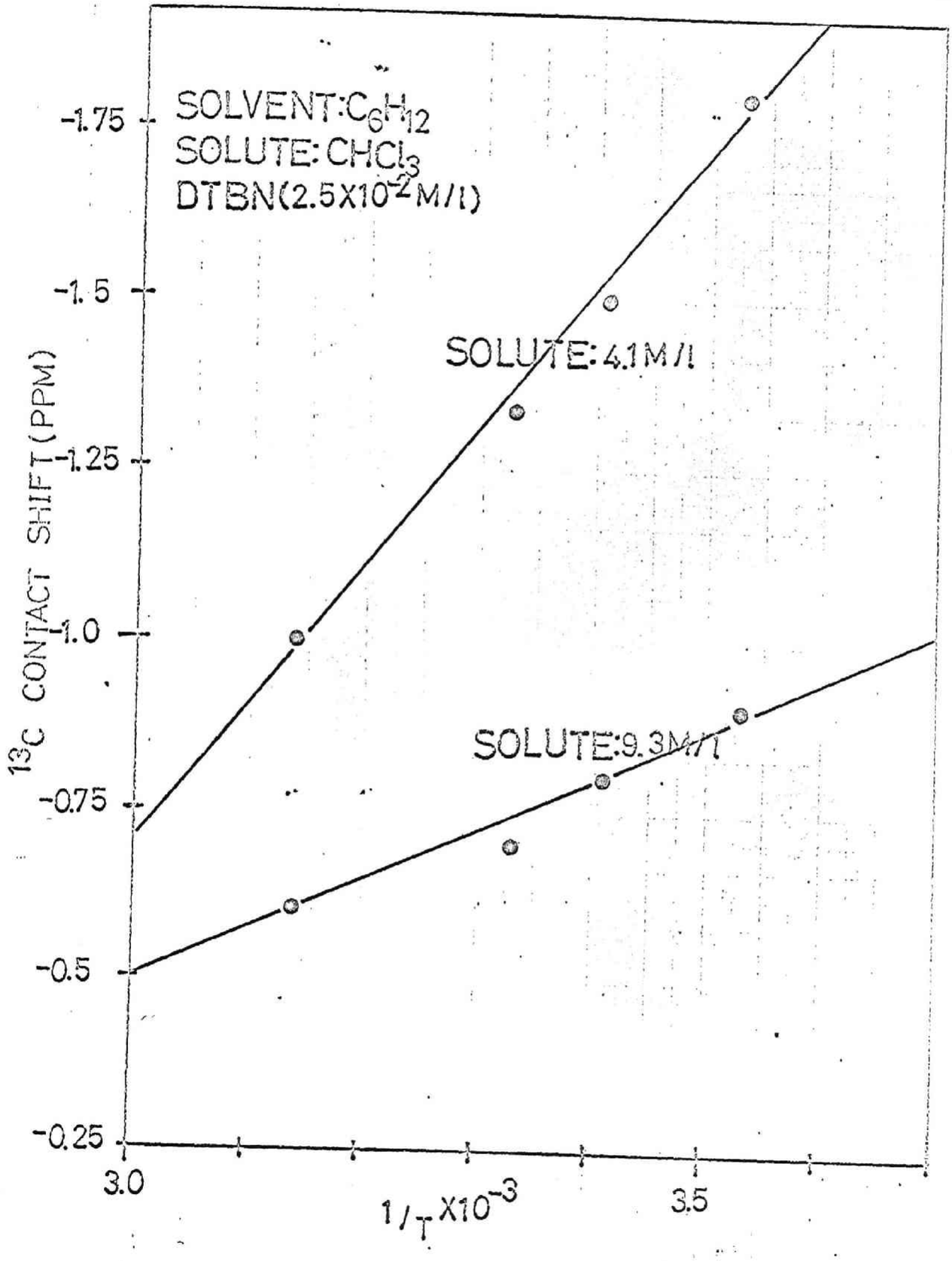

Equation 6 can be written as

$$\frac{1}{\Delta} = \frac{1}{K[DTBN]_0 \Delta_0} + \frac{[XH]_0}{[DTBN]_0 \Delta_0} \qquad (7)$$

Using this equation we have determined K and Δ_0 values from the measurement of contact shifts with varying initial concentrations [DTBN], [XH] for some typical proton donor molecules (see Figure 3). From the temperature dependence of K, we have also determined enthalpies(ΔH) for the H-bond formation (Figure 4). The results are summarized in Table I. From the limiting contact shift, we are able to estimate spin density on the X-H proton using equations (1) and (2). With the relation of $a_H = 379.34 \rho_H$,6 spin densities were obtained, as is given in Table I. Substantially large upfield proton contact shift for chloroform, comparable with that for methanol appears to reflect appreciably large value of the limiting contact shift. On the other hand, smaller contact shift for aniline(see Figure 1) results from quite small value of the limiting shift.

^{13}C Contact Shifts. For the C-H proton donor molecules, we have studied ^{13}C contact shifts induced by the addition of DTBN. Figure 5 shows DTBN-induced downfield ^{13}C contact shifts for various C-H proton donor molecules. Figure 6 exhibits the Curie law behavior of the DTBN-induced ^{13}C shift. We have also determined the equilibrium constant(K), the limiting ^{13}C contact shift(Δ_0) , the enthalpy(ΔH) and spin density on the carbon(ρ_C) for $CHCl_3$, CH_2Cl_2 and C_6H_5C CH by the method

Table II. Formation Constants, Enthalpies, ^{13}C Limiting Shifts, and spin Densities on the Carbon for Hydrogen Bond Complex Formation with DTBN

Proton Donor	K(l/mol)	ΔH(kcal/mol)	^{13}C Limiting Shift(ppm)	Spin Density on the carbon
$\underline{C}HCl_3$	0.56±0.03 (10°C)	-3.5±1.5	-410±30	0.00160
	0.45±0.03 (20°C)		-370±30	0.00150
	0.35±0.03 (27°C)		-330±20	0.00140
	0.25±0.03 (45°C)		-320±20	0.00140
			Av.	0.00150
CH_2CL_2	0.23±0.04 (-5°C)	-2.3±1.5	-380±30	0.00140
	0.20±0.03 (5°C)		-360±30	0.00140
	0.16±0.03 (20°C)		-340±30	0.00140
	0.14±0.03 (33°C)		-320±20	0.00130
			Av.	0.00140
$C_6H_5C{=}C{-}H$	0.30±0.03 (10°C)	-1.0±0.6	-150±20	0.00060
	0.29±0.03 (20°C)		-140±20	0.00059
	0.28±0.03 (30°C)		-130±20	0.00050
	0.26±0.03 (40°C)		-110±20	0.00048
			Av.	0.00055

Figure 7. Model of the hydrogen donded CH_3OH/DMNO bimolecular system with various configurations.

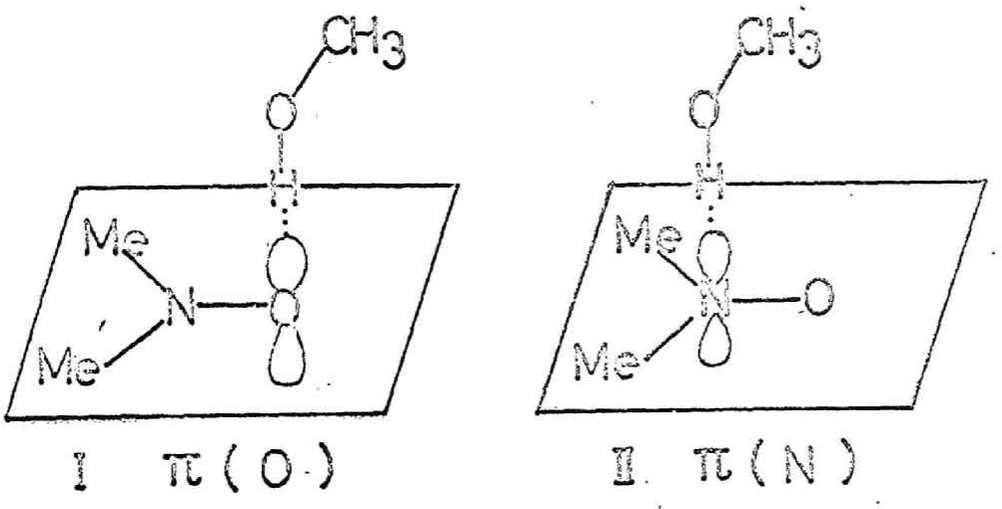

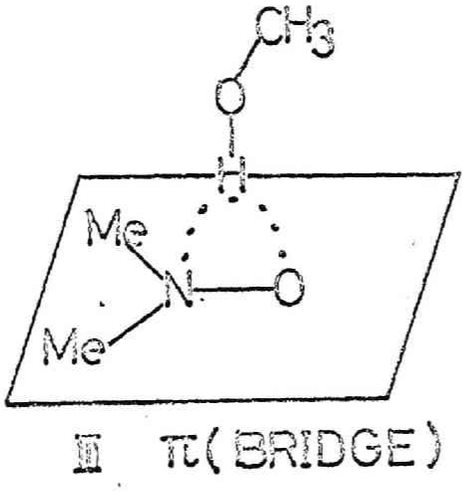

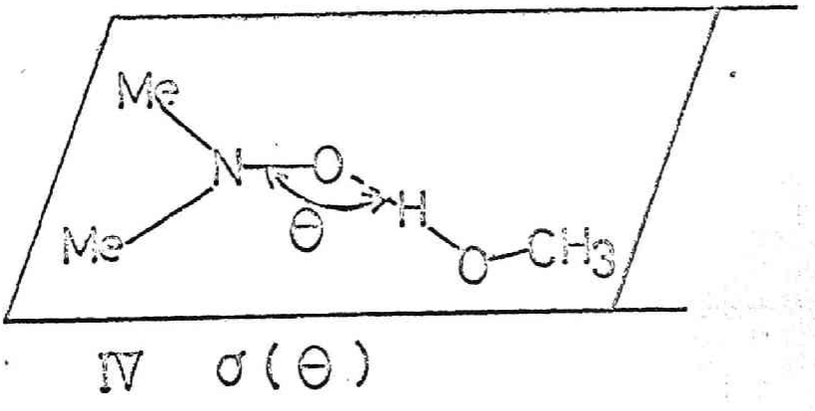

employed for the proton contact shift study. The results are tabulated in Table II. For $CHCl_3$ we have determined thermodynamic data from both ^1H and ^{13}C contact shift data. However, for CH_2Cl_2 and $C_6H_5C{\equiv}CH$, the proton contact shifts were small enough to obtain K values at various temperatures. Therefore, ^{13}C contact shifts were used to evaluate K and ΔH values for these molecules.

Molecular Orbital Calculations for Proton Donor/Nitroxide Radical System. In order to substantiate theoretically the observed ^1H and ^{13}C contact shifts of the proton donor molecules and to elucidate the nature of the X-H....DTBN H-bond, we have carried out unrestricted Hartree-Fock MO calculations(Pople's INDO MO SCF method)[6,7] for the X-H/DMNO (dimethyl nitroxide) bimolecular system. We assumed that the nitrogen, oxygen and carbon atoms in DMNO are coplanar. The bond distances used are NO, 1.215 Å and NC, 1.550 Å and the CNC bond angle is assumed to be 120°. The molecular geometries for proton donor molecules were obtained from the Sutton's compilation.[8] The geometrical structures for the H-bond bimolecular system adopted here are the π and σ types, where the X-H proton is directly over the pπ orbital of the oxygen atom(π(O) type), or of the nitrogen atom(π(N) type) or over the center of the N-O bond(π(bridge) type) with X-H bond axis perpendicular to the N-O bond, or in the σ plane($\sigma(\theta)$ type) (see Figure 7). In the $\sigma(\theta)$ model, we varied the angle θ

Table III. Results of INDO MO Calculations for Dimethyl Nitroxide (DMNO)

Nucleus	π Radical[a]				σ Radical[b]		
	ρ_s[c]		a_N(G)		ρ_s[c]	a_N(G)	a_N(Exptl) (G)
	B.A.[d]	A.A.[d]	B.A.[d]	A.A.[d]	B.A.[d]		
^{1}H	0.00837	0.00540	4.52	2.9	-0.00155	-0.83	12.3
^{13}C	-0.00620	-0.00205	-5.08	-1.6	0.02210	18.12	6.1
^{17}N	0.01232	0.00416	10.95	3.5	0.01557	13.83	19.7
^{14}N	0.01666	0.00560	6.32	2.1	-0.01763	-6.68	16.8
Total Electronic Energy	-1278.717eV				-1276.765eV		

a. Odd electron resides in the lowest unoccupied π MO (the N-O antibonding π orbital).

b. Odd electron resides in the highest occupied σ MO(closely below the highest occupied π MO) and lowest vacant π MO occupies a pair of electrons.

c. Electron spin density on the s atomic orbital.

d. B.A.= Before anihilation.
A.A.= After anihilation.

Table IV. Calculated Spin Densities on Dimethyl Nitroxide

	Spin Density		
A O	O	N	C
2s	0.0123	0.0166	-0.0062
2px	0.0032	0.0149	-0.0105
2py	-0.0079	-0.0009	-0.0065
2pz	0.6760	0.3018	-0.0099

Figure 8. INDO MO stabilization energy curves plotted against the hydrogen bond length ($\pi(0)$ model).

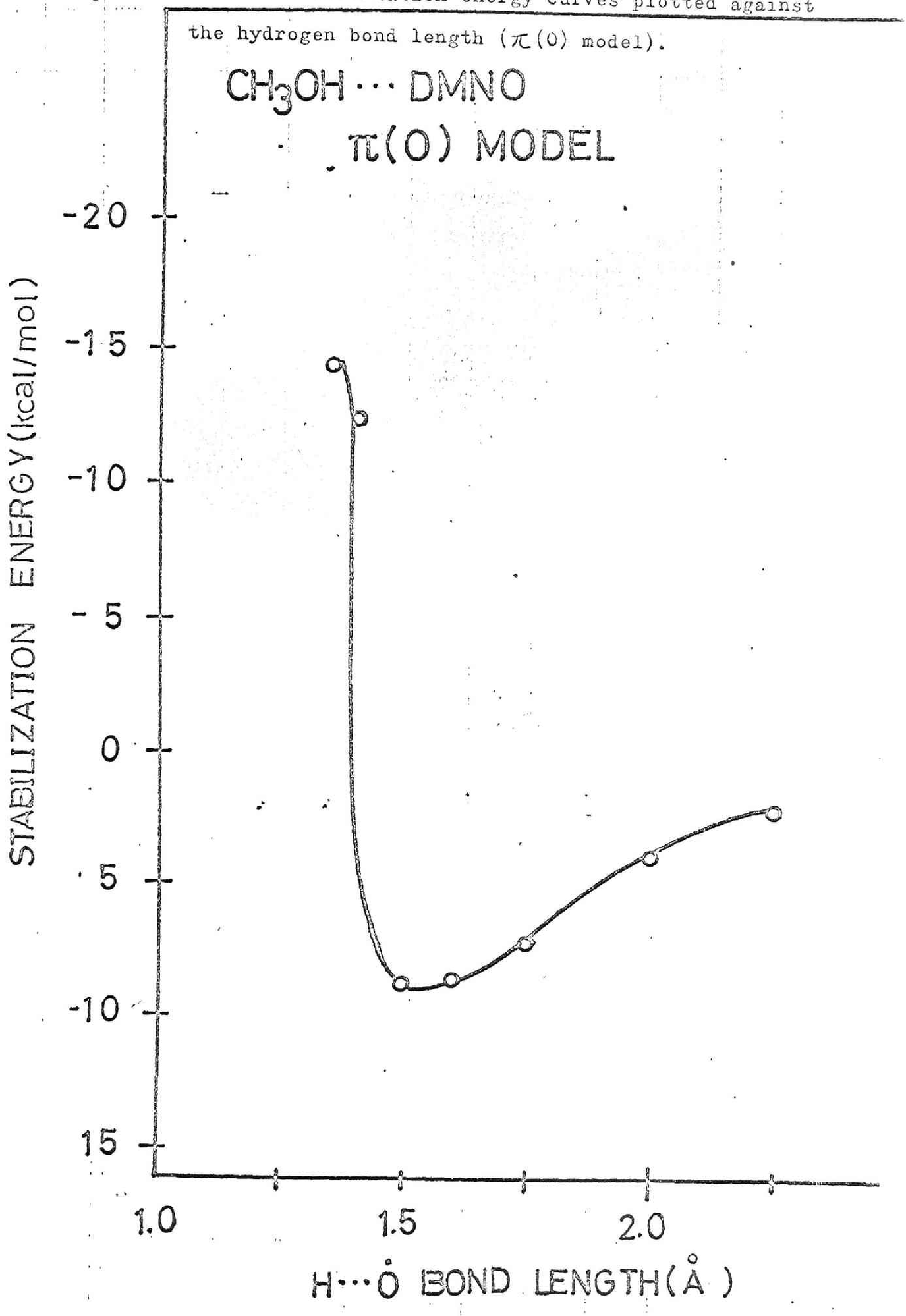

Figure 9. INDO MO stabilization energy curves plotted against the hydrogen bond length (π(N) model).

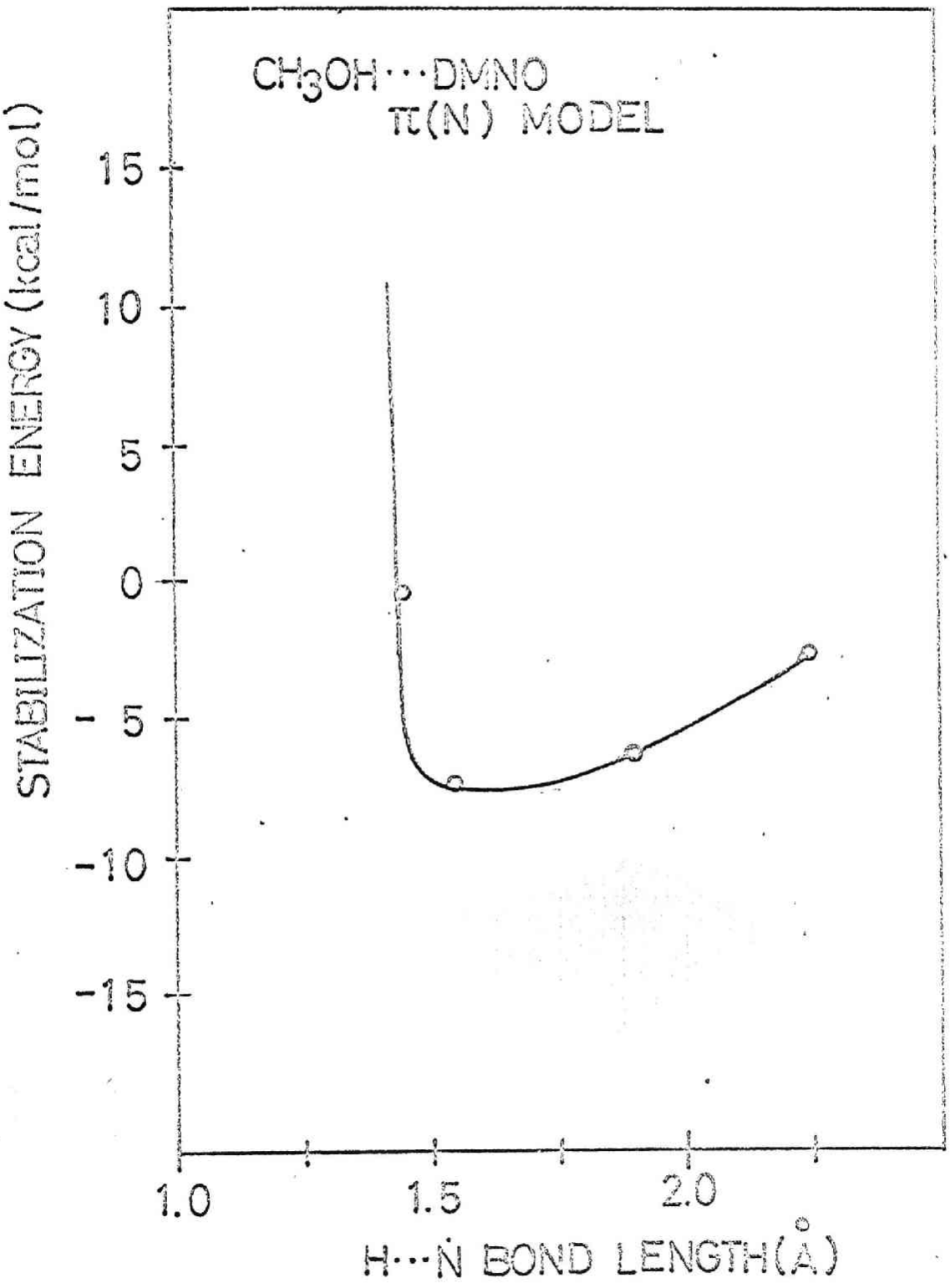

Figure 10. INDO MO stabilization energy curves plotted against the hydrogen bond length (π(BRIDGE) model).

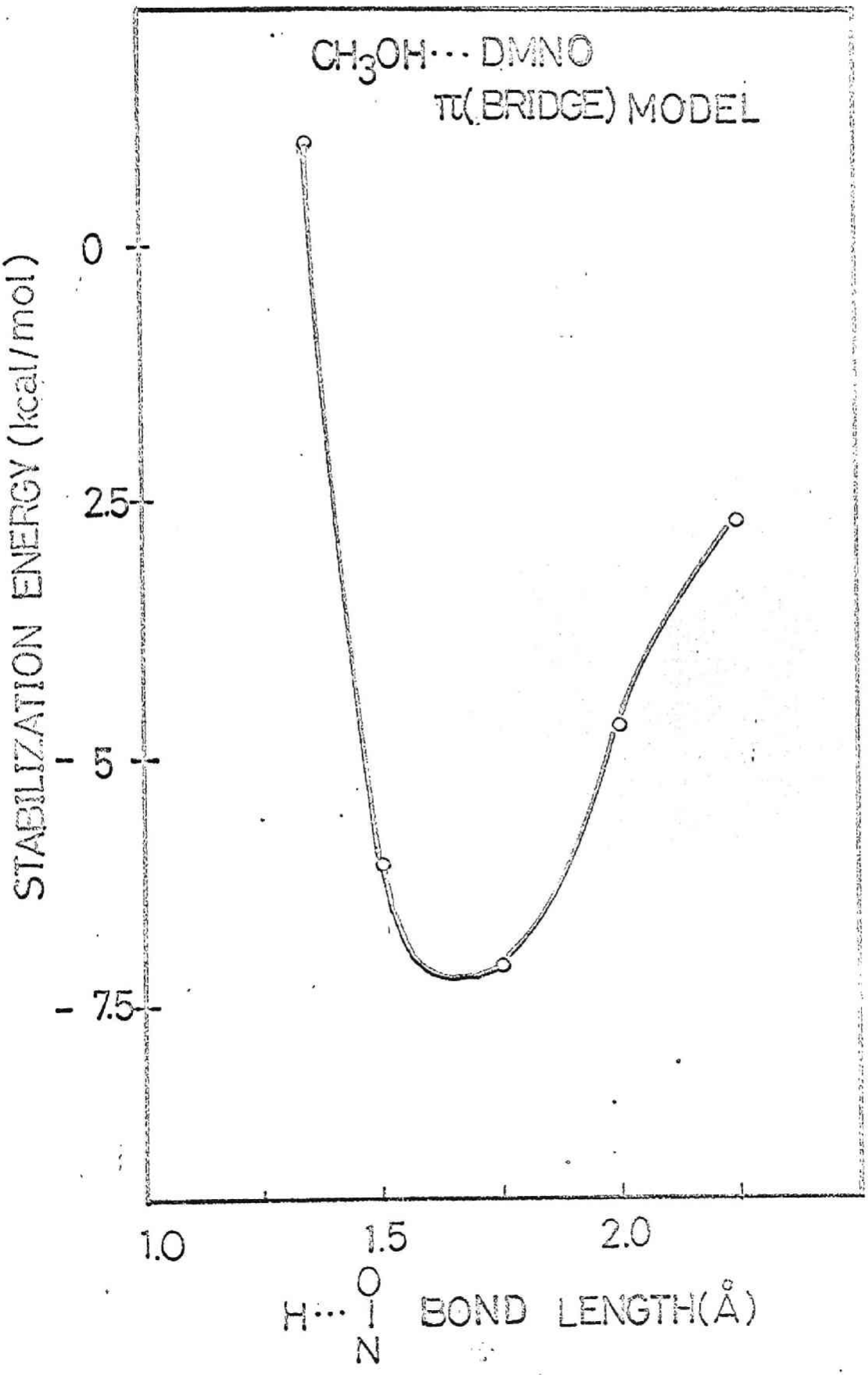

Figure 11. INDO MO stabilization energy curves plotted against the hydrogen bond length (σ(120) model).

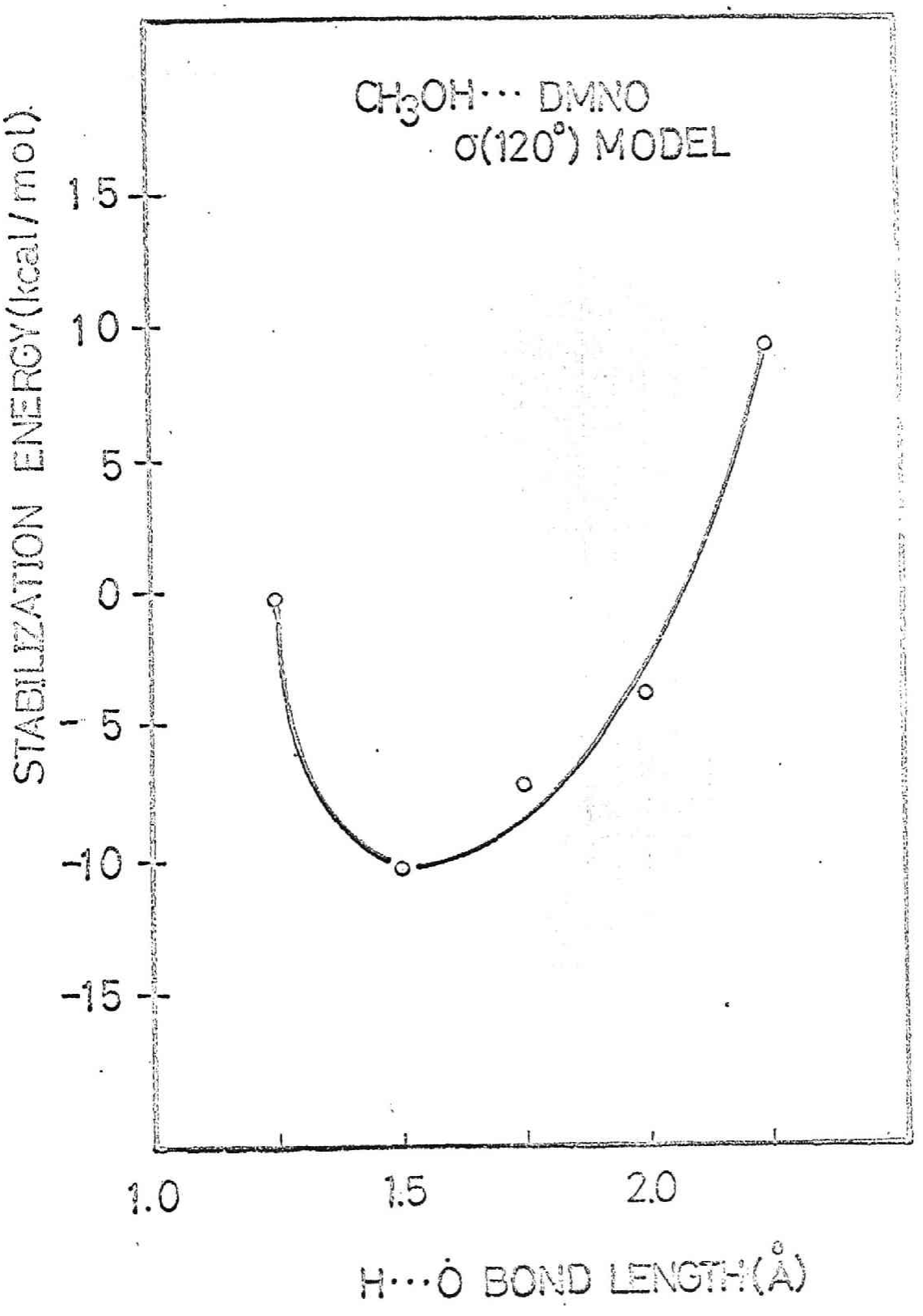

Figure 12. INDO MO stabilization energy curves plotted against the hydrogen bond length ($\sigma(180)$ model).

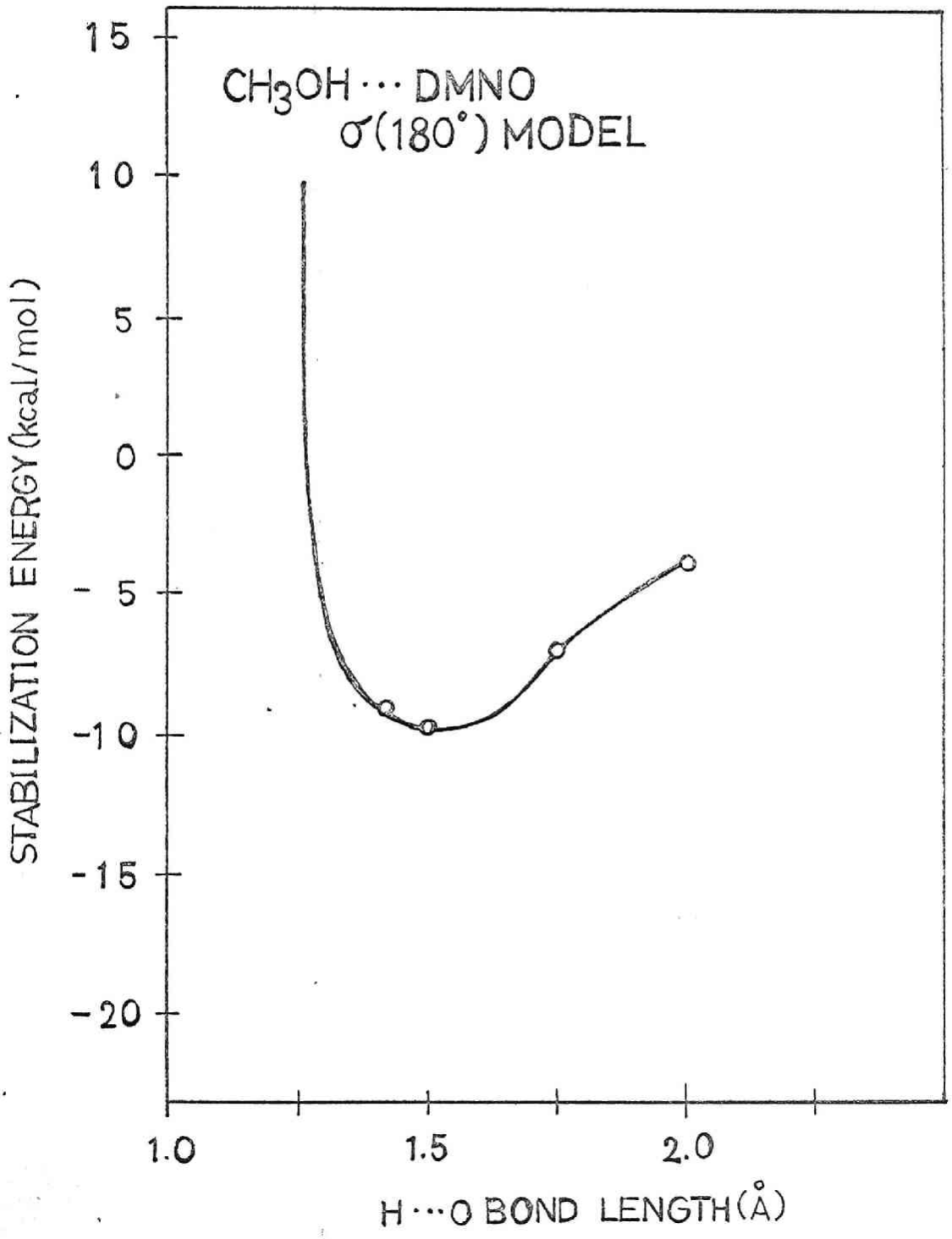

between the N-O bond and the O...H-X axis as =180°, 120°, and 90°. MO calculations were perfomed for X-H...DMNO bimolecular systems with varying X-H...O(or N) H-bond length in each model. As the X-H distance is fixed, it is equivalent to the X....O(or N) distance variation.

Before entering into X-H/DMNO bimolecular system, we have to mention the electronic structure of DMNO. We have made INDO(UHF) MO calculations for the two possible electronic structures of DMNO, the π radical and the σ radical. In the π radical odd electron resides in the lowest unoccupied π MO (the N-O antibonding π orbital) and in the σ radical odd electron occupies the next highest occupied σ MO(closely below the highest occupied π MO) and the lowest antibonding π MO occupies a pair of electrons. The results are shown in Table III. Spin densities on the s atomic orbitals and hyperfine coupling constants are given together with the total electronic energy. Calculated a_N values obtained for before anihilation in the π radical agree with the observed trend. Also in light of the electronic energy the π radical is preferable to the σ radical, as expected. Hereafter we adopt the π radical for the calculation of DMNO. Table IV exhibits the calculated values of spin density on each atomic orbital of O, N and C atoms in DMNO.

Energy curves for limited examples of X-H/DMNO bimolecular systems with various configurations are given in Figures 8~12. Table V summarizes optimum H-bond lengths, stabilization

energies(ΔE) and electron spin densities on the various X-H molecules for the configuration with the optimal stabilization. There is substantial difference in the configuration that gives optimal stabilization. We have performed detailed calculations for methanol/DMNO system in every configuration. With the other X-H molecules, only passable models were examined for MO calculation. At a glance at the table, one is easily informed that the observed negative spin density on the X-H proton is reproduced by the calculation only for the π model. The observed result of positive spin density on the carbon in $CHCl_3$ and $C_6H_5C{\equiv}CH$ are also explained theoretically in terms of the π model. Of the two π models, the $\pi(O)$ model yields negative spin density on the hydroxyl proton in methanol more sensitively than the π (N) model. The stabilization energies for these models, however, are comparable each other. For C-H and N-H proton donor molecules, we have chosen acetylene and amines as the model molecules of MO calculation. These are to be compared with observed results of phenyl acetylene and aniline.

Discussion

Observed spin densities on the proton and carbon are smaller than MO theoretical values by a factor of 2(see Tables I, II and V). This may be interpreted as in the following. MO calculation for methanol/DMNO system shows that the σ model in which the hydroxyl proton interacts with the oxygen lone-pair is energetically comparable with or more favored than the π model. However, the

Figure 13. Plots of calculated spin density on the X-H proton v.s. the hydrogen bond length for the π (O) model.

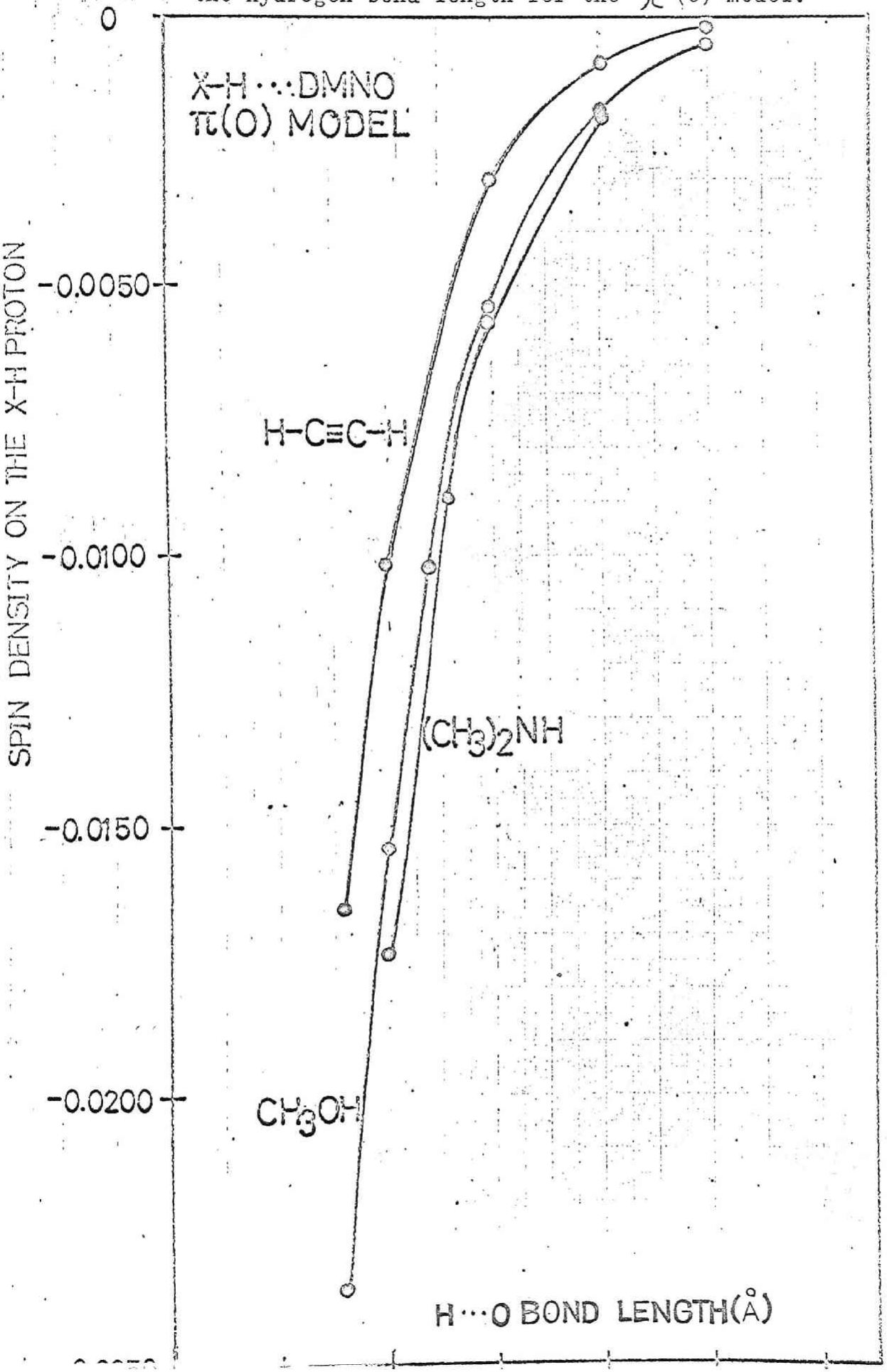

induced spin densities on the hydroxyl proton for these two models are opposite in sign. Accordingly, quite a small value of the observed spin density may allow us to expect the substantial contribution of the σ model which yields positive spin density on the proton. This is probably true for other proton donor molecules. Preference of the σ model to the π model is required to produce the observed spin density. This is substantiated by MO theoretical calculations of stabilization energy for the π and σ models (Table V). In methanol/DMNO system, the σ model is more stable than the π model by 1 - 2 kcal/mol. From above discussion it follows that the π H-bond is responsible for the observed negative spin density on the X-H proton and positive spin density on the C-H carbon although the σ type H-bond appears to contribute preferably. The observed spin density on the amine proton is much smaller than methanol and chloroform. This is also reproduced by the calculation for the π(O) model. The magnitude of the induced spin density on the X-H proton appears to be related to the optimal H-bond length. Figure 13 shows the plots of the calculated spin density on the X-H proton vs. the H-bond length for methanol, acetylene and dimethyl amine. Calculated spin density varies quite sensitively with the H....O H-bond length almost irrespective of the nature of the X atom. Therefore, the different values of spin density in these molecules are due to the difference in the optimal H-bond length. For methanol in which the H-bond length is smallest

Table V. Results of INDO MO Calculations for Proton Donor /DMNO Bimolecular Systems with Various Configurations

Proton Donor	Configuration	Optimum H-bond Length (A)	Stabilization Energy, $-\Delta E$ (Kcal/mol)	Spin Density on the Donor Molecule		
				H(1s)	O(2s)	C(2s)
CH_3OH	π(O)	1.50	+8.87	-0.0154	-0.0010	-0.0003
	π(N)	1.60	+7.33	-0.0039	-0.0003	+0.0002
	π(BRIDGE)	1.75	+7.08	+0.0030	-0.0006	+0.0001
	σ(180°,x)	1.50	+9.89	+0.0036	-0.0004	+0.0001
	σ(120°)	1.50	+10.10	+0.0023	-0.0004	+0.0000
	σ(90°,y)			+0.0014	-0.0002	+0.0000
				$\underline{H}$(1s)	C_1(2s)	C_2(2s)
$-C_2=C_1-H$	π (O)	1.75	+1.31	-0.0030	+0.0021	$+0.0000_3$
	π (N)	2.00	+0.85	+0.0001	-0.0000_3	-0.0000_0
	σ (120°)	1.75	+1.63	+0.0009	-0.0008	-0.0000_4
				H(1s)	C(2s)	
HCl_3	π (O)	1.50	+1.73	-0.0121	+0.0056	
				$\underline{H}$(1s)	N(2s)	
	π (O)	1.65	+4.52	-0.0090	-0.0004	
$(CH_3)_2N\underline{H}$	π (N)	1.75	+3.11	-0.0008	-0.0000_2	
H_3	σ (120°)	1.65	+4.12	+0.0016	-0.0005	

(1.50 Å) the hydroxyl proton senses largest negative spin density, while for acetylene(1.75 Å) the C-H proton senses smallest spin density. Relatively greater value of spin density on the C-H proton in chloroform, which is experimentally recognized, is likely due to relatively closer H-bond length(1.50 Å). Accordingly the observed trend of the limiting proton contact shifts in methanol, chloroform and aniline reflects the H-bond length, rather than the nature of the O-H, C-H and N-H bonds.

It seems of interest to note that only the π(O) model produces negative spin density on the methyl carbon 2s AO in methanol(see Table V). The observed downfield ^{13}C contact shift of methyl carbon in methanol is not due to this cause but results from the H-bond between methyl proton and DTBN(H-C-C-H...DTBN interaction). The calculated negative spin density on the carbon in H-C-O-H....DTBN H-bonded system is well reflected in the observed upfield ^{13}C contact shift of the junction carbon of phenol in the presence of DTBN where only the C-O-H---DTBN interaction is available. Therefore in this sense the π(O) model is important in the H-bond with DTBN.

It should also be noted that the observed spin density on the carbon in $CHCl_3$ is smaller than that on the proton, contrary to the MO theoretical result. This is probably due to the contribution os the C-Cl....DTBN charge transfer interaction[9,1d] in addition to the C-H...DTBN H-bond, where both interactions induces positive spin density on the carbon.[1d] The greater downfield shifts of $CHBr_3$, CH_2Br_2 and CH_2I_2 compared with $CHCl_3$ and CH_2Cl_2

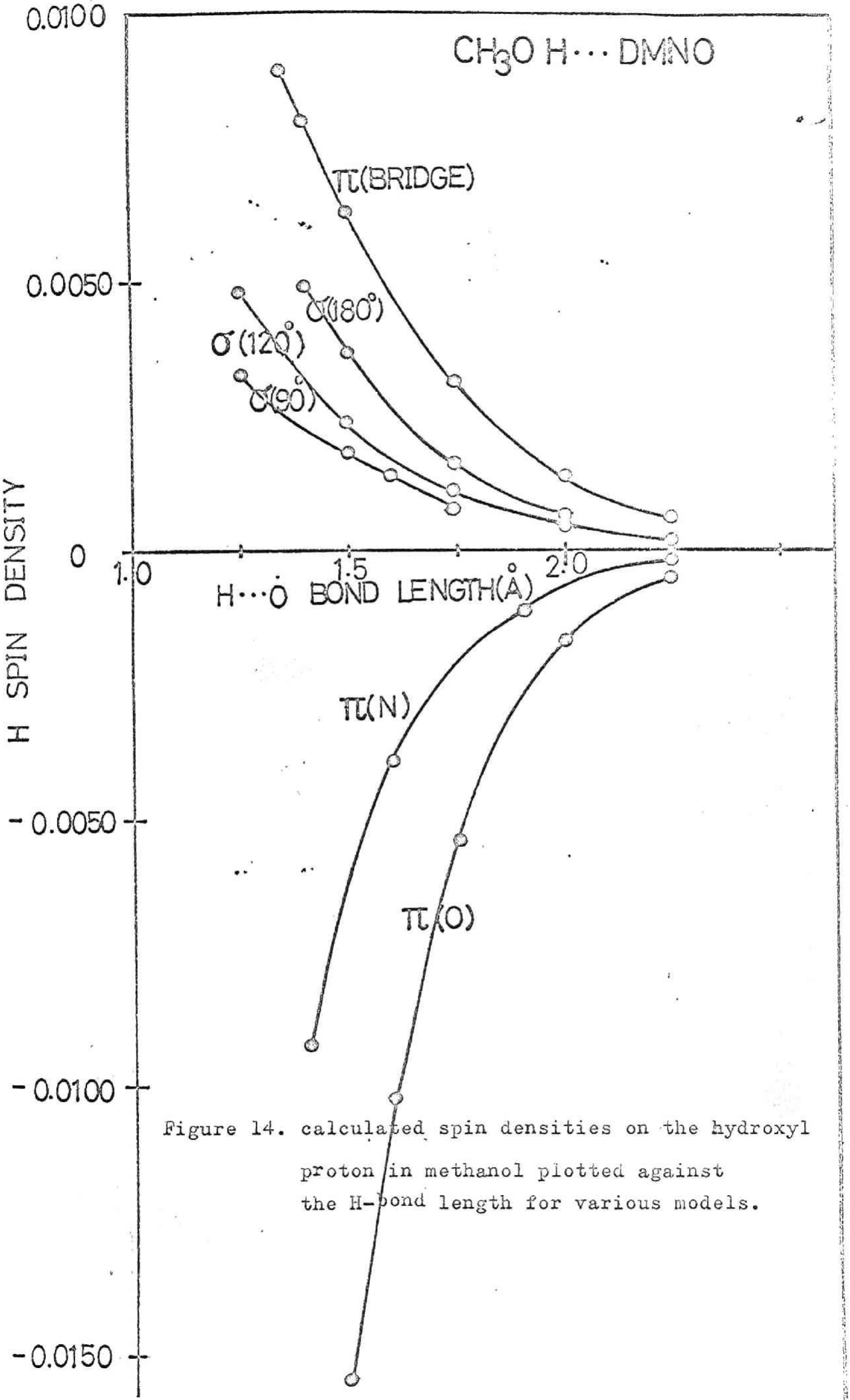

Figure 14. calculated spin densities on the hydroxyl proton in methanol plotted against the H-bond length for various models.

(see Figure 5) are most likely due to this cause.[9]

The observed H-bond energies(ΔH) ranging from 1 to 5 Kcal/mol are not so different from those for usual closed-shell H-bond system. The MO theoretical value of stabilization energy also follows this trend. As the odd electron occupies N-O π antibonding orbital in the nitroxide radical, the π H-bond is expected to gain greater H-bond energy than the usual H-bond for the closed-shell molecules if charge transfer interaction contributes substantially in the H-bond with nitroxide radical. The experimental results imply the minor contribution of the charge transfer interaction. As indicated previously,[1] electron spin transfers from DTBN to the X-H molecule by the spin polarization mechanism, not by the spin delocalization mechanism which allows the direct electron spin delocalization from nitroxide radical to the antibonding orbital of the X-H bond. The delocalization mechanism favors positive spin density on all the atoms of the X-H molecule and corresponds to the charge transfer interaction. The mechanism of electron spin transfer by the H-bond from radical to the proton donor molecule is interesting in relation to the elucidation of the nature of the H-bond, and will be published elsewhere with more theoretical method.[10]

References

(1) Preliminary studies: (a)I,I.Morishima, K.Endo and T.Yonezawa, J.Amer.Chem.Soc.,93,2048(1971);(b)II,I.Morishima, K.Endo and T.Yonezawa, Chem phys.Lett.,9,143(1971);(c) III,ibid.,9,203 (1971);(d)IV,I.Morishima, T.Inubushi,K.Endo and T.Yonezawa, J.Amer.Chem.Soc.,submitted for publication;(e)V,I.Morishima, T.Matsui and T.Yonezawa,ibid.,submitted for publication.

(2) (a)N.A.Sysoeva,A.U.Stepanyants, and A.C.Buchachenko,J.Struct. Chem.,9,248(1968);(b)y.y.Lim and R.S.Drago,J.Amer.Chem.Soc., 93,891(1971).

(3) Y.Deguchi,Bull.Chem.Soc.Japan,35,260(1962);T.Kawamura,S. Matsunami, and T.Yonezawa, ibid.,40,1111(1967).

(4) R.Briere, H.Lemaire, and A.Rassat,Bull.Soc,Chim.Fr.,P.3273 (1965).

(5) H.M.McConnell and D.B.Chesnut,J.Chem.Phys.,28,107(1958).

(6) J.A.Pople,D.L.Beveridge and P.A.Dobosh,J.Amer.Chem.Soc., 90,4201(1968).

(7) J.A.Pople,D.L.Beveridge and P.A.Dobosh,J.Chem.Phys.,47,2026 (1967).

(8) L.E.Sutton,Ed.,Chem.Soc.,Spec.Publ.,No.11(1958).

(9) I.Morishima,K.Endo,T.Inubushi,T.Yonezawa, and K.Goto, the forthcoming paper (VII).

(10) I.Morishima,K.Endo and T.Yonezawa, to be published.

Chapter 3

^{13}C Contact Shifts and Molecular Orbital Studies on the Charge-Transfer Interaction between Halogenated Molecules and Nitroxide Radical.

INTERACTION BETWEEN CLOSED AND OPEN-SHELL MOLECULES. V. ^{13}C CONTACT SHIFT AND MOLECULAR ORBITAL STUDIES ON THE INTERACTION BETWEEN HALOGENATED MOLECULES AND NITROXIDE RADICAL

^{13}C NMR contact shifts induced by the addition of the di-*tert*-butyl nitroxide (DTBN) radical were observed for halomethanes, haloethanes, haloethylenes and halobenzenes. The sensitively induced downfield ^{13}C contact shifts for the carbon bonded directly to halogen were of the order of I > Br > Cl. These results were interpreted in terms of electron donor–acceptor interaction of halides with the DTBN radical with the aid of INDO MO calculations of electron spin density on the carbon atoms of halide molecules.

Recently we have demonstrated [1] that the ^{1}H and ^{13}C NMR shifts are quite sensitive to the presence of a small amount of a stable free radical (the nitroxide radical, for example) and the resulting ^{1}H and ^{13}C contact shifts are very useful for the studies of weak molecular interactions such as the hydrogen bond; in this sense the nitroxide radical may serve as "*a spin label reagent*" for the study of a weak intermolecular interaction [2]. The hydrogen bond with the nitroxide radical induces upfield or downfield contact shifts quite sensitively on the various nuclei of the proton donor molecules. These contact shifts were interpreted in terms of the electron spin transfer by the polarization mechanism [3, 4]. Here we wish to report the preliminary results of the ^{13}C contact shift study of the electron donor–acceptor interaction between halogenated molecules and the nitroxide radical. There has been a lot of evidence for the weak donor–acceptor complex formation between halogenated methanes and electron donor molecules from UV [5], IR [6], and Raman [7] spectroscopic studies and from the measurements of the heat of mixing [8]. However, these studies were associated with the interaction of closed-shell molecules and there has been no work on the donor–acceptor interaction between closed- and open-shell molecules*. The study of the radical-induced NMR contact shift is expected to provide fruitful information on this type of interaction, particularly on the nature of the intermolecular electron spin transfer for the halogenated molecule–nitroxide radical bimolecular system.

The addition of the di-*tert*-butyl nitroxide radical (DTBN) to CCl_4 and $CBrCl_3$ caused substantial downfield shifts of ^{13}C chemical shifts of these halomethanes. The spectra of naturally occurring ^{13}C were obtained by a complete proton decoupling technique from a JEOL-C-60HL spectrometer equipped with the ^{13}C NMR assembly (at 15.1 MHz). ^{13}C chemical shifts were measured with reference to cyclohexane of which the ^{13}C chemical shift was hardly affected by the addition of DTBN. The ^{13}C chemical shifts of these halomethanes were hardly affected by the addition of a diamagnetic donor molecule such as pyridine. Therefore, the downfield ^{13}C shift can most probably be attributed to the contact shift characteristic of the positive spin density on the carbon. We have also observed downfield ^{13}C contact shifts for CHX_3 and CH_2X_2 where X = Cl, Br, and I are induced by the

* At the final stage of the present study, we noticed a paper of Murata and Mataga [12] dealing with ESR and optical studies on the electron donor–acceptor complexes of DTBN. Quite recently, a paper related to the present study appeared [13].

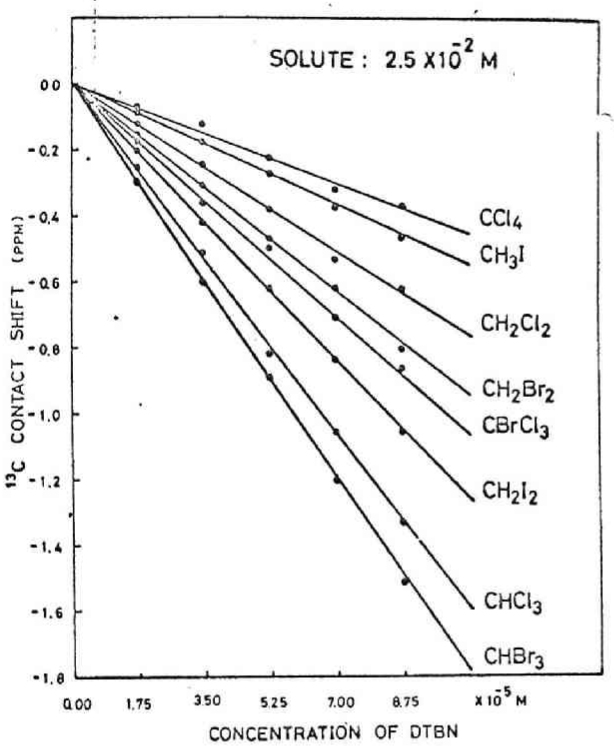

Fig. 1. Plots of ^{13}C contact shifts versus the concentration of added DTBN radical for various halomethanes.

addition of DTBN. Fig. 1 shows the linear plots of the observed ^{13}C contact shifts of various halomethanes versus the concentration of added DTBN (at room temperature). It is generally seen that the ^{13}C contact shifts for halomethanes are of the order of X = I > Br > Cl. Previously we have reported [1] DTBN-induced ^{1}H and ^{13}C contact shifts for $CHCl_3$ and CH_2Cl_2 which were interpreted in terms of the hydrogen bond between the C–H proton and the nitroxide oxygen. Negative and positive spin densities are induced on the proton and carbon respectively by the spin polarization mechanism. The above trend of the ^{13}C contact shifts for CHX_3 and CH_2X_2 (X=I > Br > Cl) is opposite to the hydrogen donor ability of these halomethanes. As is easily seen in fig. 1, $CBrCl_3$ shows an even larger downfield ^{13}C contact shift than the CH_2X_2 (X=Cl and Br) molecules. Interaction here cannot involve hydrogen bonding with DTBN. Therefore, the above observations immediately suggest the existence of an interaction between the DTBN radical and halomethanes that is quite independent of any

Table 1
^{13}C contact shift of alkyl halides a)

X	CH_3CH_2- a	CH_3CH_2- b	$(CH_3)_2CH-$ a	$(CH_3)_2CH-$ b	$(CH_3)_3C-$ a	$(CH_3)_3C-$ b
Cl	–	–	−0.43	−0.52	−0.36	+0.18
Br	−0.64	−1.50	−0.43	−0.62	−0.41	+0.13
I	−0.58	−1.59	−0.42	−0.69	−0.23	+0.04

a) ^{13}C contact shifts are given in ppm at the DTBN concentration of 3×10^{-4} M.

hydrogen bond. Thus, the ^{13}C contact shift behavior of halomethanes containing DTBN is that which would be expected if halomethanes form a weak complex with DTBN of the interaction type C–X...DTBN. The importance of this interaction can also be recognized by the experimental trend of the ^{13}C contact shifts, $CBrCl_3 > CCl_4$ (see fig. 1). However, when we compare the results for CCl_4 and $CHCl_3$, the hydrogen bond with DTBN appears to be still important for the $CHCl_3$–DTBN system. For CHX_3 and CH_2X_2, both of the C–H...DTBN hydrogen bonds and the C–X...DTBN donor–acceptor interaction could concurrently occur.

The above features of DTBN-induced ^{13}C contact shifts could be recognized more easily by the results for other halogenated molecules such as various alkyl halides, haloethylenes and halobenzenes. We have obtained similar ^{13}C contact shifts–concentration of DTBN linear plots for ethyl, isopropyl and *tert*-butyl halides and results are summarized in table 1. The data show the ^{13}C contact shift values at the DTBN concentration of 3×10^{-4} M obtained from the linear plots. For ethyl and isopropyl halides, the substituted carbon (C_b) exhibits the downfield ^{13}C contact shifts in the order of I > Br > Cl as expected. However, the downfield ^{13}C contact shift for methyl carbon has the opposite trend, Cl > Br > I. This is easily understood if the methyl C–H proton interacts with DTBN as a proton donor in the C–H....DTBN hydrogen bond: the C–H proton of the methyl group in ethyl bromide is more acidic and is here more susceptible to the hydrogen bond with DTBN than ethyl iodide. However, for *t*-butyl halides the substituted carbon shows an upfield ^{13}C contact shift, contrary to the results for ethyl and isopropyl halides, to the extent

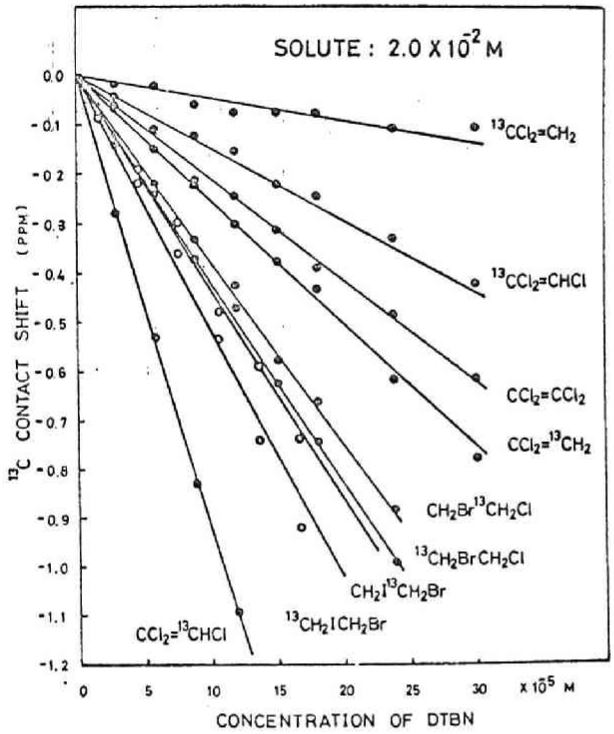

Fig. 2. Plots of the ^{13}C contact shifts versus the concentration of added DTBN radical for 1,2-dihaloethanes and chloroethylenes.

in the order of Cl > Br > I. This implies that for *t*-butyl halides the methyl C–H....DTBN hydrogen bond is preferentially important, which induces positive and negative spin densities on the methyl and tertiary carbons respectively by the spin polarization mechanism. This feature of *t*-butyl halides–....DTBN interaction is probably due to the steric inhibition of the direct C–X....DTBN interaction and this inhibition would favor the methyl C–H....DTBN weak hydrogen bond interaction.

The preferential interaction of the C–I group with DTBN was also recognized from the greater downfield contact shift of C_2 than C_1 in 1-bromo–2-iodoethane (fig. 2). For 1-chloro–2-bromoethane, the preferential downfield shift of C_2 was observed, as expected. Fig. 2 also shows the results for chlorinated ethylenes. The ^{13}C contact shift for CCl_2 carbon increases in the order of dichloro-, trichloro-, tetrachloroethylene, implying the importance of the C–Cl....DTBN interaction. The preferential downfield contact shifts for

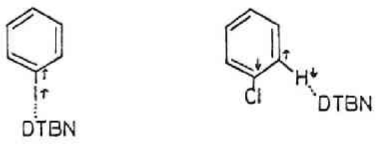

Fig. 3.

CHCl and CH_2 carbons in trichloro- and dichloroethylenes (fig. 3) could be attributed to the C–H....DTBN hydrogen bond-induced ^{13}C contact shift, as in the case of the methyl carbon contact shift in monohaloethanes.

All of these features of the ^{13}C contact shift were also encountered for halobenzenes. Fig. 4 and table 2 give the results of DTBN-induced ^{13}C contact shifts for chloro-, bromo- and iodobenzenes. The substituted carbon (C_1) of iodobenzene sensitively exhibits greater downfield contact shift than other ring carbons (fig. 4). On the other hand, the C_1 resonance of bromobenzene is quite insensitive to DTBN. In chlorobenzene, C_1 shows a contact shift slightly upfield, contrary to iodo- and bromobenzenes. These results again suggest that the C–I....DTBN interaction for iodobenzene is important while in bromo- and chlorobenzenes the C_2–H....DTBN weak hydrogen bond could be responsible for the small downfield or upfield contact shift of C_1. The fact that the aromatic C–H group is able to act as a proton donor to DTBN has previously been shown for various aromatic hydrocarbons [2]. The carbon of benzene exhibited substantial downfield contact shift by the addition of DTBN. The relative ^{13}C contact shifts with respect to benzene are given for halobenzenes in table 2. The upfield contact shift for the substituted carbon was also encountered for nitrobenzene and fluorobenzene. This upfield contact shift for C_1 is possibly due to the negative spin (↓) density induced by C_1–C_2–H....DTBN weak hydrogen bond interaction through the spin polarization mechanism. This interaction may reduce the positive spin (↑) density induced by the C_1–Br....DTBN donor–acceptor interaction and leads to a small downfield contact shift for C_1 in bromobenzene.

From these experimental results it is likely that the C–X....DTBN interaction could induce positive spin density on the carbon by the spin delocalization mechanism which permits the electron spin transfer

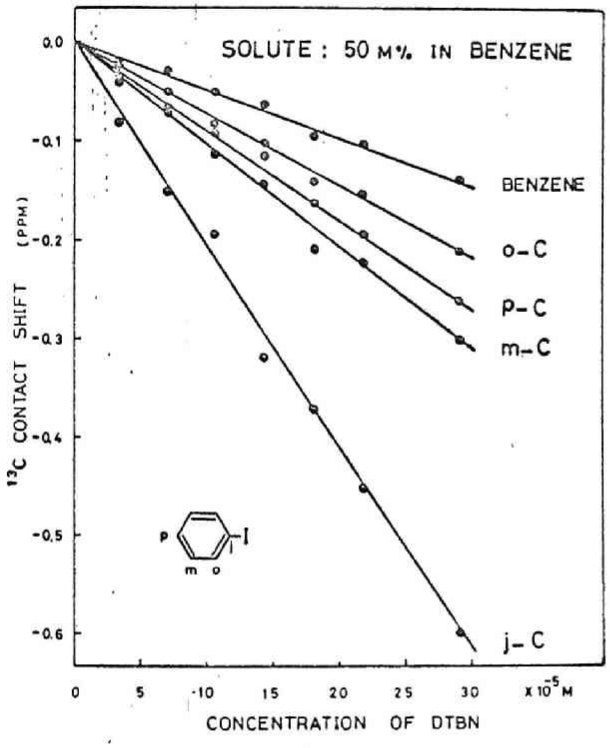

Fig. 4. Plots of ^{13}C contact shifts versus the concentration of DTBN radical for the benzene solution of iodobenzene.

Table 2
^{13}C contact shifts for halobenzenes [a]

position	X=H (benzene)	Cl	Br	I
1		+0.42	−0.49	−4.23
2, 6	(−1.00) [b]	−1.80	−1.65	−1.48
3, 5		−2.27	−2.03	−2.11
4		−2.12	−1.77	−1.84

a) ^{13}C contact shifts are given with reference to benzene.
b) The observed value of ^{13}C contact shift is 0.13 ppm at the DTBN concentration of 3×10^{-4} M (see fig. 3).

Table 3
INDO MO calculations for CH_3X.... dimethyl nitroxide bimolecular system

Complex model	X	R [a] (Å)	ΔE [a] (kcal/mole)	Calculated spin density on CH_3X $\rho_{C(2s)}$	$\rho_{X(2s)}$
I π(O)	F	1.5	20.3	0.0369	0.0177
	Cl	1.5	4.8	0.0249	0.0407
II π(N)	F	1.5	6.0	0.0298	0.0169
III σ	F	1.5	4.3	−0.0026	−0.0031

a) $\Delta E = E - E_\infty$, the energy of stabilization. The R values are at the energy minimum.

from DTBN directly to the unoccupied molecular orbital of the C–X bond. This is easily recognized by the parallel relation between ^{13}C contact shifts and the polarographic reduction potential ($E_{1/2}$) of halomethanes [9]. In order to substantiate theoretically the DTBN-induced ^{13}C contact shift for C–X carbon and to elucidate the nature of the C–X.... DTBN interaction, we have performed unrestricted Hartree–Fock MO calculations (INDO method [10]) for the H_3C–X....DMNO (dimethyl nitroxide) bimolecular system arranged in the three different geometries [4]. In models I and II, the C–X bond is placed perpendicular to the p_π orbital of the oxygen and nitrogen atom respectively, while in model III the C–X bond is placed on the σ-plane and directed toward an oxygen lone-pair orbital (the N–O–X angle = 120°). We have examined fluoride and chloride for CH_3X in INDO calculations. Because of the difficulty of including the chlorine atom in the original INDO calculation for CH_3Cl, we tentatively used the input parameters (I_p, E_A and β) of the chlorine atom in place of fluorine, and other variables such as various types of integrals were the same as in the fluorine atom. The results are summarized in table 3. The energy of stabilization, ΔE, was obtained at R (= X....O or X....N distance) = 1.5 Å for most of the bimolecular systems. The ΔE value depends largely on the parametrization but the calculated spin density appears to be rather insensitive to the above parametrization. Since the models for MO calculations are too simple, comparison between the calculated results and the experimental ones is not realistic in the present case. However, it should be noted that the π model appears to be responsible for the observed value of the positive spin density on the carbon. Another feature of the results of the INDO calculation is that positive spin density is induced on both the X and C 2s atomic orbitals, which is possibly due to the electron spin transfer directly to the C–X antibonding orbital by the spin delocalization mechanism. This should be compared with the results for the case of the C–H....DTBN hydrogen bond [1]

in which negative and positive spin densities are induced on the H and C s atomic orbitals by the spin polarization mechanism. The study of the mechanism of intermolecular electron spin transfer using more rigorous theory will be given elsewhere [11].

References

[1] I. Morishima, K. Endo and T. Yonezawa, J. Am. Chem. Soc. 93 (1971) 2048.
[2] I. Morishima, T. Matsui, T. Yonezawa and K. Goto, J. Chem. Soc., to be published.
[3] I. Morishima, K. Endo and T. Yonezawa, Chem. Phys. Letters 9 (1971) 203.
[4] I. Morishima, K. Endo and T. Yonezawa, Chem. Phys. Letters 9 (1971) 143; J. Chem. Phys., to be published.
[5] D.P. Stevenson and G.M. Coppinger, J. Am. Chem. Soc. 84 (1962) 149;
R. Anderson and J.M. Prausnitz, J. Chem. Phys. 39 (1963) 1225.
[6] P. Datta and G.M. Barrow, J. Am. Chem. Soc. 87 (1965) 3053.
[7] D.A. Bahnick and W.B. Person, J. Chem. Phys. 48 (1968) 1251.
[8] K.W. Morcom and D.N. Travers, Trans. Faraday Soc. 63 (1966) 2063.
[9] I. Morishima, T. Inubushi, K. Endo and T. Yonezawa, J. Am. Chem. Soc., to be published.
[10] J.A. Pople, D.L. Beveridge and P.A. Dobosh, J. Chem. Phys. 47 (1967) 2026; J. Am. Chem. Soc. 90 (1968) 4201.
[11] I. Morishima, K. Endo and T. Yonezawa, in preparation.
[12] Y. Murata and N. Mataga, Bull. Chem. Soc. Japan 44 (1971) 354.
[13] O.W. Howarth, Mol. Phys. 21 (1971) 949.

Interaction between Closed- and Open-Shell Molecules. VII. Carbon-13 Contact Shift and Molecular Orbital Studies on the Charge-Transfer Interaction between Halogenated Molecules and Nitroxide Radical[1]

Abstract: ^{13}C nmr contact shifts induced by the addition of di-*tert*-butyl nitroxide radical (DTBN) were observed for halomethanes, haloethanes, and halobenzenes. The downfield ^{13}C contact shifts for the carbon bonded directly to halogen were more pronounced for bromide and iodide than chloride. These results were interpreted in terms of the charge-transfer (CT) interaction between the DTBN radical and halogenated molecules in the manner of C–X···DTBN interaction. Approximate values of the formation constants, enthalpies, limiting ^{13}C contact shifts, and spin densities on the carbon were also determined for this CT complex formation. Theoretical studies on this interacting system were also performed by the unrestricted Hartree–Fock SCF–MO (INDO method) calculations. The stabilization energies and spin densities on the acceptor carbon were well reproduced by the MO calculation. The positive spin density on DTBN is transferred directly onto the C–X antibonding orbital of halomethane by the spin delocalization mechanism. On the basis of the present experimental and theoretical studies, the mechanism of halogen abstraction reaction was discussed briefly.

Recently we have demonstrated[3] that the nmr contact shift study provides a potential tool for the investigation of molecular interaction between free radical and various closed-shell molecules. The hydrogen bond between the nitroxide radical and various proton donor molecules induces quite sensitively upfield and downfield proton and ^{13}C contact shifts for proton donor molecules.[3a,b] It has been shown that the spin densities on the donor molecules induced by the hydrogen bond with nitroxide radical yield fruitful information on the nature of the hydrogen bond with the free radical. As a part of our continuing studies on the interaction between closed-shell and open-shell molecules, we here report ^{13}C nmr contact shift studies on nitroxide radical–alkyl halide interaction which are interpreted in terms of a charge-transfer (CT) interaction.

There has been much evidence of weak donor–acceptor complex formation between halogenated methanes and electron donor molecules from uv,[4] ir,[5] and Raman[6] spectroscopic studies and from measurements of heat of mixing.[7] However, these studies were associated with the interaction between closed-shell molecules and there have been only limited studies on the donor–acceptor interaction between closed- and open-shell molecules.[8] The study of radical-induced nmr contact shift is expected to provide direct information on this type of interaction, particularly on the mode of electron spin transfer from radical (electron donor) to halogenated molecules (electron acceptor). The use of ^{13}C nmr spectroscopy appears to be relevant to the present study because tetrahalomethane is most appropriate to this work as an electron acceptor and ^{13}C nmr shift is quite sensitive to the presence of the paramagnetic species.[3,9] It seems also quite interesting to investigate the CT interaction between free radical and halogenated molecules from the viewpoint that this interaction is considered to be associated with the transition state of the halogen abstraction reaction.

Here we used di-*tert*-butyl nitroxide (DTBN) as an electron donor free radical and halomethanes, haloethanes, halobenzenes, and some other halogenated molecules as an electron acceptor. We followed ^{13}C contact shifts induced by the addition of DTBN to the solution of halogenated molecules. The ^{19}F nmr contact shift was also measured for some fluorinated molecules.

Experimental Section

Materials. DTBN was prepared by referring to Briere and Rassat.[10] 1-Bromo-2-iodoethane was synthesized according to the method of Simpson.[11] All other chemicals used in this study were commercially available.

^{13}C Nmr Measurement. Completely proton-decoupled ^{13}C nmr spectra were obtained at 15.1 MHz on a Jeolco C-60HL spectrom-

(1) Presented at the 10th Nmr Symposium of Japan at Tokyo, Oct 1971. Part VI: I. Morishima, K. Endo, and T. Yonezawa, *J. Chem. Phys.*, in press.

(2) Japan Electron Optics Laboratory Co. Ltd. (JEOL), Akishima, Tokyo, Japan.

(3) (a) I. Morishima, K. Endo, and T. Yonezawa, *J. Amer. Chem. Soc.*, 93, 2048 (1971); (b) *Chem. Phys. Lett.*, 9, 143 (1971); (c) *ibid.*, 9, 203 (1971); (d) I. Morishima, T. Inubush, K. Endo, and T. Yonezawa, *ibid.*, in press.

(4) D. P. Stevenson and G. M. Coppinger, *J. Amer. Chem. Soc.*, 84, 149 (1962); R. Anderson and J. M. Prausnitz, *J. Chem. Phys.*, 39, 1225 (1963).

(5) P. Datta and G. M. Barrow, *J. Amer. Chem. Soc.*, 87, 3053 (1965).

(6) D. A. Bahnick and W. B. Person, *J. Chem. Phys.*, 48, 1251 (1968).

(7) K. W. Morcom and D. N. Travers, *Trans. Faraday Soc.*, 63, 2063 (1966).

(8) Y. Y. Lim and R. S. Drago, *J. Amer. Chem. Soc.*, 93, 891 (1971); Y. Murata and N. Mataga, *Bull. Chem. Soc. Jap.*, 44, 354 (1971).

(9) I. Morishima, T. Yonezawa, and K. Goto, *J. Amer. Chem. Soc.*, 92, 6651 (1970); I. Morishima, K. Okada, T. Yonezawa, and K. Goto, *ibid.*, 93, 3922 (1971); I. Morishima, K. Okada, and T. Yonezawa, *ibid.*, 94, 1425 (1972).

(10) R. Briere, H. Lemaire, and A. Rassat, *Bull. Soc. Chim. Fr.*, 273 (1965).

(11) M. Simpson, *Ber.*, 7, 130 (1874).

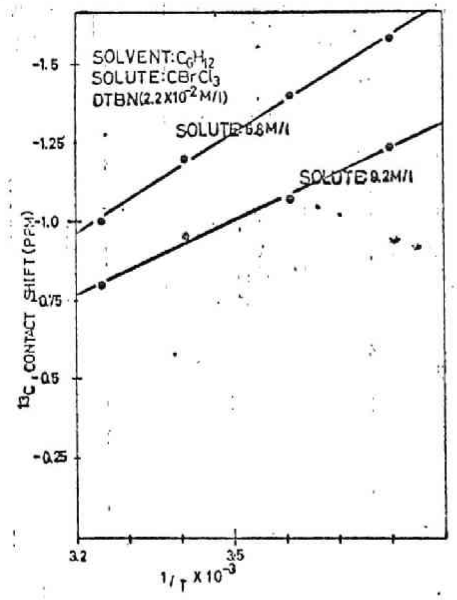

Figure 1. Curie law test of the ^{13}C contact shift for $CBrCl_3$.

eter equipped with the SD-HC heterospin decoupler and IS-60 field-frequency synchronous sweep system of the proton irradiating frequency. Spectra were measured with the external locking mode at various temperatures. ^{13}C chemical shifts were determined on an expanded scale (18 ppm per full scale) with the precision of ± 0.10 ppm. Samples were made in the neat liquid or cyclohexane solution in the absence or presence of the given amount of DTBN in the 8-mm sample tube. The ^{13}C chemical shift of cyclohexane was hardly affected by the addition of DTBN within an experimental error and was used as an internal reference for ^{13}C chemical shift measurements of halogenated molecules in the presence of DTBN radical. The susceptibility shift was also too small to be measured. Samples used for the determination of the equilibrium constant were made in the cyclohexane solution with various concentrations. The concentration of added DTBN radical was varied from 0 to 2×10^{-4} *M*. The DTBN-induced ^{13}C contact shift is the shift change from the diamagnetic solution to the paramagnetic one in the presence of a given amount of DTBN.

Results and Discussion

Halomethanes. The addition of DTBN radical to neat CCl_4 and $CBrCl_3$ caused substantial downfield shift of the ^{13}C chemical shifts of these molecules. However, they were hardly affected by the addition of diamagnetic donor molecules such as pyridine and triethylamine. The temperature dependence of DTBN-induced ^{13}C shifts followed the Curie law behavior, characteristic of the Fermi contact shift (Figure 1). Therefore, the downfield ^{13}C shift induced addition of DTBN is most probably attributable to the Fermi contact shift, indicating positive spin density on the carbon s atomic orbital. We have also observed downfield ^{13}C shifts induced by the addition of DTBN for CHX_3 and CH_2X_2 molecules where X = Cl, Br, and I. The shifts were proportional to the concentration of added DTBN. Figure 2 shows the linear plots of the observed ^{13}C shifts of various halomethanes *vs.* the concentration of DTBN at room temperature. It is generally seen that the ^{13}C contact shifts for halomethanes are in the order of X = I > Br > Cl. However, slightly upfield proton contact shifts for CH_2X_2 and CHX_3 molecules were almost the same or in the opposite trend, X = Cl > Br > I. Previously we have reported[3,12] DTBN-induced ^{1}H and ^{13}C contact shifts

(12) Paper VI: I. Morishima, K. Endo, and T. Yonezawa, *J. Chem. Phys.*, in press.

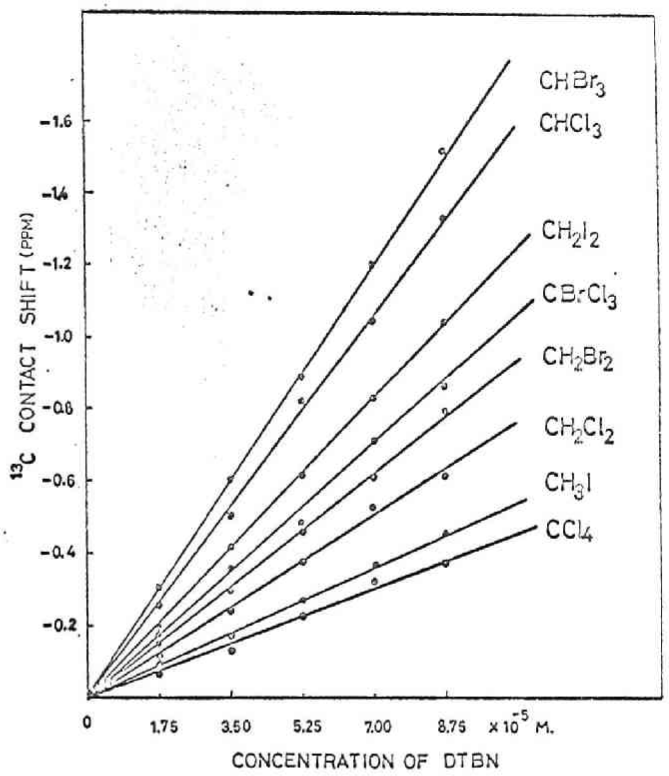

Figure 2. Observed ^{13}C contact shifts plotted against the concentration of DTBN.

for $CHCl_3$ and CH_2Cl_2 together with other proton donor molecules which were interpreted by the hydrogen bond between the C–H proton and the nitroxide oxygen or nitrogen.[12] Negative and positive spin densities on the proton and carbon, respectively, are induced by the spin polarization mechanism.[3,12] However, the above trend of the ^{13}C contact shifts for CHX_3 and CH_2X_2 (X = I > Br > Cl) is opposite to the hydrogen donor ability of these halomethanes. This suggests that C–X···DTBN interaction is important in these systems. As may be seen in Figure 2, $CBrCl_3$ shows even larger downfield ^{13}C contact shifts than CH_2X_2 (X = Cl and Br) molecules. Interaction here cannot involve the hydrogen bonding with DTBN. Therefore, the above observations immediately suggest the existence of an interaction between DTBN and halomethanes that is quite independent of any hydrogen bond. The ^{13}C contact shift behavior of solutions of halomethanes containing DTBN is that which would be expected if halomethanes form a CT complex with DTBN of the type C–X···DTBN. The CT character of halomethane–DTBN interaction can also be recognized experimentally (Figure 2) from the fact that the ^{13}C contact shift increases in the order $CBrCl_3 > CCl_4$ as might be expected. However, when we compare the results of CCl_4 and $CHCl_3$, the hydrogen bond with DTBN appears to be still important in the $CHCl_3$–DTBN system. For CHX_3 and CH_2X_2, both of the C–H···DTBN hydrogen bond and C–X··· DTBN CT interactions could concurrently occur. The CT interaction could induce positive spin density by the spin delocalization mechanism[9] which permits electron spin transfer from DTBN directly to the antibonding orbital of the C–X bond. The C–H···DTBN hydrogen bond also induces positive spin density on the carbon by the spin polarization mechanism as has been

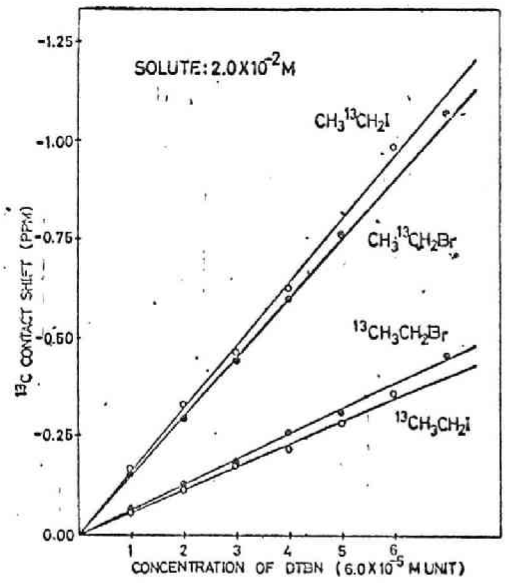

Figure 3. Observed ^{13}C contact shifts plotted against the concentration of DTBN for bromo- and iodoethanes.

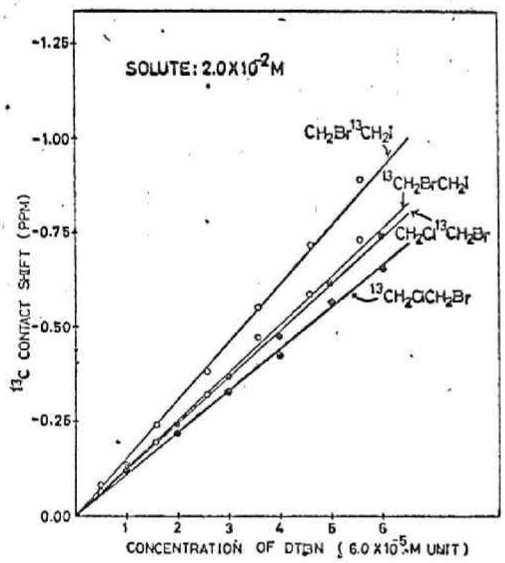

Figure 4. Observed ^{13}C contact shift plotted against the concentration of DTBN for 1,2-dihaloethanes.

revealed previously.[3,12] Therefore, the carbon of halomethanes senses positive spin density induced by the hydrogen bond and the CT interactions as in the following way.

DTBN···H–C–X hydrogen bond (spin polarization)

H–C–X···DTBN charge-transfer interaction

(spin delocalization)

In order to substantiate further the CT nature of DTBN···halomethane interaction, we have measured the ^{19}F and ^{13}C contact shifts of $CFCl_3$ induced by the presence of DTBN. The downfield shifts of both nuclei may support the CT interaction stated above.[13]

Haloethanes. Figures 3 and 4 show the plots of DTBN-induced ^{13}C contact shifts *vs.* the concentration

(13) We have observed the DTBN-induced ^{19}F nmr contact shift of $CFCl_3$ in 50 mol % CCl_4 solution using a Jeolco PS-100 spectrometer at 94.1 MHz. The addition of 1.5×10^{-1} *M* DTBN caused 0.15 ± 0.05 ppm downfield shift of the ^{19}F resonance for $CFCl_3$. The ^{13}C contact shift for the corresponding paramagnetic solution was 0.60 ± 0.10 ppm downfield shift.

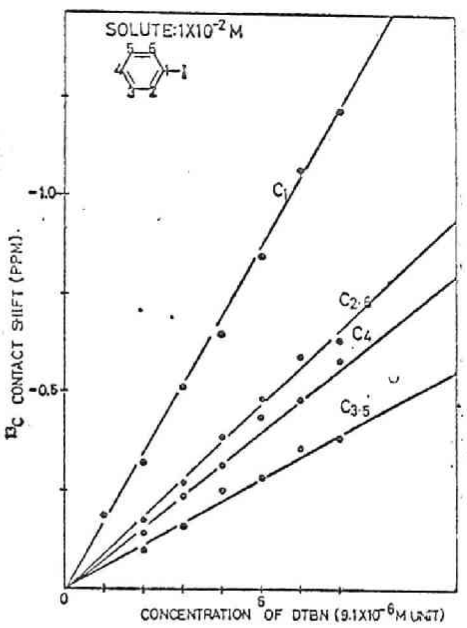

Figure 5. Observed ^{13}C contact shifts plotted against the concentration of DTBN for iodobenzene.

of DTBN for several haloethane molecules. The downfield ^{13}C contact shifts for the methylene carbon in ethyl halides are more pronounced for iodide than for bromide, while that for the methyl carbon is greater for bromide than for iodide. This trend of the ^{13}C contact shifts in the methyl group is easily expected if the methyl C–H proton interacts with DTBN as a proton donor in the C–H···DTBN hydrogen bond; the C–H proton of the methyl group in ethyl bromide is more acidic and therefore more susceptible to the hydrogen bond with DTBN than ethyl iodide. On the other hand, the ^{13}C contact shifts in the methylene carbon bonded directly to the halogen atom follow the trend encountered for halomethanes in the order of ethyl iodide > ethyl bromide. The preferential interaction of the C–I group with DTBN was also recognized from the greater downfield contact shift of C_2 than C_1 in 1-bromo-2-iodoethane (see Figure 4). For 1-chloro-2-bromoethane, preferential downfield shift of C_2 was observed, as expected. In addition to this C–X···DTBN interaction, the C–H···DTBN hydrogen bond interaction could occur concurrently for 1,2-dihaloethanes. However, the results of the ^{13}C contact shifts for these haloethanes strongly suggest relative importance of the C–X···DTBN CT interaction.

Halobenzenes. We have also studied the ^{13}C contact shift for the halobenzene–DTBN system. Figures 5 and 6 show the DTBN-induced ^{13}C contact shifts for bromo- and iodobenzenes. The substituted carbon (C_1) of iodobenzene exhibits quite sensitively greater downfield contact shift than other ring carbons. On the other hand, the C_1 resonance of bromobenzene is quite insensitive to DTBN, compared with other ring carbons. This was also confirmed from the facts that in chlorobenzene the substituted C showed a slightly upfield DTBN-induced shift while the other C's exhibited substantial downfield shifts comparable with those in iodo- and bromobenzenes. These results show that the C–I···DTBN interaction in iodobenzene is important while in bromo- and chlorobenzenes the

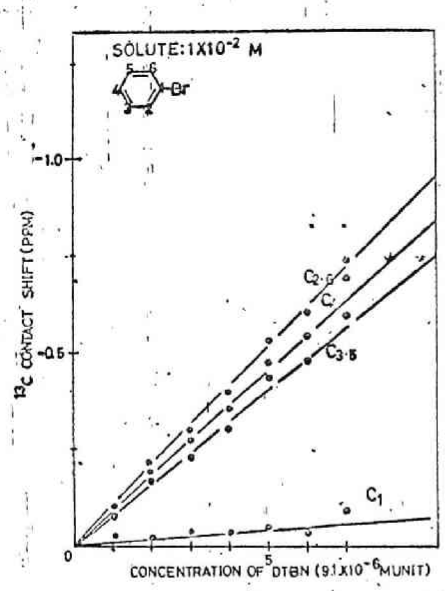

Figure 6. Observed ^{13}C contact shift plotted against the concentration of DTBN for bromobenzene.

C–H···DTBN hydrogen bond interaction is predominant. The fact that the aromatic C–H group can act as a proton donor to DTBN has previously been shown for various aromatic hydrocarbons.[14] The carbon of benzene exhibited substantial downfield ^{13}C contact shift by the addition of DTBN.[14] The aromatic carbon senses positive spin density induced by the C–H···DTBN hydrogen bond through the spin polarization mechanism.[14] The substituted carbon of nitrobenzene in which the nitro group is inert to DTBN showed *upfield* contact shift while other ring carbons exhibited usual downfield contact shifts (Figure 7). This upfield ^{13}C contact shift for C_1 in nitrobenzene is possibly due to the negative spin density induced by the C_1–C_2–H···DTBN interaction through the spin polarization mechanism (see below). Of course, in halobenzenes the C_2–H···DTBN hydrogen bond induces negative spin density on the substituted carbon and reduces positive spin density induced by the C_1–X···DTBN CT interaction. This is probably responsible for quite a small magnitude of downfield contact shift for C_1 of bromobenzene.

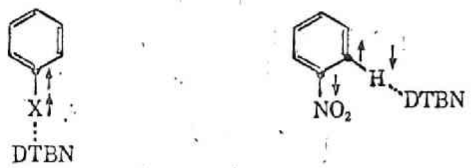

charge transfer interaction (spin delocalization) — hydrogen bond interaction (spin polarization)

In chlorobenzene, positive and negative spin densities on C_1 induced by both interactions cancel; this appears to be responsible for the observation of a slightly upfield ^{13}C contact shift of the substituted C. In fluorobenzene, DTBN-induced ^{13}C shifts were quite similar to those in nitrobenzene; the substituted C was shifted upfield and other carbons were moved downfield. This finding implies the relative importance of the C_2–H···DTBN hydrogen bond compared with the C_1–F···DTBN interaction. In nitro- and

(14) Paper IV: I. Morishima, T. Matsui, T. Yonezawa, and K. Goto, *J. Chem. Soc., Perkin Trans. 2*, 633 (1972).

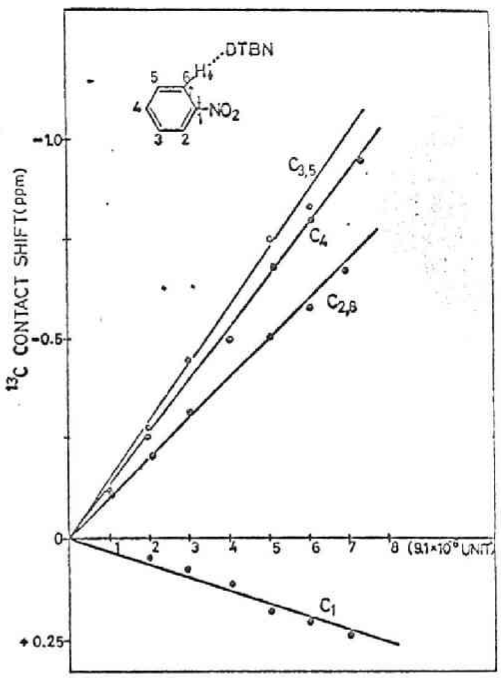

Figure 7. Observed ^{13}C contact shift plotted against the concentration of DTBN for nitrobenzene.

fluorobenzenes with the electronegative substituent, the C_2–H bond is more acidic and susceptible to the hydrogen bond with DTBN, which induces negative spin density on the C_1. We have also measured the ^{19}F contact shift for fluorobenzene. The observed downfield ^{19}F contact shift may suggest that there is still weak CT interaction between the C–F bond and DTBN. These findings for halobenzenes correspond reasonably to the preferential donor–acceptor interaction between C–X bond and DTBN radical.

Equilibrium Constants and Limiting Contact Shifts. To facilitate a quantitative analysis of the interaction between DTBN radical and halogenated molecules, the formation constant, limiting contact shift, and spin density on the carbon are needed. There is a vast literature on the spectrophotometric study of weak CT complexes. For the 1:1 donor–acceptor complex formation between halomethane and DTBN with the condition of $[A]_0 \gg [D]_0$, the following linear equation is obtained[15]

$$1/\Delta = 1/K[D]_0\Delta_0 + [A]_0/[D]_0\Delta_0$$

where K is the formation constant, $[A]_0$ and $[D]_0$ are the initial concentration of electron acceptor (halomethane) and electron donor (DTBN), respectively, Δ_0 the limiting ^{13}C contact shift for the pure complex relative to the ^{13}C shift for the free halomethane, and Δ is the observed ^{13}C shift of halomethane in the presence of DTBN relative to the free halomethane. However, as shown by Person[16] and Deranleau,[17] simultaneous evaluation of K and Δ_0 values for weak complex formation is difficult and these values obtained from the above straight-line fitting procedure should contain substantial uncertainty. The separation of

(15) R. Foster and C. A. Fyfe, "Progress in Nmr Spectroscopy," Vol. 4, Pergamon Press, Oxford, 1969.
(16) W. B. Person, *J. Amer. Chem. Soc.*, 87, 167 (1965).
(17) D. A. Deranleau, *ibid.*, 91, 4044 (1969).

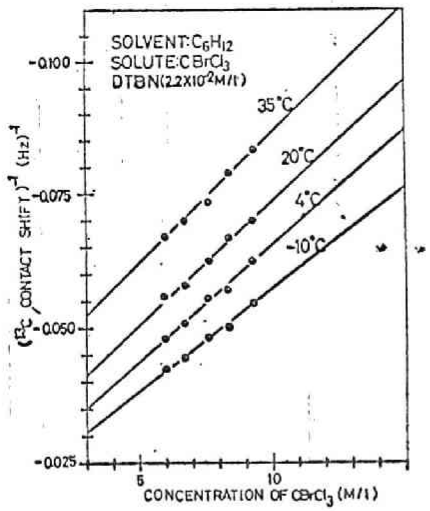

Figure 8. Plots of the inverse of the observed ^{13}C contact shifts against the initial concentration of $CBrCl_3$ at various temperatures.

K and Δ_0 requires special conditions that K is large and DTBN is completely complexed.[16,17] However, this is rarely possible. In this respect, we carried out only order estimation of K and Δ_0 values by the above standard procedure. Therefore, the results of K and the limiting ^{13}C contact shifts are not realistic when we use these values for a quantitative discussion.

Figure 8 shows the linear plots of $1/\Delta$ *vs.* the initial concentration of $CBrCl_3$, as an example, at various temperatures. The K values at various temperatures obtained from these linear plots lead to the heat of complex formation. The results are summarized in Table I. According to the critical works of Person and Deranleau, it is generally possible to make an error analysis of K and Δ_0. However, in our case where $[A]_0 \gg [D]_0$ and the signal of A is observed, the equations of Deranleau are not applicable. Therefore,

Table I. Approximate Values of Formation Constant, Limiting ^{13}C Contact Shift, Heat of Complex Formation, and Spin Densities on the Carbon for CH_2Br_2 and $CBrCl_3$–DTBN Interactions

T, °K	K, l./mol[a]	ΔH, kcal/mol[b]	Limiting ^{13}C shift,[c] ppm	Spin density,[d] ρ_C
		CH_2Br_2		
306	0.28		−250	0.00102
293	0.38	−3.8	−280	0.00102
279	0.50		−300	0.00113
268	0.63		−310	0.00113
				Av 0.00108
		$CBrCl_3$		
308	0.12		−650	0.00270
293	0.14	−1.7	−710	0.00280
277	0.17		−740	0.00280
263	0.20		−810	0.00290
				Av 0.00280

[a] Uncertainty of the K value is ±0.20 l./mol at least. [b] Uncertainty of the ΔH value is at least ±2.5 kcal/mol. [c] Uncertainty of the limiting shift is at least 150 ppm. [d] Spin density on the carbon was obtained from the limiting ^{13}C contact shifts by using the equation, $(\Delta H/H = -a_C(\gamma_e g\beta S(S+1)/\gamma_e 3kT)$ where $a_C = -820.10\rho_C$ (see ref 12 and 19).

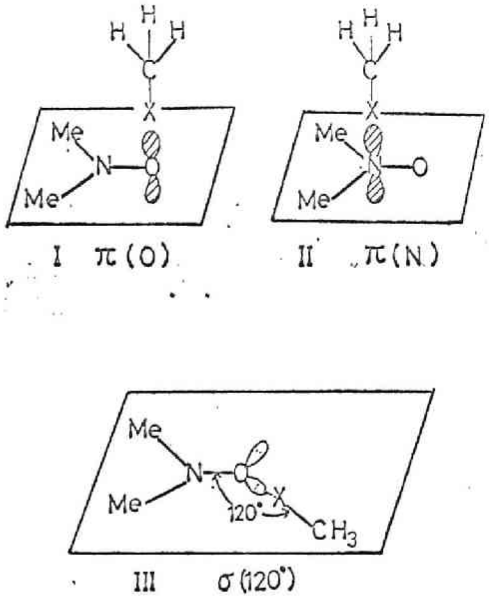

Figure 9. Models of the $CH_3X\cdots$DMNO bimolecular system with various configurations.

the results in Table I may have serious uncertainty.[18] Only order of magnitude is important. It is likely that the observed trend of ^{13}C contact shifts for halomethanes results partly from the difference in K values and partly from the large difference in the limiting ^{13}C contact shifts. It is also probable that the ΔH values for adducts of the nitroxide radical with halomethanes appear to be not so different from those for the diamagnetic donor–acceptor interactions.[4–7]

A Theoretical Study on the Halomethane–Dimethyl Nitroxide Bimolecular System by Molecular Orbital Calculations. In order to substantiate theoretically the DTBN-induced ^{13}C contact shift for halogenated molecules and to elucidate the nature of DTBN–halomethane interaction, we have performed unrestricted Hartree–Fock MO calculations (INDO–SCF method)[19] on the DMNO (dimethyl nitroxide)–halomethane bimolecular system. This type of MO calculation has been proved to be successful in reproducing spin densities and interaction energies for the proton donor–DMNO hydrogen bonding system. INDO–MO calculations were carried out here for the H_3C–X$\cdots$DMNO bimolecular system arranged in the three geometries (Figure 9).[20] In models I (π(O)) and II (π(N)), the C–X bond is placed perpendicularly over the $p\pi$ orbital of the oxygen and nitrogen atoms of DMNO, respectively, while in model III (σ(120°)) the C–X bond is placed on the σ plane and directed toward an oxygen lone-pair orbital (the N–O–X angle = 120°). We have examined fluoride and chloride for CH_3X in INDO calculations.

The results are summarized in Table II. Figures 10 and 11 show the stabilization energies varying with

(18) According to Deranleau,[17] the limit for accurate simultaneous determination of K and Δ_0 constants is approximately $0.2 \leq s \leq 0.8$ where s is the saturation fraction and equivalent to $[AD]/[D]_0$ in the present case. However, in the present study we cannot estimate the s value.

(19) J. A. Pople, D. L. Beveridge, and P. A. Dobosh, *J. Chem. Phys.*, 47, 2026 (1967); J. A. Pople, D. L. Beveridge, and P. A. Dobosh, *J. Amer. Chem. Soc.*, 90, 4201 (1968).

(20) The d orbitals are not considered in the INDO method even though these undoubtedly play a significant role in reality.

Table II. INDO-MO Calculations for the $CH_3X\cdots$Dimethyl Nitroxide Bimolecular System

Complex model	X	R, Å	ΔE,[a] kcal/mol	Calculated spin density on CH_3X $\rho_{C(2s)}$	$\rho_{X(2s)}$	$\rho_{\pi(1s)}$	a_N,[b] Gauss	Δq_C[c]	Δq_X[c]	$\Delta\rho_{CX(p-\sigma)}$[d]	$\Delta\rho_{CX(s-s)}$[d]
I π(O)	F	1.5	20.3	0.0369	0.0177	−0.0022	−3.15	+0.132	−0.291	−0.013	−0.026
	Cl	1.5	4.8	0.0249	0.0407	−0.0023	−2.50	+0.005	−0.007	−0.059	+0.027
II π(N)	F	1.5	6.0	0.0298	0.0169	−0.0007	+4.21	+0.187	−0.267	−0.004	−0.047
III σ(120°)	F	1.5	4.3	−0.0026	−0.0031	0.0004	+0.58	+0.152	+0.142	+0.217	−0.046

[a] $\Delta E = E - E_\infty$, the energy of stabilization. The R values are at the energy minimum. [b] The change of the a_N value for DMNO caused by $CH_3X\cdots$DMNO interaction. The plus and minus signs mean the increase and decrease in the a_N value, respectively. a_N was obtained by $a_N = 379.34\rho_{N(2s)}$ (ref 12). [c] Δq_C and Δq_X denote the change in the total charge densities on the carbon and halogen atoms in CH_3X. The plus and minus signs mean the increase and decrease in electron densities. [d] $\Delta\rho_{CX(p-\sigma)}$ and $\Delta\rho_{CX(s-s)}$ mean the change in the total p–σ and s–s bond orders for the C–X bond in CH_3X. The plus and minus signs mean the increase and decrease in the bond order.

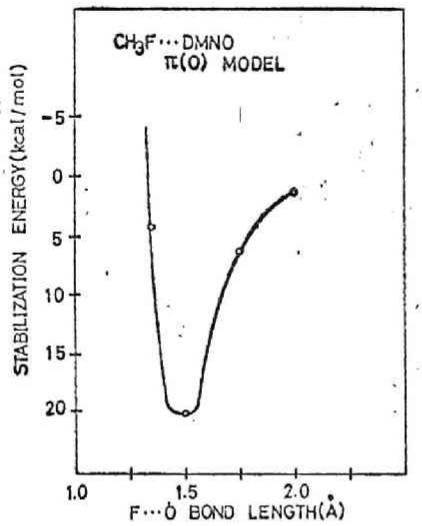

Figure 10. INDO stabilization energy curve plotted against the F···O distance for CH_3F–DMNO bimolecular system (the π(O) model).

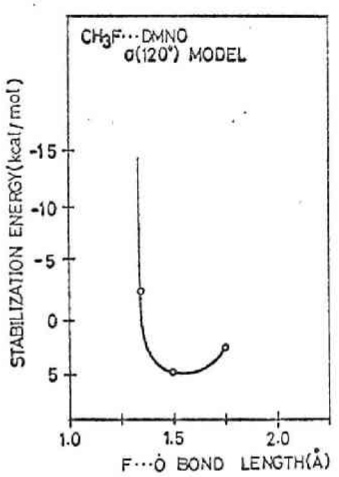

Figure 11. INDO stabilization energy curve plotted against the F···O distance for CH_3F bimolecular system (σ(120°) model).

X···O (or N) distance for methyl fluoride. The energy of stabilization, ΔE, was obtained at R (X···O (or N) distance) = 1.5 Å for most of the bimolecular systems. The results of calculated spin densities allow us to conclude that the π model is responsible for the downfield ^{13}C contact shift of halomethane interacting with DTBN. This is also the case for the hydrogen bond with DTBN.[3,12] Positive spin density is induced both on the X and C 2s atomic orbitals, which is possibly due to the electron spin transfer directly to the C–X antibonding orbital by the spin delocalization mechanism. This should be compared with the results for the case of the C–H···DMNO hydrogen bond in which negative and positive spin densities are induced on the proton and carbon s atomic orbitals by the spin polarization mechanisms.[3,12]

Quite a large value of the stabilization energy is obtained for the π(O) model of fluoromethane, compared with the other two models. However, when we use tentatively the input parameters (I_p, E_A, and β)[21] of chlorine in place of fluorine atom and other variables, such as various types of integrals in INDO method, are not varied, we obtain quite a reasonable value of the stabilization energy (4.8 kcal/mol), comparative with the experimental value. Spin density, on the other hand, appears to be rather insensitive to the above parametrization (Table II). Therefore, comparison between calculated stabilization energy and observed interaction energy is not realistic in the present case, but it seems worthwhile to compare the theoretical and experimental values of spin density on the carbon of CH_3X. Quite a small value of observed spin density on the carbon (Table I), compared with the theoretical value for the π(O) or the π(N) model, may allow us to expect the contribution of the σ(120°) model in addition to the π model; the σ model yields negative spin density on the carbon and diminishes the absolute value of the positive spin density. The importance of the σ model has also been encountered for the hydrogen bond between proton donor and nitroxide radical.[3,12] However, it should be noted that the π model is responsible for the observed value of the positive spin density on the carbon.

Another feature of the results of INDO calculations (Table II) is that the hyperfine coupling constant of nitrogen, a_N, in DMNO is substantially affected by halide–DMNO interaction. The experimental study on the solvent effect of a_N showed that the a_N value is slightly increased on going from cyclohexane to CCl_4 or to $CBrCl_3$.[22] This trend is reproduced by the calculation for models II and III. Also in this sense, the contribution of the σ model should not be ignored.

Table II also contains the changes of charge density and bond order due to the C–X···DMNO complex

(21) The UHF–INDO calculations including chlorine atom are not available in the original method.[19]

(22) We have studied the solvent effect of a_N of DTBN in the various halomethane solvents using Jeolco 3BX esr spectrometer with a 100-Kc modulation. The value of a_N increased slightly on going from CCl_4 (15.30 G) to $CBrCl_3$ (15.40 G). In both solvents a_N is larger than in cyclohexane (15.20 G). This trend of experimental results is in agreement with the Drago's recent work (ref 8).

formation. The results for the σ model show that total charge densities on the F and C atoms increase and s–s and p–σ bond order between C add F atoms decreases. This indicates that in the above complex formation halomethane accepts the electron into the antibonding orbital of the C–X bond, causing the weakening of the C–X bond. In fact, when DTBN was added to the solution of CHI_3, they reacted immediately and no esr signal was observed. For CH_2I_2 solution, this reaction was slow and the esr signal gradually disappeared. These results appear to correspond with the above interpretation of the charge-transfer interaction.

Finally we briefly comment on the charge-transfer interaction between free radical and halomethane in light of the mechanism of the halogen abstraction reaction. Recently it has been suggested[23] that the transition state of the halogen abstraction reaction process produces anionic character on the carbon from which the iodine is being removed.

$$R\text{–}I + \cdot Rad \longrightarrow [R^{\delta-}\cdots I\cdots Rad^{\delta+}] \longrightarrow \cdot R + I\text{–}Rad$$

The above scheme corresponds to the abovementioned charge-transfer model of the transition state in which an odd electron transfers to the antibonding orbital of the R–X bond, causing the release of the C–X bond.[24] The anionic character and release of the C–X bond was well reproduced by INDO–MO calculations for the model molecule, CH_3F. The failure to observe the esr spectrum and the ^{13}C contact shift of the CHI_3 + DTBN system may result from the strong CT interaction, leading to the iodine abstraction reaction. It has been shown by Fukui, *et al.*,[25] that the polarographic reduction potential of haloalkanes is connected with the energy of their lowest unoccupied σ level. The parallel relation between the DTBN-induced ^{13}C contact shift and reduction potential ($E_{1/2}$) [$CHBr_3$ ($E_{1/2}$ = −0.64) > $CHCl_3$ (−1.67), CH_2I_2 (−1.12) > CH_2Br_2 (−1.48) > CH_2Cl_2 (−2.33)][25] also shows that the lowest unoccupied orbital is important in the DTBN–halomethane interaction.

Acknowledgment. We are greatly indebted to Professor H. Kato and Mr. K. Okada for helpful discussions. Technical assistance of Mr. T. Matsui in the ^{13}C nmr measurements is also gratefully acknowledged.

(23) W. C. Danen and D. G. Saunders, *J. Amer. Chem. Soc.*, 91, 5924 (1969); W. C. Danen and R. L. Winter, *ibid.*, 93, 716 (1971).

(24) A similar discussion along with the CT interaction has been made on the photochemical halogen abstraction reaction of halomethanes in the presence of amines using as the electron donor (see ref 4).

(25) K. Fukui, K. Morokuma, H. Kato, and T. Yonezawa, *Bull. Chem. Soc. Jap.*, 36, 217 (1963).

Chapter 4. Conclusion

In part II of the present thesis, the author aimed to show that the ^{1}H and ^{13}C n m r contact shifts are quite sensitive to the presence of a small amountof a stable free radical and the resulting ^{1}H and ^{13}C contact shifts are very useful for the studies of weak molecular interactions.

In Chapter 2, the intermolecular interaction between the proton-donor molecules and the nitroxide radical was investigated by the n m r contact shifts measurements and molecular orbital calculations. In section 2 the author mentions a correlation between ^{13}C contact shifts and ^{13}C-H nuclear spin coupling constants. This correlation is explained in terms of finite perturbation theory of nuclear spin coupling constants in which the ^{13}C-H coupling constant is related to the electron spin density of the ^{13}C nucleus induced when spin density is placed finitely on the proton. The potential utility of this relation in the prediction of sign and magnitude of long-range ^{13}C-H coupling constants was stated. In section 4, in order to provide fruitful information on the nature of the hydrogen bond between the proton donor molecules and a DTBN radical, ^{1}H and ^{13}C Fermi contact shifts induced by the hydrogen bond with DTBN radical were observed for various proton-donor molecules. The upfield ^{1}H contact shifts and downfield ^{13}C contact shifts of the donor molecules are interpreted in terms of the spin polarization mechanism of electron spin transfer from DTBN to the protic substances. The formation constants, enthalpies, limiting ^{1}H and ^{13}C contact shifts and spin densities on the H and C atoms were determined for the proton donor/DTBN hydrogen bond interaction from ^{1}H and ^{13}C contact shifts measurements at various temperatures. Also the theoretical studies on this closed-and open-shell bimolecular system are performed by unrestricted Hartree-Fock SCFMO(INDO method) calculations.

The hydrogen-bond energies and spin densities on the X-H molecules were well reproduced by MO calculations.

Chapter 3 described ^{13}C n m r contact shifts study of the electron donor-acceptor interaction between halogenated molecules and the nitroxide radical. These results are interpreted in terms of the charge-transfer interaction between the DTBN radical and halogenated molecules in the manner of C-X...DTBN interaction. Approximate values of the formation constants enthalpies, limiting ^{13}C contact shifts and spin densities on the carbon were determined for this C.T. complex formation. Also MO calculations reproduced the stabilization energies and spin densities on the DTBN is transferred directly onto the C-X antibonding orbital of halomethane by the spin delocalization mechanism.

PART III

NUCLEAR RELAXATION OF THE HYDROGEN BOND IN PROTON DONOR/A FREE RADICAL SYSTEM

Part III

Chapter 1. Introduction

Since the experiment of Bloch, Hansen and Packard[1] for protons in aqueous solution of Fe^{3+} ions, investigations on the proton relaxation time in various solutions of paramagnetic ions and solutions of organic free radicals have been carried out by the nuclear magnetic resonance technique. The relaxation times of nuclei in various circumstances give the useful informations in the dynamic field.

The relations describing the spin-lattice and spin - spin relaxation[2,3] of nuclei due to coupling with a paramagnetic species depend upon the nature of the chemical interaction between the diamagnetic molecules under observation and the paramagnetic species. There exists three cases,

(a) no chemical interaction,

(b) formation of a labile complex,

(c) formation of a nonlabile complex (i. e., one whose lifetime is long compared with the difference between the relaxation times of the nucleus under observation in the complexed and uncomplexed species).

In each case the nucleus-electron relaxation has both dipolar and scalar components. When there is no chemical interaction between the diamagnetic and paramagnetic species, the nucleus-electron coupling is intermolecular and the dipolar component is modulated by relative translational diffusion.[2] Also, when molecules containing the nucleus under observation form a complex with those containing the electron spins, the nucleus-electron coupling is modulated by rotational motion[3] of the complex as a whole. (It is assumed that contributions from uncomplexed paramagnetic species are negligible.)

For proton-donor/a free radical hydrogen-bond system which belongs to the case(b), the author considers that the uncleus-electron relaxation has the dipolar rotational and translational contributions and scalar coupling term.

Until now, although many investigations have been done on the proton relaxation times in various solutions of paramagnetic ions and some in solutions of organic free radicals, similar work does not appear to have been made for proton-donor/DTBN radical hydrogen-bond system. Here the author aims to obtain informations about dynamic behaviors for this hydrogen-bond system, by exploring the effect of a dissolved free radical upon relaxation mechanism of the proton-donor nuclei.

In Chapter 2, the author describes the study on the proton relaxation of the hydrogen bond in proton-donor/DTBN radical system. This study will extend the informations about the hydrogen-bond in that system described in Part II.

Refernces

1. F.Bloch, W.W.Hansen, and M.E.Packard, Phys.Rev. 70, 474,(1946).
2. P.S.Hubbard,Proc.Roy.Soc.(London) A291,537(1966).
3. D.R.Eaton and W.D.Phillips, advances in Magnetic Resonance, edited by J.S.Waugh(Academic, New York, 1965), Vol.1,Chap.3.

Chapter 2. ^{1}H Relaxation of the Hydrogen Bond in Proton-Donor/A Free Radical System.

1. Introduction

Recently Morishima et al. [1] have reported a series of studies on the interactions between the closed- and open-shell molecules by the measurements of n m r contact shifts, using free radicals and paramagnetic metals as "a spin label reagent." Their papers gave worthy informations on the molecular interactions between the closed-shell molecules and free radicals; the hydrogen-bond and the charge-transfer interactions. However the useful informations about intermolecular dynamic behaviors cannot be obtained from their studies standing a static view-point. Thus, here, the author attempts to investigate the relaxation mechanisms for protic substances / a free radical system.

Already there have been some works on the interactions between free radicals and solvent molecules by the pulse n m r and nuclear-electron double resonance experiments. Gutowsky et al. [2] studied the solvent-effects from measurements of the relaxation times by the pulse methods. They described that the ^{1}H relaxation mechanism for solvent free radicals systems was explained by nucleus-electron dipole-dipole interaction from a combination of translational and rotational motions. Kramers et al. [3] and Dewek et al. [4] pointed out that, from the dynamic nuclear polarization experiments, proton and electron spin relaxation in organic solutions of free radicals results from a pure dipole-dipole interaction governed by translational random motions of the spin-carrying molecules.

In this thesis, the author performs the ^{1}H relaxation study using the high-resolution n m r, in order to obtain the new informations on the relaxation mechanism, chemical exchange lifetimes, activation

energies and the closest distance that the proton approaches the odd electron for proton-donor/DTBN radical H-bond system.

2. Experimental section

Materials; DTBN was prepared by referring to Briere and Rassat. All samples were redistilled, sealed under vacuum by the freeze-thaw pump technique in order to eliminate dissolved oxygen. All samples containing DTBN were stored in liquid nitrogen.

nmr measurement; ^1H spectra in wide temperature ranges were obtained at a Varian HR220MHz spectrometer. All other ^1H spectra in frequency ranges were measured by Jeolco 60 and 100 MHz spectrometers. The spin-lattice relaxation time T_1 was measured by a Jeolco pulsed F.T. spectrometer at 100 MHz. The line shape of ^1H spectra is assummed to be lorentzian type. All T_2's were evaluated from the half widths which are full width at half height.

3. Results and Discussions

a) Preliminary Studies

First, the dependence of the proton T_2 upon the concentration of DTBN in proton-donor molecules was measured at room temperature. The observed values of $1/T_2$ for the DTBN solutions are plotted vs. concentration in Fig. 1. The linear relation found is well within experimental error over the concentration range studied, up to 4.2×10^{-4} M in DTBN, which predicts for relaxation governed by nucleus-free radical interactions.

Then the frequency-dependence of T_2 at room temperature was measured for the proton donor/DTBN radical system shown in Fig. 2. The experimental data was analyzed by Swift and Connick [5] Eqs..

Figure 1. Concentration dependence of the ^1H relaxation time, T_2, in the proton-donor/DTBN radical H-bond system.

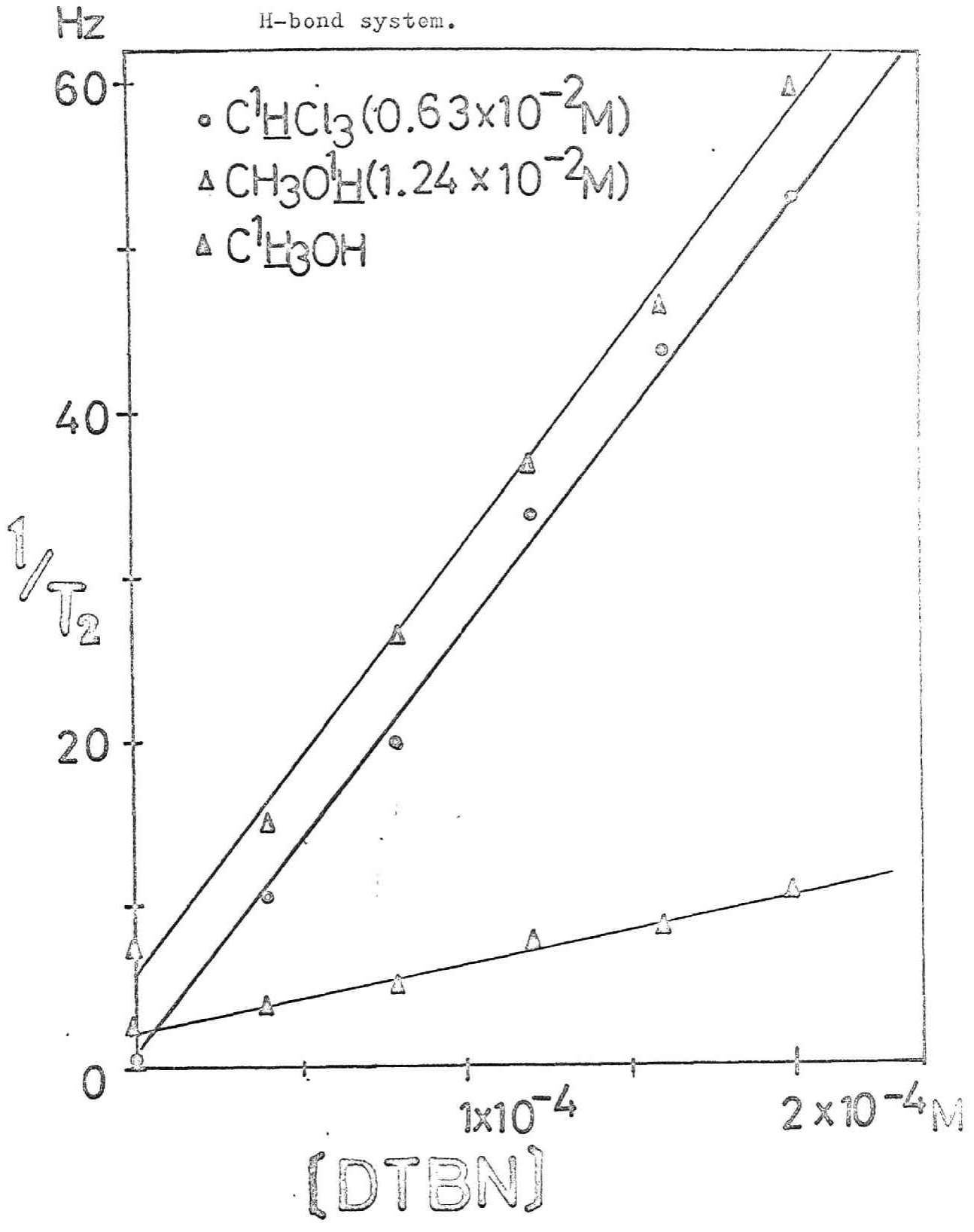

According to their theory, when the chemical exchange is rapid, the two following limiting cases are considered;

(a) $1/\tau_M^2 \gg \Delta\omega_M^2 \gg 1/T_{2M}\tau_M$; $1/T_2 = P_M \tau_M \Delta\omega_M^2$ (1)

(b) $1/(T_{2M}\tau_M) \gg 1/T_{2M}^2, \Delta\omega_M^2$; $1/T_2 = P_M/T_{2M}$ (2)

where τ_M is the lifetime for the chemical exchange, $\Delta\omega_M$ is given by Bloembergen [6], T_{2M} is the transverse-relaxation time which has been considered by Bloembergen et al. [7] and Solomon [8], and T_2 means the observed transverse-relaxation time.

For the four proton-donor molecules in Fig. 2, T_2 does not depend upon the frequency, so we can deal with the proton-donor/radical H-bond system as the case of (b). Therefore, T_2 in this system can be discussed by Bloembergen et al. and Solomon. Under the condition $\omega_I \tau_c \ll 1$, the equation(2)[11] is

$$\frac{1}{T_2} = \left(\frac{1}{T_2}\right)_{rot} + \left(\frac{1}{T_2}\right)_{trans} + \left(\frac{1}{T_2}\right)_{ex}$$

$$= \frac{\gamma_I^2\gamma_S^2\hbar^2 Nn}{20r_0^6 N_0}\left(7\tau_c + \frac{13\tau_c}{1+\omega_S^2\tau_c^2}\right) + \frac{2\pi\gamma_I^2\gamma_S^2\hbar^2}{30r_0'^3}N\left(7\tau_{c'} + \frac{13\tau_{c'}}{1+\omega_S^2\tau_{c'}^2}\right)$$

$$+ \frac{1}{4}\left(\frac{A}{\hbar}\right)^2 \frac{N}{N_0} n\left(\tau_e + \frac{\tau_e}{1+\omega_S^2\tau_e^2}\right) \quad (3)$$

r_0 = the effective separation between the nucleus and the odd electron.

r_0' = the closest distance that the nucleus approaches the odd electron.

N = the solute particles per milliliter.

N_0 = the solvent particles per milliliter.

n = the number of solvent molecules in solvation sphere.

τ_c = the correlation time for the rotation.

$\tau_{c'}$ = the correlation time for the translation.

τ_e = the correlation time for the exchange coupling.

Figure 2. A log-log plot of the frequency dependence of the proton T_2 in the proton-donor...DTBN radical system.

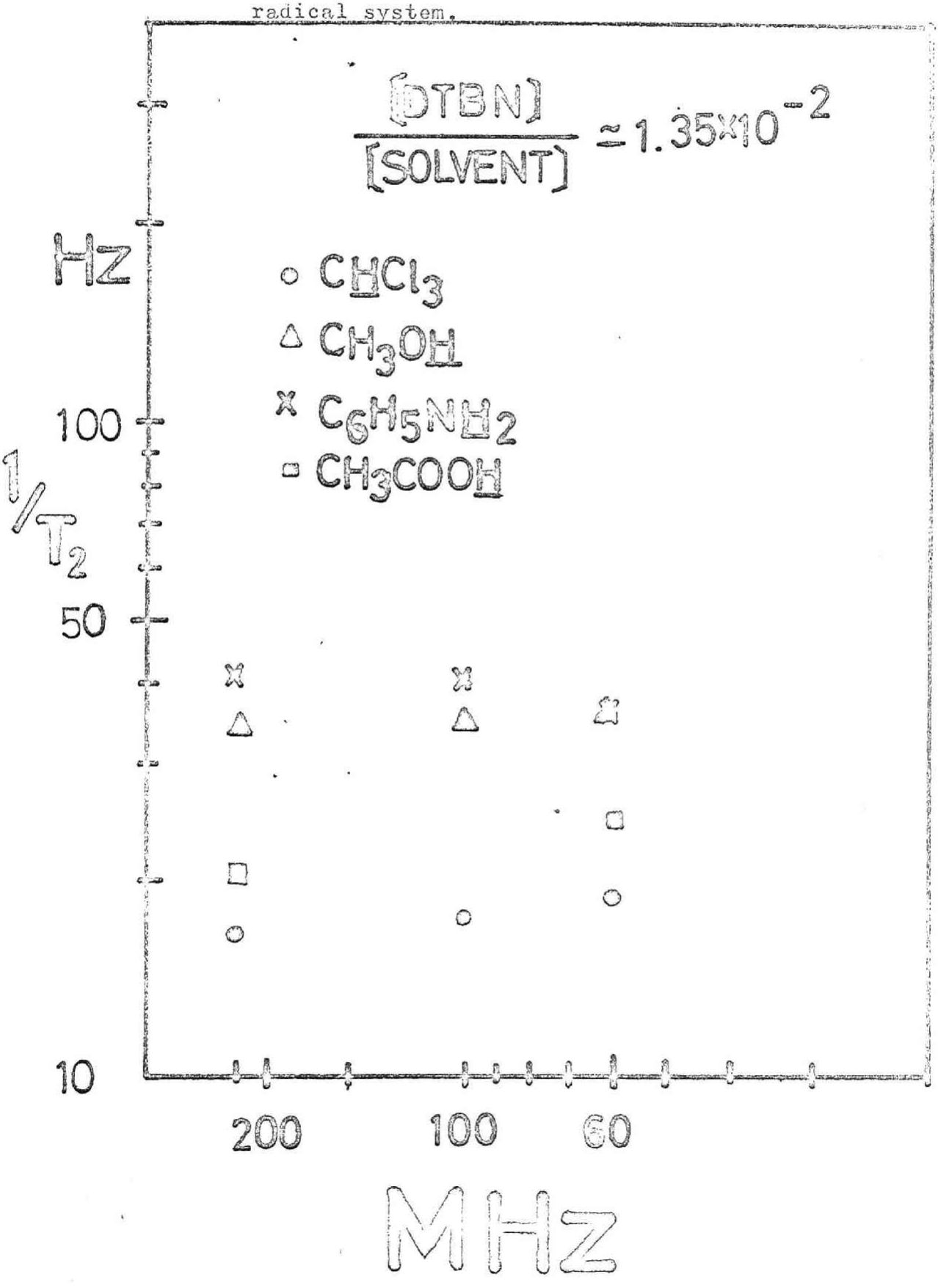

Also, the spin-lattice relaxation time T_1 is given as follows;

$$\frac{1}{T_1} = \left(\frac{1}{T_1}\right)_{rot} + \left(\frac{1}{T_1}\right)_{trans} + \left(\frac{1}{T_1}\right)_{ex}$$

$$= \frac{\gamma_I^2 \gamma_S^2 \hbar^2 N}{10 r_0^6 N_0} n \left(3\tau_c + \frac{7\tau_c}{1+\omega_S^2 \tau_c^2}\right) + \frac{2\pi N \gamma_I^2 \gamma_S^2}{15 r_0'^3} \hbar^2 \left(3\tau_{c'} + \frac{7\tau_{c'}}{1+\omega_S^2 \tau_{c'}^2}\right)$$

$$+ \frac{1}{2}\left(\frac{A}{\hbar}\right)^2 \frac{N}{N_0} n \left(\frac{\tau_e}{1+\omega_S^2 \tau_e^2}\right) . \qquad (4)$$

In addition, a search was made for T_1/T_2 ratios using three solutions of $CHCl_3$, CH_3OH and $C_6H_5NH_2$. These values are summarized in table 1. It is shown that the T_1/T_2 ratios fall in the narrow range about $1.1 \sim 1.2$. These results indicate the predominance of nucleus electron dipole-dipole relaxation, as seen readily from Eqs.(3)and(4). The small differences from unity can result from the internuclear scaler coupling and from the diffusional shortening of T_2.

b) Relaxation by the exchange coupling

It can be seen from Eqs.(3)and(4)that the T_1/T_2 ratio would differ significantly from unity if $(A/\hbar)^2 \tau_e$ were comparable to, or larger than, the dipole-dipole contribution to $1/T_1$ and if $\omega_S \tau_e \gg 1$. The value of τ_e is the sum of two terms

$$1/\tau_e = 1/\tau_s + 1/\tau_h , \qquad (5)$$

where τ_h is the lifetime of the solvated complex characterized by the effective hyperfine interaction constant A, and τ_s is

Table 1. Relaxation times and chemical exchange liftetimes for proton-donor/DTBN radical system at 100 MHz and 24.5°C.

Proton-donor molecules (0.5ml)	DTBN (M)	T_1 (m sec)	T_2 (m sec)	T_1/T_2	A_H[10] (MHz)	τ_e (sec)
$C^1\underline{H}Cl_3$	8.4×10^{-5}	19.6±1.3	16.9±0.9	1.16	1.3	$(0.9\times10^{-11})^{n=4}$
$CH_3O^1\underline{H}$	8.4×10^{-5}	14.8±1.1	13.8±0.7	1.07	1.2	(1.7×10^{-11})
$C_6H_5N^1\underline{H}_2$	8.4×10^{-5}	8.4±0.8	7.5±0.3	1.15	0.18	1.0×10^{-9}

(10) I.Morishima, K.Endo and T.Yonezawa, J.Chem.Phys., in press (1973)

Contact Shift

$$\Delta H/H = -(\gamma_e/\gamma_H) \cdot s(s+1)A_H/(3kT)$$

the spin-lattice relaxation time of the odd electron.

In the free-radical solutions, $\tau_h \ll \tau_s$ [9] and τ_e is governed by τ_h. Thus the lifetime τ_e (τ_h) for the solvated complex (the chemical exchange) can be estimated by assuming that the T_1/T_2 of 1.07~1.15 in table 1 differ from 1 because of the exchange interaction and $\omega_s^2 \tau_e^2 \gg 1$.

Upon combining this ratio with Eqs.(3)and(4), we find for $CHCl_3$/DTBN H-bond system,

$$0.16(1/T_1) \simeq 1/4(A_H/\hbar)^2(N/N_o)n\tau_e \qquad (6)$$

Here, the value for A_H has already obtained from ^1H nmr contact shifts [10], and a reasonable value for n is 4 to 10. [2]

In table 1, τ_h for n= 4 was given . The results for $CHCl_3$ and CH_3OH are too small, which makes $\omega_s \tau_e \simeq 1$: these do not satisfy the condition of $\omega_s^2 \tau_e^2 \gg 1$. However, it may be stressed that one can estimate the order of τ_h in this H-bond system for the first time.

c) Temperature-Dependence Studies

If the motions responsible for nuclear relaxation are simple and thermally activated events, τ_a can be given as $\tau_a = \tau_a^o \exp(V_a/RT)$, where V_a is the activation energy for the motion characterized by τ_a. Eqs.(3)and(4)indicate that, if the relaxation is governed by one motion, then $1/T_2$ will have an exponential dependence on 1/T only when $\omega_s^2 \tau_a^2 \gg 1$ or $\omega_s^2 \tau_a^2 \ll 1$. So we can learn something about motions from the temperature-dependence studies of T_2.

Figure 3. Temperature dependence of relaxation time and viscosity for $CHCl_3$

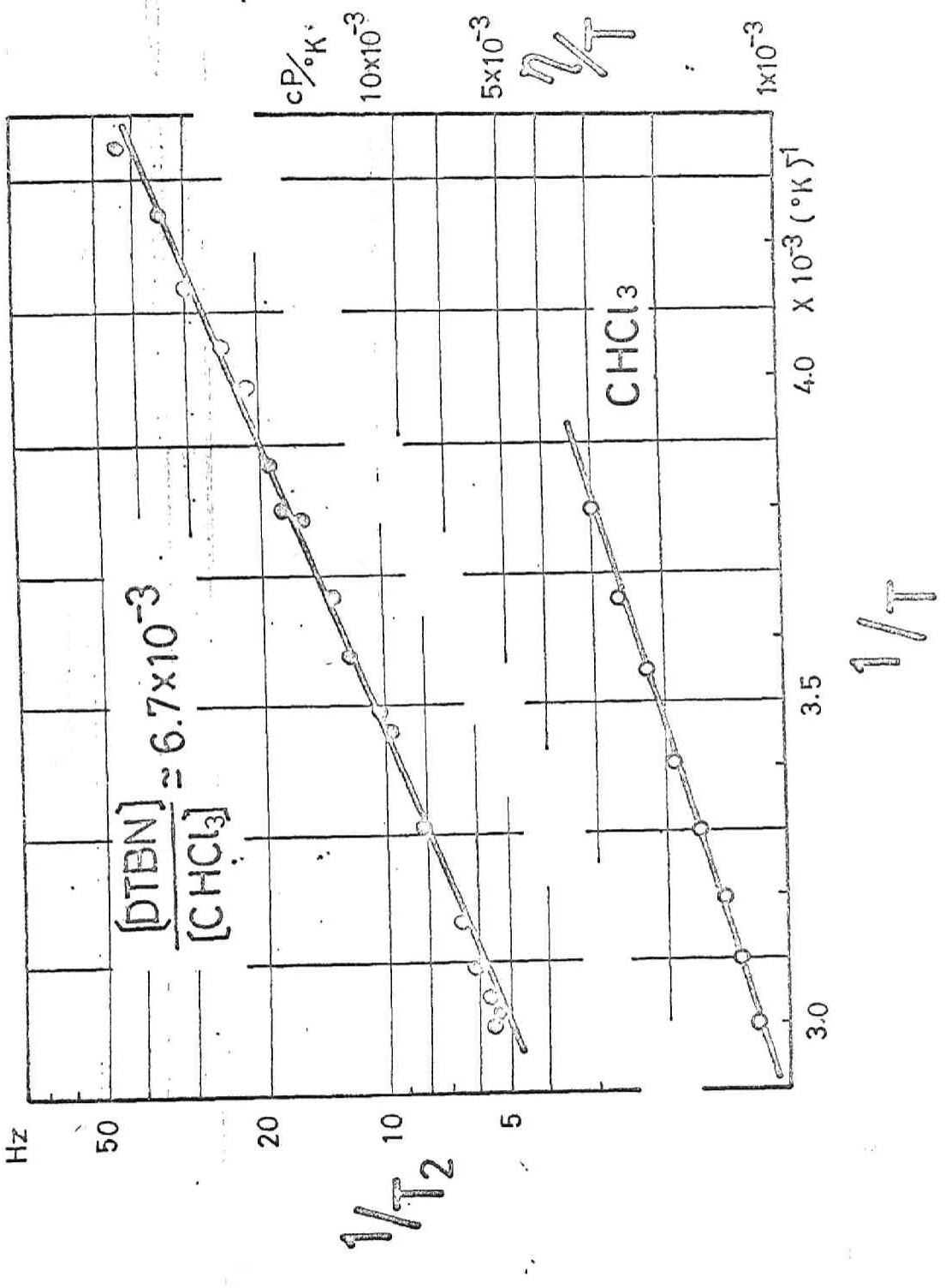

Figure 4. Temperature dependence of relaxation time and viscosity for CH_3OH

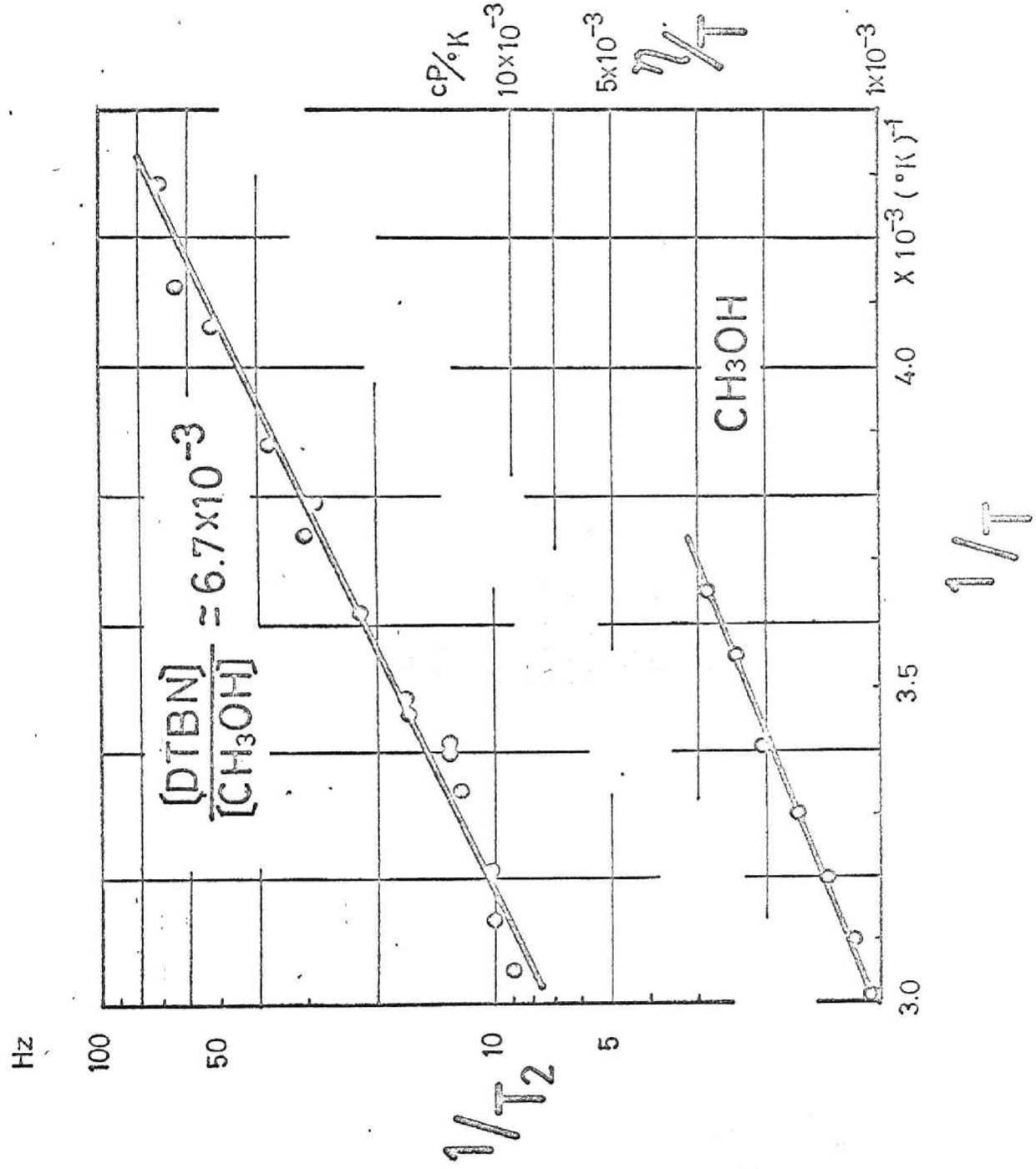

Figure 5. Temperature dependence of relaxation time and viscosity for $C_6H_5NH_2$

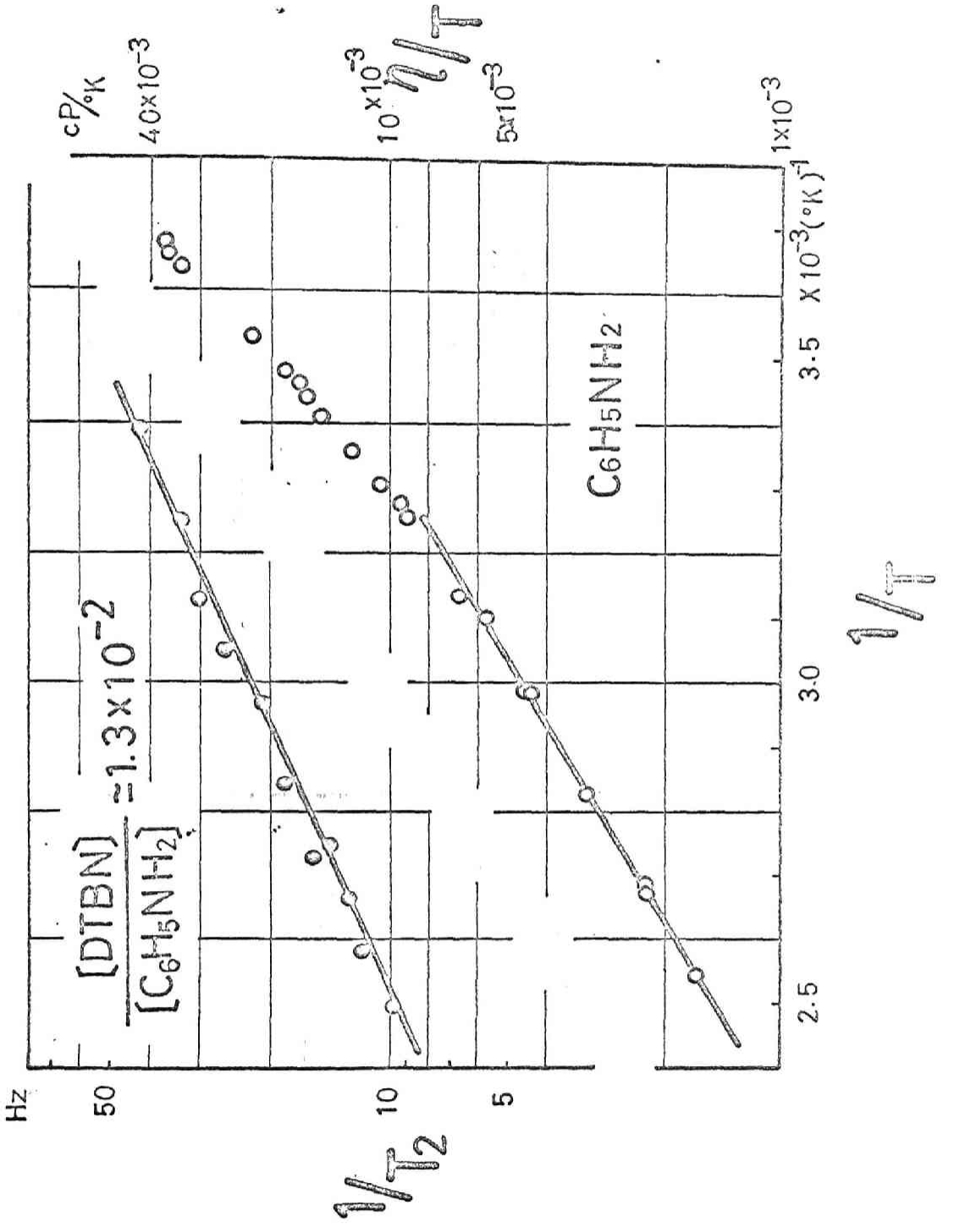

T_2 was measured for the solutions of $CHCl_3$, CH_3OH and $C_6H_5NH_2$ in wide temperature ranges ; this covers about 100°C. The results are plotted as log(the inverse of T_2) vs. 1/T in Fig. 3 ~ 5, where T is the absolute temperature. From the slope of the straight line through T_2 data in Fig. 3 ~ 5 , we have obtained the apparent activation energies for the process involved. The activation energies are listed in table 2. From these results, it is pointed out that the temperature-dependences of T_2 in this H-bond system correspond to apparent activation energies of about 3 ~ 4 kcal/mole for the motion characterized by one correlation time.

Besides, since the slope of $\log(1/T_2)$ vs. 1/T expresses the correlation time τ_a, it may be interesting to consider some correspondences to other macroscopic parameters describing the behaviours of liquids. If diffusion is proved to be the chief mechanism of motion , a comparison with the viscosity seems reasonable. The viscosity of the liquid may also be explained by the random motion of molecules tending to disturb each other such as to reduce their velocities.

So, using the Stokes expression for the various force on a sphere and the theory of Brownian motion, one obtains the Debye expression for τ ;

$$\tau = 4\pi\eta a^3 / 3kT \quad , \qquad (7)$$

where η is the viscosity.

In Fig. 3~5, η/T is plotted vs. the inverse of temperature. The viscosity data of the proton-donor molecules were taken

from the literature [12] . The similarities of the slope of $1/T_2$ and η/T in Fig. 3~5 suggest that a similar mechanism is responsible for both T_2 and η . The plots of log $(1/T_2)$ vs. $1/T$ and log (η/T) vs. $1/T$ are nearly parallel. Therefore, using τ obtained from the viscosity and T_2 at the same temperature , we may evaluate the closest distances that the proton approaches the odd electron approximately. If the relaxation results from the dipolar translational motion, and if $\omega_s^2 \tau_{c'}^2 \ll 1$, Eq. 3 becomes

$$1/T_2 \simeq (4\pi/3r_o'^3)\gamma_I^2\gamma_s^2\hbar^2 N \tau_{c'} . \qquad (8)$$

The values of r_o' are shown in table 2. The results are too small,[13] because $\tau_{c'}(=\tau)$ is caculated with the values of the viscosity of the pure solvent. Here, the rotational contribution was excluded , because $r_o < 1$ (Å) when the relaxation mechanism is governed by the rotational motion.

Table 2. The correlation times from the viscosity, the activation energies, and the closest distance that the proton approaches the odd electron.

proton-donor molecules (0.5 ml)	DTBN (M)	τ_c (27°C) ($\mu\mu$sec)	∇_a (kcal/mole)	r_0 (trans.term) (Å)
$C^1\underline{H}Cl_3$	4.2×10^{-5}	1.3	3.0 ± 0.8	1.3
$CH_3O^1\underline{H}$	8.4×10^{-5}	1.2	3.8 ± 1.0	1.2
$C_6H_5N^1\underline{H}_2$	8.4×10^{-5}	7.6	3.2 ± 0.7	1.8

References

(1) (a) I.Morishima, K,Endo, and T.Yonezawa, J.Amer. Chem.Soc., 93, 2048(1971)

(b) Chem.Phys.Lett., 9, 143(1971).

(c) ibid 9, 203(1971)

(d) I.Morishima, T.Inubushi, K,Endo, and T.Yonezawa, ibid 14, 372(1972)

(e) J.Amer. Chem,Soc.,94, 4812 (1972),

(2) H.S. Gutowsky and Julia Chow Tai, J.Chem.Phys. 39, 208(1963)

(3) K.D.Kramer, W.Muller-Warmuth, and J.Schinder, J.Chem.Phys., 43, 31(1965)

(4) R.A.Dwek, O.W.Howarth, D.F.S.Natusch and R.E.Richards, Molec.Phys., 13, 457(1967).

(5) T.J.Swift and Robert E.Connick, J.Chem.Phys., 37,307(1962).

(6) N.Bloembergen, J.Chem.Phys., 27, 595(1957).

(7) I.Solomon and N.Bloembergen, J.Chem.Phys., 25, 261(1956).

(8) I.Solomon,Phys. Rev., 99, 559(1955).

(9) D.J.E.Ingram, Free Radicals as Studied by E S R (Butter-worths Scientific Publications, Ltd., London, 1958)

(10) I.Morishima, K,Endo and T.Yonezawa, J.Chem.Phys. in press(1973)

(11) the relaxation term by the translational motion was added as well as Gutowsky et al. (2) used.

(12) The National Research Council of the U.S.A.,"International Critical Tables of Numerical Data, Physics, Chemistry and Technology (Mcgraw-Hill Book Co.Inc. New York and London,1929)

(13) the closest distance means when the proton of the proton-donor molecule approaches the odd electron of DTBN in the closest separation because of τ obtained from

the viscosity of the pure solvent. For the correlation time of the proton-donor molecule which interacts with DTBN will be larger than the correlation time of the pure proton-donor molecule.

Chapter 3. Conclusion

The investigation summarized in Part III gives the informations on the interaction between the closed- and open-shell molecules by use of nmr from the dynamic standpoint.

Part III dealed with the ^1H relaxation study of the H-bond in the proton-donor/DTBN radical system. The results are in agreement with the ralaxation mechanism governed by the dipolar magnetic interaction in previous papers. From this study the author obtained the informations about the relaxation mechanism, the lifetimes for the chemical exchange, the activation energies and the closest distances that the proton approaches the odd electron for this H-bond system.

From the discussions in Chapter 2, the conclusions are stated as follows;

(a) The relaxation mechanism for the proton of the protic substance is determined chiefly by the nucleus-electron dipole-dipole interaction but partly characterized by the exchange interaction.

(b) The lifetimes for the chemical exchange indicate about $10^{-9}\sim10^{-11}$ sec ; the chemical exchange of this H-bond is rapid.

(c) The activation energies due to the motion dominated by the translational correlation time are 3～4 kcal/mole.

(d) The ^1H relaxation time corresponds to the correlation

time from the viscosity of the pure proton-donor molecule. Thus, a similar mechanism of motion (owing to the translational diffusion) is responsible for relaxation time and viscosity.

SUMMARY AND GENERAL CONCLUSION

In the studies summarized in this thesis, the author intended to understand the nmr parameters such as the chemical shielding constants, coupling constants, and relaxation times based on the perturbation theory. These parameters have been shown to be quite sensitive to the local electronic structures of molecules and subject to the environmental effects. Throughout present thesis, the author investigated the heavy atom effect on the chemical shielding constant and the molecular interaction between the proton-donor molecules and a free radical from the measurements of nmr contact shifts and nuclear relaxation times.

Part I, by use of the third order perturbation method, the new typed expression (LS shift) for the shielding constant including the spin-orbit interaction was given in order to interprete the abnormal upfield trend of the chemical shift for the nucleus bonded to the heavy atom. As the application of this theory, the proton chemical shift for the hydrogen halides was calculated in detail. Thus. it is emphasized that the σ_{LS} term cannot be neglected in comparison with σ_{para}, and has an important contribution to the abnormal upfield trend of the proton chemical shift in hydrogen halides.

From the studies given in Part II, the author showed that the ^{1}H and ^{13}C nmr contact shifts are quite sensitive to the presence of a small amount of a stable free radical and

the resulting ^{1}H and ^{13}C contact shifts are very useful for the studies of weak molecular interactions. In the course of this study, the author mentions a correlation between ^{13}C contact shifts and ^{13}C-H nuclear spin coupling constants. This correlation is explained in terms of finite perturbation theory of nuclear spin coupling constants in which the ^{13}C-H coupling constant is related to the electron spin density on the ^{13}C nucleus induced when spin density is placed finitely on the proton. The potential utility of this relation in the prediction of sign and magnitude of long-range ^{13}C-H coupling constants is described. Also in order to give the fruitful informations on the nature of the H-bond for proton-donor/DTBN radical system, the formation constants, enthalpies, limiting ^{1}H and ^{13}C contact shifts and spin densities on the H and C atoms were determined from ^{1}H and ^{13}C contact shifts measurements at various temperatures. The H-bond energies and spin densities on the X-H molecules were well reproduced by MO calculations. As a part of these continuing studies on the interaction between closed- and open-shell molecules , he performed ^{13}C nmr contact shifts studies on DTBN...alkyl halides interaction which are interpreted in terms of a charge-transfer interaction.

In the studies given in Part III, the author dealed with the molecular interaction between the proton-donor molecules and a free radical from the measurement of ^{1}H relaxation times.

An analysis of proton relaxation data yielded the informations about the dynamic behaviors in proton-donor/DTBN radical H-bond system. For this H-bond system which belongs to the formation of a labile complex, the relaxation mechanism is governed by the translational dipolar magnetic interaction, but partially characterized by the exchange coupling. The chemical exchange is rapid. (This lifetimes are of the order of $10^{-9} \sim 10^{-11}$ sec.) From the temperature dependence study, the activation energies corresponding to the translational motion indicate about 3 ~ 4 kcal/mole. Also the closest distance that the proton approaches the odd electron was evaluated.

From the studies summarized in Part II and III, it is expected that one may obtain the worthy informations on the interaction between the closed- and open-shell molecules by nmr. These studies enable us to use the magnetic moment of a stable free radical as a probe to investigate the molecular interaction in biological system.